For Reference

NOT TO BE TAKEN FROM THIS ROOM

Ex libris
Universitatis
Albertaensis

QUAECUMQUE VERA

Digitized by the Internet Archive
in 2024 with funding from
University of Alberta Library

https://archive.org/details/Wattamaniuk1973

THE UNIVERSITY OF ALBERTA

RELEASE FORM

NAME OF AUTHOR Walter J. Wattamaniuk

TITLE OF THESIS Non-equilibrium Effects in Tunnel Junctions

DEGREE FOR WHICH THESIS WAS PRESENTED Ph.D.

YEAR THIS DEGREE GRANTED Spring 1973

Permission is hereby granted to THE UNIVERSITY OF ALBERTA LIBRARY to reproduce single copies of this thesis and to lend or sell such copies for private, scholarly or scientific research purposes only.

The author reserves other publication rights, and neither the thesis nor extensive extracts from it may be printed or otherwise reproduced without the author's written permission.

THE UNIVERSITY OF ALBERTA

NONEQUILIBRIUM EFFECTS IN TUNNEL JUNCTIONS

by

© WALTER J. WATTAMANIUK

A THESIS

SUBMITTED TO THE FACULTY OF GRADUATE STUDIES AND RESEARCH
IN PARTIAL FULFILLMENT OF THE REQUIREMENTS FOR THE DEGREE
OF DOCTOR OF PHILOSOPHY IN THEORETICAL PHYSICS

DEPARTMENT OF PHYSICS

EDMONTON, ALBERTA

SPRING 1973

THE UNIVERSITY OF ALBERTA

FACULTY OF GRADUATE STUDIES AND RESEARCH

The undersigned certify that they have read, and recommend to the Faculty of Graduate Studies and Research, for acceptance, a thesis entitled "NONEQUILIBRIUM EFFECTS IN TUNNEL JUNCTIONS", submitted by Walter J. Wattamaniuk in partial fulfillment of the requirements for the degree of Doctor of Philosophy in Theoretical Physics.

ABSTRACT

Structure in the conductance σ of normal metal-insulator-metal junctions at very low bias is explained through a nonequilibrium treatment of the tunneling process. In particular, the related peak in the derivative $d\sigma/dV$ is quantitatively accounted for by the blocking of otherwise-available electron tunneling states due to the finite electron relaxation rates in the metal electrodes. A transport model which includes the effects of elastic and inelastic scattering of electrons in the metal electrodes is used to obtain expressions for σ and $d\sigma/dV$. The results are compared with the temperature dependence of the peaks of $d\sigma/dV$ obtained from measurements on Al-Al and Pb-Au tunnel junctions. The nonequilibrium theory is extended to the case of tunneling in superconducting junctions and results in a non-discontinuous rise in the tunneling current at the gap edge.

ACKNOWLEDGEMENTS

I wish to express my deep gratitude to Dr. H.J. Kreuzer, my research supervisor, for captivating my interest in electron tunneling and for his encouragement and guidance.

I am indebted to Dr. J.G. Adler for providing me with the experimental data for this project and for many interesting discussions.

To Dr. P.N. Trofimenkoff I express my gratitude for many illuminating and informative discussions about tunneling and solid state physics.

I would like to thank Mr. R. Teshima for assistance with the numerical calculations required in this work and Mrs. Mary Yiu for her patience and excellent typing performance on this thesis.

Finally, and most important of all, I thank my wife and children for their understanding and perseverance during the past years.

TABLE OF CONTENTS

Chapter Page

I INTRODUCTION 1

1.1 General Background 1

1.2 Historical Resumé of Tunneling Investigations 5

1.3 Experimental Procedures in Tunneling 8

1.4 Aim and Scope of the Present Investigation 11

II CONVENTIONAL TUNNELING THEORY (NORMAL METALS) 13

2.1 The One-Electron Picture of Tunneling 13

2.2 Barrier Models and Transmission Coefficients 23

2.3 Magnitude and Angular Dependence of the Transmission Coefficient 27

2.4 Nonlinear Characteristics of Tunnel Junctions Due to Barrier Dependence 31

2.5 Perturbation Formulation of Tunneling 37

III THE ZERO BIAS ANOMALY 46

3.1 Nonequilibrium Tunneling 46

3.2 Relaxation Times 55

3.3 Calculation of the Current, Conductance and Derivative of Conductance Due to the Blocking Effect 65

Chapter Page

III (cont'd)

3.4 Comparison of Theory with Experiment 74

IV INELASTIC ELECTRON TUNNELING 91

4.1 The Inelastic Current 91

4.2 Inversion For G(ω) in Terms of The Second Derivative of Inelastic Tunneling Current 102

V TUNNELING IN SUPERCONDUCTORS 106

5.1 The Semiconductor Picture 106

5.2 Nonequilibrium Tunneling in Superconductors 116

5.3 Superconducting Relaxation Times 118

5.4 The Nonequilibrium Tunneling Current 121

VI GEOMETRICAL EFFECTS IN TUNNEL JUNCTIONS AND CONCLUSION 127

6.1 Structure of The Tunnel Junction and Splitting of the ZBA 127

6.2 Conclusion and Discussions 132

REFERENCES 136

CHAPTER I

INTRODUCTION

1.1 General Background

A transport phenomenon which has been of particular interest over the past decade is the transport of electrons through thin insulating films. One system (commonly called a tunnel junction) that is used to study such effects is made by depositing a metal film onto a glass slide, letting it oxidize for a few minutes and then depositing a second film crossing the first. Such an oxide film on metals like aluminum, lead or tin will ordinarily be continuous and may be of the order of 20 Å thick. The two metal films are therefore not in electrical contact; yet if a voltage is applied across the two, a current is found to flow and is in fact proportional to the applied voltage. This is the behavior expected if the current was conducted through small metal bridges in the oxide. However, when the metallic films are superconducting, it becomes clear that the current is carried by a tunneling mechanism. To understand the phenomenon of electron tunneling through thin insulating films, we must understand the behavior of an electron in the vicinity of a metal surface. We shall return to tunneling in superconductors in Chap. V.

Theories of metal surfaces adjacent to a vacuum or an insulator have, relatively speaking, lagged far behind the bulk theories of metals which are now capable of giving quantitatively accurate descriptions of wide classes of metals. This is primarily due to the loss of translational invariance at the surface of the metal and the rapid decrease of electron density there. In contrast, the translational invariance of the lattice in the bulk metal introduces important elements of simplicity into the calculations of the bulk theorist.

The earliest model calculations of the metal interface were made by Frenkel (1928). He replaced the lattice of the metal by a constant positive "jellium" density which ended as a step discontinuity at the metal surface. He applied the Thomas-Fermi Method together with Poisson's Equation to calculate the electron density near the interface. Integrated charge neutrality as well as the vanishing of electronic charge density at large distances exterior to the metal were used as boundary conditions in his calculations. Bardeen (1936) used the same approach except that he used the many-electron Schrödinger equation rather than the Thomas-Fermi Approximation to relate the electron potential to its charge density. Recently, a new formulation was developed in a series of papers by Kohn and his collaborators (1964-1971). Kohn uses the (presumed known) results for the ground

state energy of a uniform system to calculate the energy of an inhomogeneous system by writing the latter as a functional of the local electron density.

The picture of the metallic interface that has emerged from these studies is very similar to what one feels should happen intuitively. The potential an electron sees inside a metal is periodic with the period of the lattice, going through deep depressions in the neighborhood of each atomic nucleus. It rises sharply at the surface, forming a potential barrier which keeps the electrons confined to the metal. This transition zone at the surface is of the order of an electron Fermi wavelength wide. The potential energy within a metal is lowered due to the actions of the attractive restoring forces of the atomic nuclei and the exchange forces between electrons of the same spin. The translational invariance of the bulk lattice forces the electrons in a solid to be grouped into energy bands separated by gaps of forbidden energy. The lower energy bands are filled with electrons, each energy level in a band having its full quota of two electrons according to the Pauli Exclusion Principle. In metals the highest energy band is only partially filled and forms the conduction band, only electrons of this band participating in conduction and transport processes.

If we consider a conduction band electron wavefunction in one of the metal strips of a tunnel junction, it is clear that the wavefunction does not drop immediately to zero at the interface with the oxide. Rather it will penetrate and decay exponentially into the oxide. The wavefunction may still have a very small but finite value at the opposite edge of the oxide and therefore it is possible for the electron to make a transition or to "tunnel" into the second strip. This is the same behavior that would be anticipated if the oxide were to be replaced by an equivalent thickness of vacuum. The conduction electrons of interest would have energy below the vacuum level, and therefore the wavefunction would have negative kinetic energy within the vacuum and again would decay exponentially. This is precisely the situation described as quantum-mechanical tunneling and treated in elementary quantum-mechanics textbooks (e.g. see Schiff for instance). Oxides are predominantly used as the barriers in tunnel junctions because of their ease of fabrication. In order to easily observe a tunneling current between two metals separated by a vacuum, the metals should, in practice, be spaced less than 50 Å apart. The construction of such a tunnel junction presents a very difficult task since the smoothness of ordinary metal surfaces is certainly not of this order, even when they are specially prepared.

The only difference with the oxide layer is that the exponential decay of the electron arises from the fact that the energies of interest lie within the forbidden energy band of the oxide rather than from negative kinetic energy as in vacuum.

1.2 Historical Resumé of Tunneling Investigations

The first application of the idea of quantum-mechanical tunneling to describe emission from a bulk metal was the calculation of Fowler and Nordheim (1928) that explained field emission from free electron metals. Frenkel (1930) soon extended this calculation to the case of current flowing across a voltage biased metal-vacuum-metal system. He accounted both for the change in character of the barrier potential (which he assumed was trapezoidal in shape) and for the thermal occupation probabilities of the electronic states in the metal electrodes. An extension of Frenkel's calculation was made by Sommerfeld and Bethe (1933) to the case in which the barrier between the two metal electrodes is an insulator rather than a vacuum. The band structure and dielectric constant of the barrier region was taken to be characteristic of a bulk insulator.

The quantum-mechanical tunnel current flowing through a thin insulating layer between normal metal

electrodes was first experimentally investigated in detail by Fisher and Giaever (1961). They measured the current-voltage characteristics of junctions made with evaporated electrodes of aluminum and a thermally grown oxide layer. Detailed comparison with the theory of Holm (1951) verified that tunneling was in fact taking place. When their devices were subsequently cooled to superconducting temperatures it was found that superconducting energy gaps and densities of quasi-particle states characteristic of the bulk films could be obtained from the now non-linear current voltage characteristics (Giaever, 1960).

Giaever's work immediately stimulated a sequence of measurements on both superconducting and normal metal-insulator-metal junctions. The early experiments on superconducting tunnel junctions provided additional confirmation of the Bardeen-Cooper-Schrieffer Theory of Superconductivity (1957, hereafter referred to as the BCS theory) for weak coupling superconductors (e.g. Al, In, Sn). Subsequent experiments also verified the theory of strong coupling superconductors (e.g. Pb, Hg). The history of developments of measurements on superconducting tunnel junctions has been reviewed in detail by McMillan and Rowell (1969).

Giaever's experiments also provided the motivation for a reexamination of the theory of tunneling in order to incorporate into it a description of the many body properties of the electrodes and thus provide an adequate base for theoretical calculations. The models of tunneling (and their experimental manifestations) prior to Giaever's pioneering measurements had the common feature that they were based upon a one-electron description of the tunneling process. Although the theory of bulk superconductivity had already been developed by BCS, the superconducting tunnel conductance, $\sigma = dI/dV$, seemed to be a direct measure of the many body bulk density of states in contrast to the predictions of a one electron theory.

The subsequent reexamination of tunneling theory led to the transfer-Hamiltonian formulation of the tunneling current by Bardeen (1961) and Cohen, Falicov and Phillips (1962). This reformulation of tunneling theory led to the prediction by Josephson (1962) and subsequent observation by Anderson and Rowell (1963) of phase coherence between two superconductors separated by a thin tunnel barrier (now commonly known as Josephson tunneling).

1.3 Experimental Procedures in Tunneling

Since experimental data is presented in this thesis and compared with theory, a brief description of the measurements and data is given to provide an orientation for subsequent theoretical analysis. Unless otherwise noted, the experimental data in this thesis is presented with the kind permission of Dr. J.G. Adler.

The steps in the fabrication of a tunnel junction are outlined in Fig. (1-1). A smoothly polished glass slide with indium contacts (a) is placed in a high vacuum environment. A metallic strip about 1 mm wide and 1000 to 3000 Å thick is deposited across the indium contacts (b). The metallic strip is then allowed to oxidize to form an insulating layer some tens of Anstroms thick (c). A second strip of metal is then evaporated in vacuum across the first one (d). The connections of current and voltage leads are shown. The junction is then taken out of the evaporator and placed into a liquid He^4 cryostat where measurements down to 1°K can be made. A superconducting magnet surrounding the junction may be used to subject the junction to magnetic fields as high as 60 kilogauss. Normally several films are evaporated across the oxidized base film to simultaneously provide several junctions for measurement.

In a typical normal metal-insulator-metal (M-I-M) junction measurement, a constant current I_o is passed

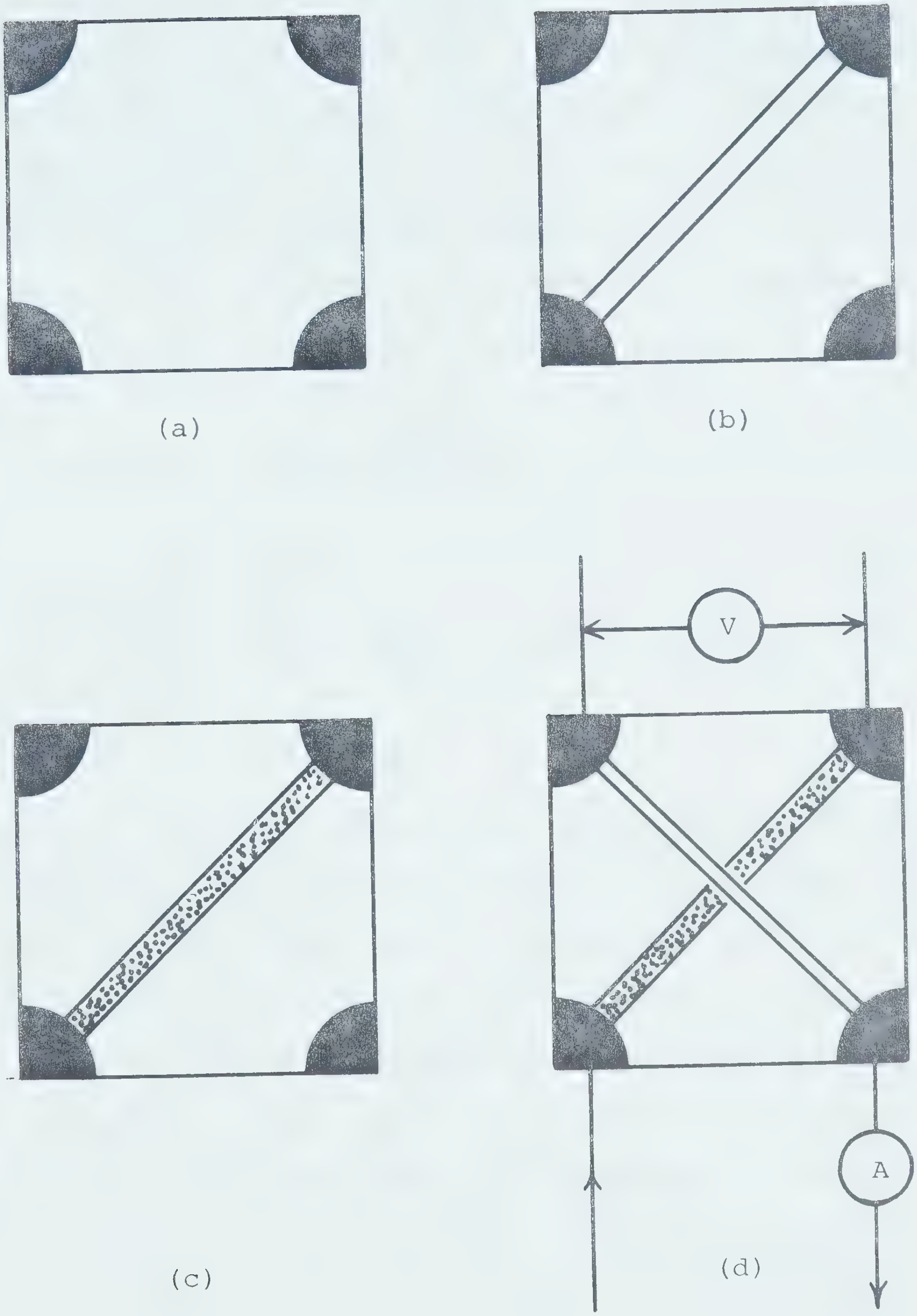

(Fig. 1-1) Preparation of an M-I-M tunnel junction.

through the junction together with a small modulation current $\delta \cos \omega t$ where δ is a small constant current modulation amplitude, ω is 2π times the modulating frequency and t is the time. The current $I = I_o + \delta \cos \omega t$ will result in a voltage response V(I) across the junction. Since the junctions are weakly non-linear, the voltage response may be expanded in powers of small δ:

$$V(I) = V(I_o) + \left(\frac{dV}{dI}\right)_{I_o} \delta \cos \omega t + \frac{1}{2}\left(\frac{d^2V}{dI^2}\right)_{I_o} \delta^2 \cos^2 \omega t + \ldots\ldots$$

$$= V(I_o) + \left(\frac{dV}{dI}\right)_{I_o} \delta \cos \omega t + \frac{1}{4}\left(\frac{d^2V}{dI^2}\right)_{I_o} \delta^2 (1 + \cos 2\omega t) + \ldots\ldots$$

$V(I_o)$ is the d.c. bias of the tunnel junction and it follows from the above equation that if δ is small compared to I_o and constant, then the component of voltage across the junction at angular frequency ω is proportional to $(dV/dI)_{I_o}$ and the component at 2ω is proportional to $(d^2V/dI^2)_{I_o}$. Both these two components are measured by means of phase sensitive instrumentation. The quantities of interest, the current I(V), the dynamic conductance $\sigma(V) = dI(V)/dV$, and derivative of conductance $d\sigma(V)/dV = d^2I(V)/dV^2$ are then reconstructed numerically from the above measurements (see Adler et.al. 1971) and form the final data for theoretical interpretation.

1.4 Aim and Scope of the Present Investigation

The objective of the present investigation was to carry out an intensive interpretation and theoretical analysis of the conductance minima centered about zero bias (hereafter called zero-bias anomalies or ZBA) occurring in normal M-I-M junctions under experimental investigation by Dr. J.G. Adler.

In Chapter II of this thesis we present a review of conventional tunneling theory both from the one-electron picture and the perturbation (transfer-Hamiltonian) point of view. This review will provide the concepts in tunneling required to explain the physical origin of the zero-bias-anomalies. It will also provide us with the means for isolating the zero-bias-anomalies from the gross background features of electron tunneling which tend to obscure these anomalies. This will allow us to compare theory with experiment in an effective manner.

The theory of the ZBA as an interference or "blocking" effect in the transport of electrons across the junction is presented in Chapter III. We compare theory to experiment in detail for two cases; an aluminum-aluminum junction and a lead-gold junction. Partial results of Chapter III have been published in Physical Review Letters (P.N. Trofimenkoff, H.J. Kreuzer, W.J.

Wattamaniuk and J.G. Adler, 1972).

Chapter IV is presented for completeness and involves a discussion and phenomenological explanation of the nonlinearities that occur in the tunneling process due to the presence of the barrier oxides.

The theory of quasi-particle tunneling in superconducting tunnel junction is reviewed in Chapter V. The extension of ideas put forward to explain the ZBA's in normal metal junctions leads to a plausible explanation of the nonideal behavior in the current-voltage characteristics of a superconducting-superconducting tunnel junction.

In the final Chapter (VI), we give a general discussion of the geometry of the tunnel junctions based on related experiments made by Dr. J.G. Adler. It is shown that tunneling occurs at restricted areas of the tunnel junctions of interest in this thesis.

CHAPTER II

CONVENTIONAL TUNNELING THEORY
(NORMAL METALS)

2.1 The One-Electron Picture of Tunneling

In this section, we derive the tunneling current across a M-I-M junction using essentially the arguments of Sommerfeld and Bethe (1933) and Fan (1942). It is assumed that the insulator may be replaced by an effective one-electron potential barrier whose thickness is equivalent to that of the oxide. Any distortion of band structure in the metals due to mismatch of metal-insulator work functions is neglected. Some justification for these assumptions has been given in Section 1.1 of the Introduction. The tunnel junction itself will be envisioned geometrically as an insulator of even thickness sandwiched between two parallel metals. The metals are treated in the free electron approximation in which the periodic potential of the crystal lattice is neglected. In accordance with this model, only the electrons in the partially filled conduction band may tunnel. A convention that is adopted throughout the remainder of this thesis is that quantities characteristic of the left and right hand metals shall be identified by subscripts ℓ and r respectively.

The energy-space diagram of two metals M_ℓ and M_r separated by an insulator of thickness s and gap energy E_g is represented schematically by Fig. (2.1). At 0°K all electronic states in the metal are occupied up to a critical value of the kinetic energy μ (the Fermi energy). If metals M_ℓ and M_r are different and are shorted out by an external conducting wire they will reach (by electron exchange) an equilibrium state in which the chemical potentials in both metals are equal (i.e. the Fermi levels coincide). In this state an intrinsic voltage V_c (the contact potential) arises so that $eV_c = \chi_\ell - \chi_r$, where e is the electron charge and χ is the metal-insulator work junction (i.e. the work required to displace an electron at the Fermi level in the metal into the conduction band of the insulator). We shall measure all energies from the bottom of the conduction band in M_r.

When an external bias V is applied to the junction so that M_ℓ is the cathode and M_r the anode, the Fermi level of M_r will be lowered by an amount eV with respect to that of M_ℓ. The change in electron potential energy in a direction x normal to the junction is represented by the trapezoidal barrier (curve (a) of Fig. (2.1)) if the interaction of the tunneling electron with the metals is neglected. However, the abrupt change in the potential barrier is only an ideal model and is physically unrealizable since abrupt changes in potential imply infinite

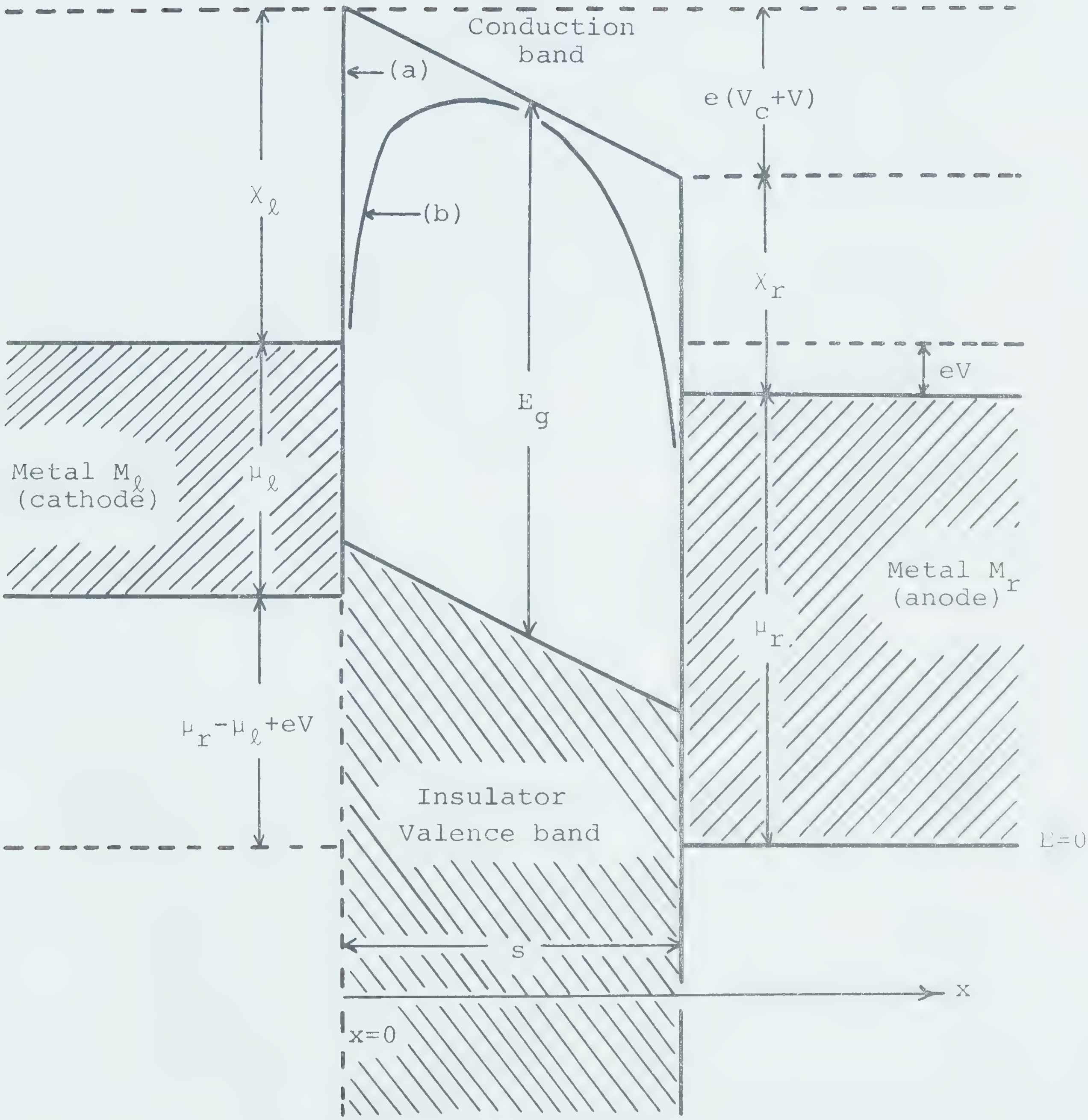
Conduction band
(a)
(b)
$e(V_c+V)$
χ_ℓ
χ_r
E_g
eV
Metal M_ℓ (cathode)
μ_ℓ
Metal M_r (anode)
μ_r
$\mu_r-\mu_\ell+eV$
Insulator Valence band
E=0
s
x
x=0

Fig. (2.1) Energy diagram for a metal-insulator-metal system.

fields. In fact, we expect that the barrier potential changes smoothly (curve(b), Fig.(2.1)) because the transition region between the metal and insulator must be of finite extent. The electron will also experience an attractive image force in the barrier region due to the metal surface (Simmons, 1969). The voltages of interest in this thesis are of the order of millivolts as contrasted to the Fermi energies and potential barrier heights which are of the order of volts. In addition the low temperatures of interest here ensure us that the Fermi surfaces are sharp. Thus electron transfer across the barrier will occur entirely by tunneling at Fermi energies.

The electron current density incident on the metal-insulator interface from the left is given by

$$J_i = \frac{2e}{V} \sum_{\underline{k}} v_x f^o(E_{\underline{k}} - \mu_r - eV) \quad , \tag{2.1}$$

where V is the volume and $\hbar\underline{k}$ is the momentum of an electron of energy

$$E_{\underline{k}} = \mu_r - \mu_\ell + eV + \frac{\hbar^2 \underline{k}^2}{2m} \quad , \tag{2.2}$$

and velocity

$$\underline{v}_{\underline{k}} = \frac{1}{\hbar} \nabla_{\underline{k}} E_{\underline{k}} = \frac{\hbar\underline{k}}{m} \quad . \tag{2.3}$$

m is the free electron mass and f^o is the equilibrium Fermi-Dirac distribution function defined by

$$f^o(E) = \frac{1}{1 + e^{E/k_B T}} \quad , \qquad (2.4)$$

where k_B is Boltzmann's constant and T is the temperature in °K. The factor of 2 in front of the summation over free electron states accounts for spin while v_x is the positive x-directed component of electron velocity ($v_x = \hbar k_x/m$). With a large number of states and box quantization

$$\sum_{\underline{k}} \longrightarrow \frac{V}{(2\pi)^3} \int d^3\underline{k} \quad ,$$

therefore

$$J_i = \frac{2e}{(2\pi)^3} \iint d\underline{k}_{||} \int_{k_x>0} dk_x \left(\frac{\hbar k_x}{m}\right) f^o(E_{\underline{k}} - \mu_r - eV) \quad , \qquad (2.5)$$

where $d\underline{k}_{||} = dk_y dk_z$.

Now let the wave vector $\underline{k}$ of an electron in the left-hand metal change to $\underline{k}'$ as it tunnels into the right hand metal. We shall assume that energy is conserved (i.e. $E_{\underline{k}} = E_{\underline{k}'}$) along with the parallel component of momentum (i.e. $\underline{k}_{||} = \underline{k}'_{||}$).

The latter simply corresponds to specular reflection at the metal-insulator interface. Now whether or

not an electron tunnels into the right hand metal depends upon:

(i) the availability of an empty state of energy $E_{\underline{k}}$ in the right hand metal. This is specified by the distribution of holes there,

$$1 - f^{o}(E_{\underline{k}} - \mu_{r}) \; .$$

(ii) the probability of the electron penetrating through the barrier into the right hand side. We specify the probability by a transmission coefficient $P(\underline{k})$ which will of course depend upon the bias and explicit shape of the barrier potential.

The transmitted current density from left to right is thus given by

$$J_{\rightarrow} = \frac{2e}{(2\pi)^{3}} \int d\underline{k}_{||} \int_{k_x > 0} dk_x \left(\frac{\hbar k_x}{m}\right) f^{o}(E_{\underline{k}} - \mu_r - eV)$$

$$\times \; [1 - f^{o}(E_{\underline{k}} - \mu_r)] \; P(k_x, \underline{k}_{||}) \; , \qquad (2.6)$$

where $E_{\underline{k}}$ is given by Eqn. (2.2).

Similarly, there will be a transmitted current from the right hand metal into the left hand metal which by symmetry is

$$J_{\leftarrow} = - \frac{2e}{(2\pi)^{3}} \int dk'_{||} \int_{k'_x > 0} dk'_x \left(\frac{\hbar k'_x}{m}\right) f^{o}(E_{\underline{k}'} - \mu_r)$$

$$\times \; [1 - f^{o}(E_{\underline{k}'} - \mu_r - eV)] \; P(\underline{k}'_x, \underline{k}'_{||}) \qquad (2.7)$$

where now $\underline{E}_{k'} = \hbar^2 \underline{k}'^2/2m$ (remember that we are measuring energies from the bottom of the right hand band). The above equation for the backcurrent must be modified slightly since a glance at Fig. (2.1) shows that an electron in the left hand metal cannot tunnel into a right hand state that is below the bottom of the band on the right hand side. In fact, it is easy to show that in such a case, the energy and momentum conservation relations that we have imposed lead to an imaginary x component of the wave vector there, implying that the wavefunction decays there. This is of course to be expected and may be rectified by imposing the following condition

$$P'(k_x', \underline{k}_{||}') = 0$$

if

$$k_x'^2 \leq \frac{2m}{\hbar^2} (\mu_r - \mu_\ell + eV) .$$

If we now define

$$k_x''^2 = k_x'^2 - \frac{2m}{\hbar^2} (\mu_r - \mu_\ell + eV),$$

then Eqn. (2.7) for the backcurrent may be written as

$$J_{\leftarrow} = - \frac{2e}{(2\pi)^3} \int dk_{||}' \int_{k_x''>0} dk_x'' \left(\frac{\hbar k_x''}{m}\right) f^{o}(E_{\underline{k}'} - \mu_r) [1 - f^{o}(E_{k'} - \mu_r - eV)]$$

$$\times P'\left(\sqrt{k_x''^2 + \frac{2m}{\hbar^2}(\mu_r - \mu_\ell + eV)}\ ,\ \underline{k}_{||}'\right) , \qquad (2.8)$$

where

$$E_{\underline{k}'} = \frac{\hbar^2}{2m}(k_x''^2 + \underline{k}_{||}^2) + \mu_r - \mu_\ell + eV \; .$$

Eqn. (2.8) now is similar structurally to Eqn. (2.6). At zero bias (eV = 0) no current can flow, therefore we must have

$$J_\rightarrow + J_\leftarrow = 0 \; .$$

This implies that

$$P(\underline{k}_x, \underline{k}_{||}) = P'\left(\sqrt{k_x^2 + \frac{2m}{\hbar^2}(\mu_r - \mu_\ell + eV)} \; , \; \underline{k}_{||}\right) . \qquad (2.9)$$

If we now combine the forward current (Eqn. (2.6)) with the backward current (Eq. (2.8)), the net current from left to right is given by

$$J = \frac{2e}{(2\pi)^3}\int d\underline{k}_{||}\int_{k_x>0} dk_x \left(\frac{\hbar k_x}{m}\right)[f^0(E_{\underline{k}} - \mu_r - eV) - f^0(E_{\underline{k}} - \mu_r)]P(\underline{k}) \, , \qquad (2.10)$$

where $E_{\underline{k}} = \mu_r - \mu_\ell + eV + \frac{\hbar^2 \underline{k}^2}{2m}$. If the barrier is translationally invariant in the parallel plane (i.e. yz plane) then the transmission coefficient $P(\underline{k})$ can only depend on k_x or the x directed kinetic energy $E_x = \hbar^2 k_x^2/2m$ available for tunneling. Let us in addition define the parallel kinetic energy of the electron by

$$E_{||} = \frac{\hbar^2 \underline{k}_{||}^2}{2m} = \frac{\hbar^2}{2m}(k_y^2 + k_z^2) \; .$$

Thus

$$\int d\underline{k}_{||} \int\limits_{k_x>0} dk_x \left(\frac{\hbar k_x}{m}\right) \longrightarrow \frac{2\pi m}{\hbar^3} \int_0^\infty dE_x \int_0^\infty dE_{||} \quad ,$$

and the tunneling current density now becomes

$$J = \frac{4\pi e m}{(2\pi\hbar)^3} \int_0^\infty P(E_x)dE_x \int_0^\infty dE_{||}[f^o(E_x+E_{||}-\mu_\ell) - f^o(E_x+E_{||}-\mu_\ell+eV)] . \tag{2.11}$$

The integral over $E_{||}$ may easily be evaluated using Eqn. (2.4). The result is commonly called the "supply function" $N(E_x)$, i.e.

$$N(E_x) \equiv \int_0^\infty dE_{||}[f^o(E_x+E_{||}-\mu_\ell) - f^o(E_x+E_{||}-\mu_\ell+eV)]$$

$$= k_BT \ln \left(\frac{1 + \exp(\mu_\ell - E_x/k_BT)}{1 + \exp(\mu_\ell - E_x - eV/k_BT)}\right) \quad . \tag{2.12}$$

Thus the current density now assumes the simple form

$$J = \frac{4\pi e m}{h^3} \int_0^\infty P(E_x)N(E_x)dE_x \quad , \tag{2.13}$$

where $h = 2\pi\hbar$ is Planck's constant. The supply function $N(E_x)$ simply represents the difference between the number of electrons per unit time and area, incident on opposite sides of the barrier, and having x-directed kinetic energy in the range E_x to E_x+dE_x. It is entirely statistical in

nature and restricts the tunneling process to those electrons whose total kinetic energy is close to the Fermi energy. The breakdown of the tunneling current into an integral over the product of geometrical and statistical factors is very convenient and provides the starting point for any quantitative analyses of the current-voltage characteristics in tunnel junctions. If we define the total kinetic energy by $E = E_x + E_{||}$, then Eqn. (2.11) may be cast into the form

$$J = \frac{4\pi em}{h^3} \int_0^\infty dE[f^o(E-\mu_\ell) - f^o(E-\mu_\ell+eV)] \int_0^E P(E_x)dE_x \quad . \qquad (2.14)$$

This equation displays more clearly the fact that tunneling is restricted to energies close to the Fermi energy. At zero temperature we have

$$\begin{aligned} f^o(E-\mu_\ell) - f^o(E-\mu_\ell+eV) &= 1 \quad \text{if} \quad -eV \le E-\mu_\ell \le 0 \ , \\ &= 0 \quad \text{otherwise} \quad . \qquad (2.15) \end{aligned}$$

Therefore Eqn. (2.14) becomes

$$J(V)\big|_{T=0} = \frac{4\pi em}{h^3} (eV) \int_0^{\mu_\ell} P(E_x)dE_x \qquad (2.16)$$

$$\text{provided} \quad |eV| << \mu_\ell \quad .$$

For small bias we expect that $P(E_x)$ will be fairly in-

sensitive to the voltage. The tunneling current expressed by Eqn. (2.16) then shows that the tunnel junction is ohmic for very small bias as confirmed by experiment.

2.2 Barrier Models and Transmission Coefficients

We now proceed to compute and discuss the probability of an electron tunneling through the oxide layer. The most natural approach is to construct incident and reflected waves in the left hand metal, match them to exponentially decaying waves of the same energy in the oxide, and finally to match these to a transmitted wave in the right hand metal.

We shall consider two different models of the potential barrier, the first of which is illustrated in Fig. (2.2a) and is characterized by sharp walls with a smoothly varying potential inside. Since we have translational invariance parallel to the barrier, we need only consider an electron incident on the barrier with an x-component of kinetic energy $E_{x_\ell} = \hbar^2 k_{x_\ell}^2/2m$ and which emerges on the other side with x-directed kinetic energy $E_{x_r} = \hbar^2 k_{x_r}^2/2m$. The incident and reflected waves will be of the form $\exp(\pm i k_{x_\ell} x)$, while the transmitted wave is given by $\exp(i k_{x_r} x)$. The potential inside the barrier is left arbitrary and is denoted by $\phi(x)$. Using the WKB approximation (e.g. see Davidov (1965)), the

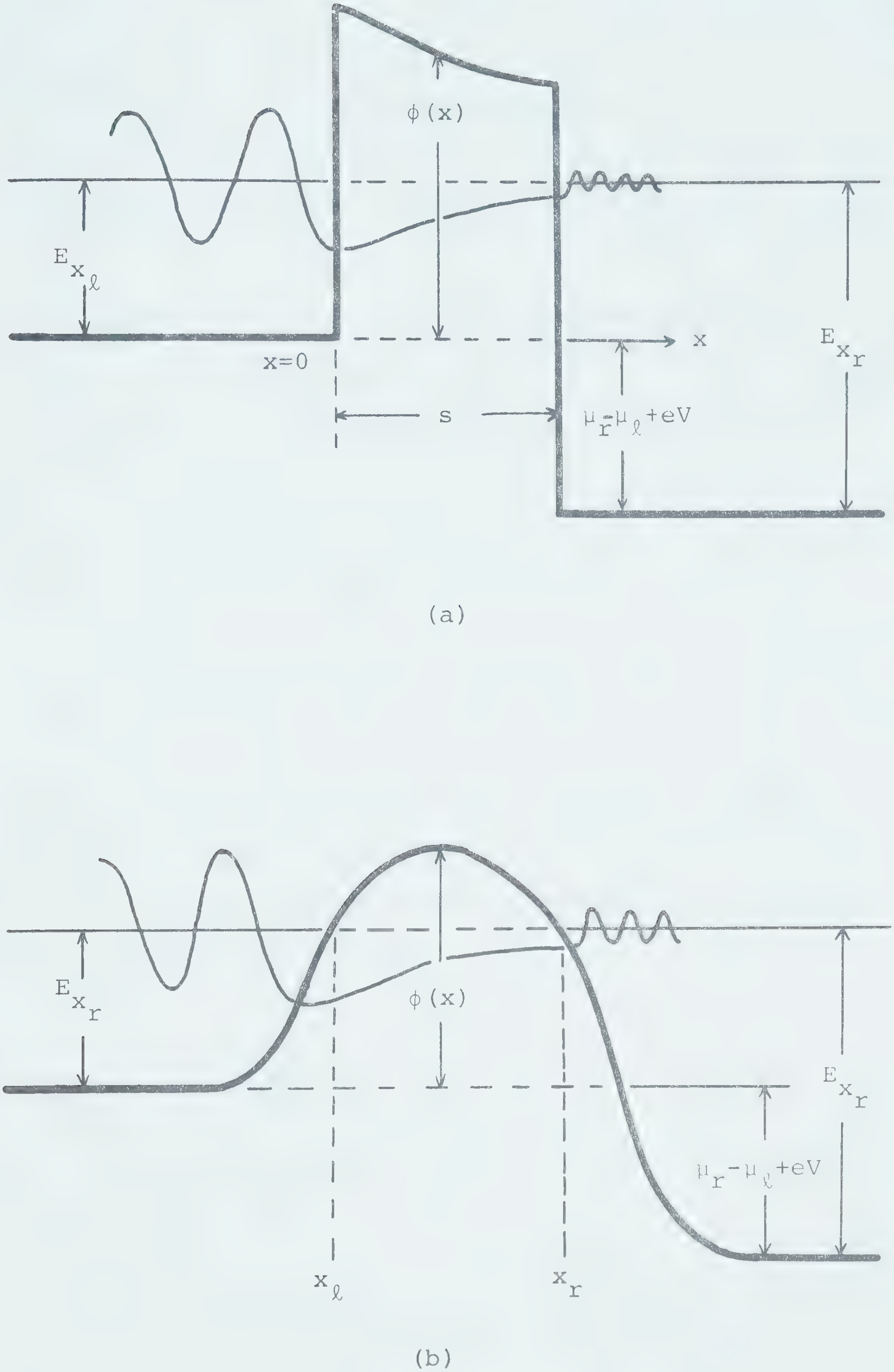
$\phi(x)$
E_{x_ℓ}
x
E_{x_r}
$x=0$
s
$\mu_r-\mu_\ell+eV$
(a)
E_{x_r}
$\phi(x)$
E_{x_r}
$\mu_r-\mu_\ell+eV$
x_ℓ
x_r
(b)

Fig. (2.2) Models of tunneling barrier.

wave functions within the barrier are

$$\frac{1}{\sqrt{\kappa(x)}} \exp(\pm\int_0^x \kappa(y)dy) \;, \quad \text{where} \quad \kappa^2(x) = \frac{2m}{\hbar^2} (\phi(x) - E_{x_\ell}) \;.$$

This approximation is justified provided that $\phi(x)$ varies sufficiently smoothly within the barrier. The conditions of smoothness on the potential may be obtained by simply substituting the wave function into the Schrodinger equation for the electron in the barrier. These conditions are simply

$$|\frac{1}{\kappa^2} \frac{d\kappa}{dx}| << 1 \qquad \text{and} \qquad |\frac{1}{\kappa^2} \frac{d^2\kappa}{dx^2}| << 1 \;.$$

If we proceed to match the wave functions and their derivatives at the walls of the barrier, we find that the transmission coefficient (the ratio of transmitted to incident particle flux) is given by the formula

$$P(E_{x_\ell}) = \frac{\dfrac{k_{x_\ell} k_{x_r}}{\kappa(0)\kappa(s)} e^{-2\int_0^s \kappa(x)dx}}{(1 + \dfrac{k_{x_\ell}^2}{\kappa^2(o)})(1 + \dfrac{k_{x_r}^2}{\kappa^2(s)})} \tag{2.17}$$

Consider the case where the barrier potential is constant (i.e. $\phi(x) = \phi_o$ = constant) and the bias is small. If the metals are similar so that $\mu_\ell = \mu_r$, Eqn. (2.17) becomes

$$P(E_x) = 16\left(\frac{E_x}{\phi_o}\right)\left(1-\frac{E_x}{\phi_o}\right) e^{-2s\sqrt{\frac{2m}{\hbar^2}(\phi_o - E_x)}} , \qquad (2.18)$$

which is just the probability for a particle to tunnel through a square barrier of height ϕ_o and width s (Davidov, 1965). The transmission probability depends exponentially on the width of the barrier as expected.

A more physical model of the oxide barrier with smooth walls is depicted in Fig. (2.2b). Unfortunately it is difficult to deal with such a model rigorously and therefore we again resort to the WKB approximation under the assumption that the potential is smooth enough. The WKB solutions are matched at the turning points x_ℓ and x_r. The transmission coefficient for such a case is given by Kemble (1937) and is discussed in detail by Miller and Good (1953). The result is simply

$$P(E_x) = e^{-2\int_{x_\ell}^{x_r} \kappa(x)dx} \qquad (2.19)$$

where x_ℓ and x_r are the turning points (i.e. $\kappa(x_\ell)=\kappa(x_r)=0$) and $\kappa(x)$ was defined in the previous model ($\kappa(x) = \sqrt{\frac{2m}{\hbar}(\phi(x)-E_x)}$). Because of its simplicity and ease of application, this approximation is frequently used in quantitative calculations of the tunneling current.

Although both models agree in their exponential dependence of the tunneling probability on the thickness and height of the oxide barrier, they differ with respect to their preexponential factors. The preexponential factors present in the model with sharp walls contain, in principle, information about the band structure and density of states of both metals. Harrison (1961) has calculated the transmission coefficient for a square barrier taking into account the structure of the metal lattice by also matching the Bloch parts of the electron wavefunction at the interface. He concludes that details of the lattice structure are also contained in the preexponential factors. However, experiments to date have not managed to confirm these details. The dependence of the tunneling probability on the details of the wavefunctions seems rather unrealistic when the boundaries are not ideal as one suspects in the case in tunneling junctions.

2.3 Magnitude and Angular Dependence of the Transmission Coefficient

In this section we shall estimate the magnitude of the transmission coefficient as well as its dependence upon the angle of incidence of the tunneling electron. Since the experiments are done at very low temperatures,

we shall make use of the current density given by Eqn. (2.16) for small bias and 0°K to relate the transmission coefficient to the resistance of the junction. We consider a typical junction with aluminum electrodes and a resistance of 50 ohms. From Eqn. (2.16) the tunneling current I is given by

$$I = \left(\frac{4\pi e^2 mAP_o\mu}{h^3}\right) V \quad , \tag{2.20}$$

where A is the effective tunneling area and P_o is a dimensionless quantity defined by

$$P_o = \frac{1}{\mu}\int_0^\mu P(E_x)dE_x \quad . \tag{2.21}$$

If the resistance of the tunnel junction is R, then from Eqn. (2.20), it follows that

$$P_o = \frac{h^3}{4\pi e^2 mA\mu R} \quad . \tag{2.22}$$

μ is the Fermi energy of aluminum and is approximately 11.6 electron volts. As mentioned previously the area common to the two metal films that make up the junction is approximately 1 mm^2. However, as we shall show in Chapter VI, tunneling occurs predominantly near the edges of the junction so that the effective tunneling area is probably of the order of 1% of the crossed strip area.

We take $A = 10^{-2}$ mm^2. Thus for a resistance of 50 ohms we find that $P_o \approx 10^{-9}$.

For convenience we choose a square well model with transmission probability given by Eqn. (2.18)

$$\text{i.e.}\quad P(E_x) = \frac{16E_x}{\phi_o}\left(1 - \frac{E_x}{\phi_o}\right) \exp\left(-2s \sqrt{\frac{2m}{\hbar^2}(\phi_o - E_x)}\right) .$$

Here ϕ_o is the height of the barrier relative to the bottom of the conduction band. The exponential factor will dominate $P(E_x)$ and we expect that tunneling will occur predominantly for those values of E_x which minimize the argument of the exponent. That is, tunneling will occur only for those values of E_x close to the Fermi energy μ. With this in mind we shall disregard the preexponential factors which are of order unity and write

$$P_o \simeq \frac{1}{\mu} \int_0^{\mu} e^{-2s\sqrt{\frac{2m}{\hbar^2}(\phi_o - E_x)}} \, dE_x \quad .$$

The integral is easily evaluated and gives the following result

$$P_o \simeq 2\left(\frac{\phi_o - \mu}{\mu}\right) \frac{(\gamma+1)e^{-\gamma}}{\gamma^2} \quad , \qquad (2.23)$$

where

$$\gamma = 2s \sqrt{\frac{2m}{\hbar^2}(\phi_o - \mu)} \quad .$$

If we take the barrier height to be one electron volt above the Fermi level, we can solve Eqn. (2.23) for γ. We obtain $e^{-\gamma} \approx 10^{-7}$ and this is simply the transmission coefficient for an electron at Fermi energy tunneling normal to the barrier.

Consider now an electron of wave vector $\underline{k}$ incident on the barrier such that θ is the angle between $\underline{k}$ and the normal barrier. Then the x-component of $\underline{k}$ is given in terms of the Fermi wave number k_f by $k_x = k_f \cos\theta$. Thus

$$E_x = \frac{\hbar^2 k_f^2}{2m} \cos^2\theta = \mu \cos^2\theta$$

and we can write down the transmission coefficient in terms of the angle of incidence

$$\text{i.e.}\quad P(\theta) \approx e^{-2s\sqrt{\frac{2m}{\hbar^2}(\phi_o - \mu\cos^2\theta)}} = e^{-\gamma\sqrt{\frac{\phi_o - \mu\cos^2\theta}{\phi_o - \mu}}} \quad .$$

If we define $\theta_{\frac{1}{2}}$ as the angle at which the transmission coefficient $P(\theta)$ reaches ½ its value at $\theta = 0$, then

$$\tfrac{1}{2} = \frac{\exp - \sqrt{\frac{\phi_o - \mu\cos^2\theta_{\frac{1}{2}}}{\phi_o - \mu}}}{\exp(-\gamma)} \quad .$$

This has the solution

$$\sin^2\theta_{\frac{1}{2}} \approx \frac{2(\phi_o - \mu)}{\mu} \frac{\mathrm{Ln}(\frac{1}{2})}{\gamma}$$

and for $\phi_o - \mu = 1$ eV, we obtain $\theta_{\frac{1}{2}} \approx 5°$. It follows then that tunneling is confined predominantly to those electrons which have velocity nearly normal to the barrier.

2.4 Nonlinear Characteristics of Tunnel Junctions Due to Barrier Dependence

Although the tunneling current is generally found to be very nearly ohmic for low bias, this is certainly not the case for high bias. A typical example is given in Fig. (2.3) where the I-V characteristic of an Al-Al_2O_3-Al junction is displayed. At voltages comparable to the barrier height, the transmission probability will become a strong function of bias and thus contribute nonlinear terms to the tunneling current. Unfortunately even at the low voltages that shall concern us in the treatment of the zero-bias-anomalies this gross nonlinear background is still in evidence. Therefore, we briefly consider the effects of the bias dependence of the barrier in order that we may separate it from other processes occurring in the junction.

We start with the basic expression given by Eqn. (2.13) for the current density. However, as we saw in the last section, the current flow across the barrier is

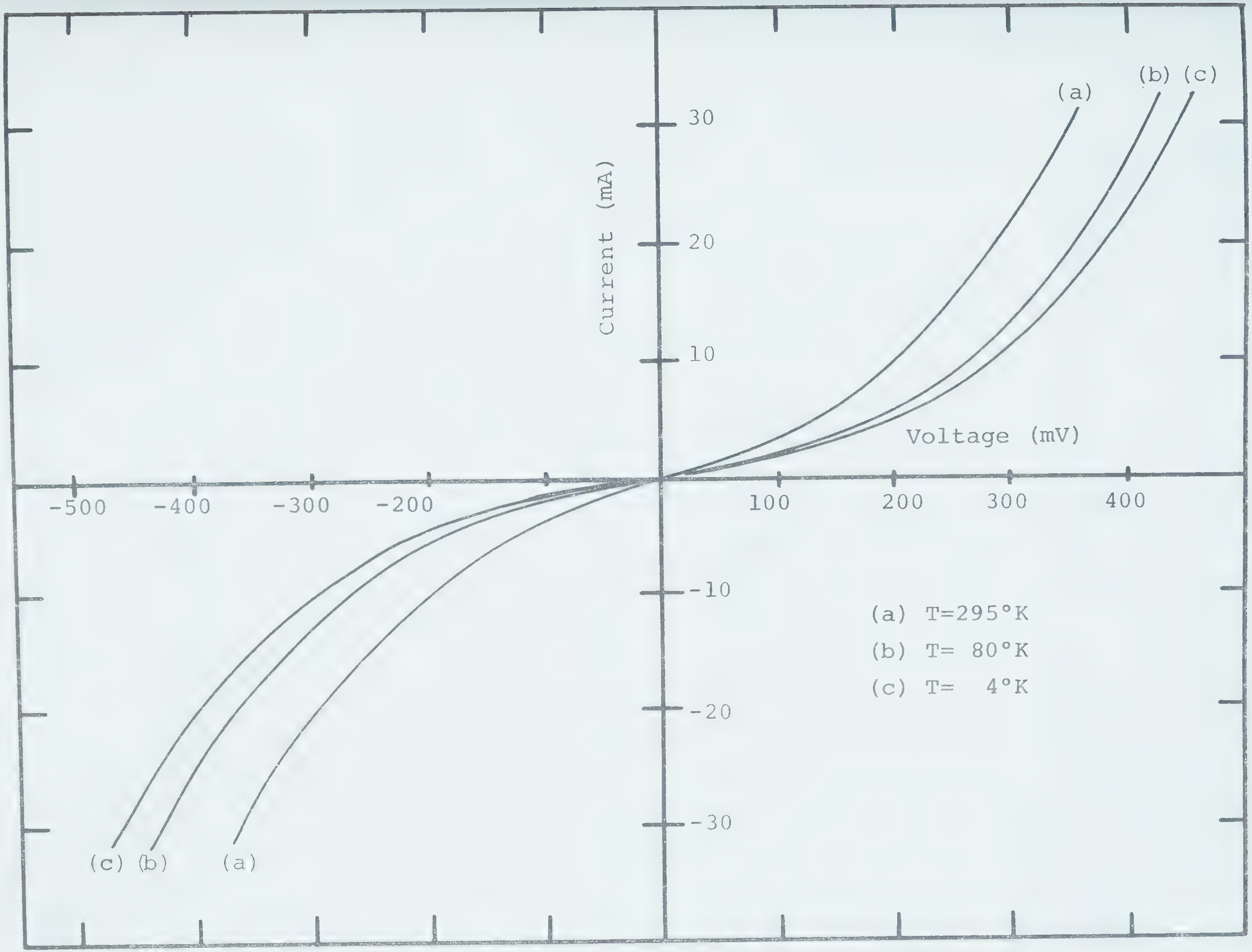

Fig. (2.3) I-V curves for an Al-Al_2O_3-Al tunnel junctions.

predominantly due to electrons whose velocity is almost normal to the barrier. Therefore it is convenient to use the variable $\varepsilon = \mu - E_x$ which is very small compared to the Fermi energy. The current density is now given by

$$J = \frac{4\pi em}{h^3} \int_{-\mu}^{\infty} P(\varepsilon)N(\varepsilon)d\varepsilon \qquad (2.24)$$

where

$$N(\varepsilon) = k_BT \, \mathrm{Ln} \left[\frac{1 + e^{\varepsilon/k_BT}}{1 + e^{\varepsilon - eV/k_BT}}\right] \quad . \qquad (2.25)$$

Following the work of Stratton (1962) we use the WKB approximation for the transition probability given by Eqn. (2.19).

i.e. $P(\varepsilon) = \exp\left[-\alpha\int_{x_1}^{x_2} [\phi(x,V) - \mu + \varepsilon]^{\frac{1}{2}} dx\right]$

where

$$\alpha = 2\left(\frac{2m}{\hbar^2}\right)^{\frac{1}{2}} .$$

We expand the argument of the exponent in $P(\varepsilon)$ in a Taylor's series for small ε and retain only the terms linear in ε. Thus we have

$$P(\varepsilon) = \exp[-b(V)-c(V)\varepsilon] \qquad (2.26)$$

where the bias dependent constants b and c are defined by

$$b(V) = \alpha \int_{x_1}^{x_2} [\phi(x,V) - \mu]^{\frac{1}{2}}\, dx \quad ,$$
$$c(V) = \frac{\alpha}{2} \int_{x_1}^{x_2} [\phi(x,V) - \mu]^{-\frac{1}{2}}\, dx \quad . \tag{2.27}$$

Eqn. (2.24) for the current density now becomes

$$J = \frac{4\pi e m k_B T}{h^3} \int_{-\infty}^{+\infty} \mathrm{Ln}\left(\frac{1 + e^{\varepsilon/k_B T}}{1 + e^{\varepsilon - eV/k_B T}}\right) \cdot e^{-b-c\varepsilon}\, d\varepsilon \quad . \tag{2.28}$$

It is possible to do the above integral in closed form with the aid of the substitution

$$z = e^{\varepsilon/k_B T}$$

and the result is

$$J = \frac{4\pi e m}{h^3 c^2} \left(\frac{\pi c k_B T}{\sin(\pi c k_B T)}\right) e^{-b} \{1 - e^{-ceV}\} \quad . \tag{2.29}$$

At a given voltage the temperature dependence of the current is then given by

$$\frac{I(V,T)}{I(V,T=0)} = \frac{\pi c k_B T}{\sin(\pi c k_B T)} \simeq 1 + \frac{1}{6} (\pi c k_B T)^2 \quad . \tag{2.30}$$

For 0°K and small bias we note that

$$I = \frac{4\pi e^2 mAe^{-b}}{h^3 c} V \quad . \qquad (2.31)$$

Thus from Eqn. (2.20) we obtain

$$P_o = \frac{e^{-b}}{\mu c} \quad . \qquad (2.32)$$

For a square barrier one can confirm from the definitions of b and c given by Eqn. (2.27) that Eqn. (2.32) for P_o is identical to that of Eqn. (2.23), where $\gamma = b$. If we use the estimates made of $e^{-\gamma}$ and P_o in the previous section, we can estimate the magnitude of c and hence deduce the temperature dependence of the current

$$\text{i.e.} \quad c = \frac{e^{-\gamma}}{P_o \mu} \approx \frac{10^{-7}}{10^{-9}\mu} \approx \frac{100}{\mu} \quad .$$

Hence

$$\frac{I(V,T)}{I(V,T=0)} \approx 1 + \frac{1}{6}\left(\frac{100\pi k_B T}{\mu}\right)^2 \quad .$$

Since $k_B \approx .086$ meV/°K and $\mu \approx 11.6$ eV, the temperature factor becomes appreciable only at room temperature and can be disregarded at low temperatures. This crude estimate is somewhat justified by the I-V curves in Fig. (2.3).

Stratton (1962) has shown that Eqn. (2.29) may be simplified further by expanding b(V) and c(V) in a power

series in V. He obtains the power series expansion for the current

$$I = \sigma_o V + \sigma_1 V^2 + \sigma_2 V^3 + \ldots.$$

where σ_o is the zero bias conductance and σ_1, σ_2, ... are constants that depend upon the geometry of the barrier at zero bias. He further shows that the even terms in this expansion are zero if the barrier is symmetric and one has then $I(V) = -I(-V)$. However, for asymmetric barriers, he points out that this is no longer the case and asymmetry in the conductance curves is possible. One finds experimentally that this is the rule rather than the exception. Both Rowell (1969) and Hartman (1964) have discussed tunneling through asymmetric barriers.

We can summarize this section by saying that the ideal current through a junction should be very weakly temperature dependent at low temperatures, and it should be ohmic at small bias with a small amount of deviation present from the non-linear terms.

2.5 Perturbation Formulation of Tunneling

Up to this point the phenomenon of tunneling in simple normal metals has been described as the transmission of electron waves through the oxide barrier. In this regard the theory appears to explain the experimental details. It was found necessary to take a somewhat different approach to explain the observed results in superconductive tunneling. This alternative approach, advanced by Bardeen (1961), is based on time-dependent perturbation theory. The tunneling process is regarded as a transition of an electron across the oxide with the barrier itself acting as the perturbing potential. The electron (or quasi-particle in the case of a superconductor) densities of states then enter the problem explicitly and this is essential to explain the experimental results in the case of superconductive tunneling.

It is not difficult to see that this is a valid description. We first imagine, as in Fig. (2.4a), an unperturbed system of two metals separated by a sufficiently thick oxide layer that no tunneling occurs. The total Hamiltonian for the system then contains one term, H_ℓ, which describes the left hand metal, and a term H_r, which describes the right hand metal. Each of these has a one-electron series of eigenstates. Let us denote one of the eigenstates in the left hand metal as

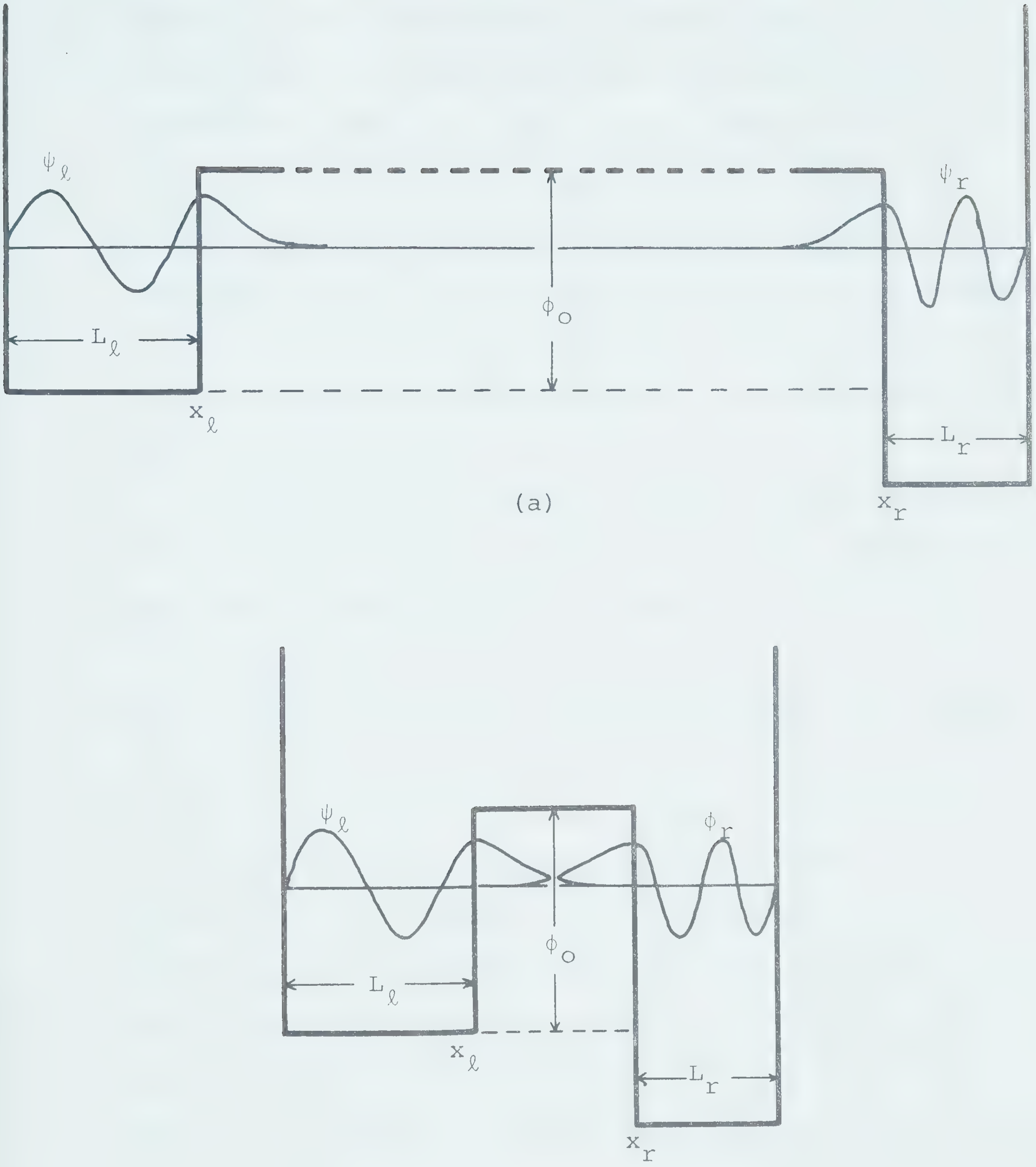
ψ_ℓ
ψ_r
ϕ_o
L_ℓ
x_ℓ
L_r
x_r
ψ_ℓ
ϕ_r
ϕ_o
L_ℓ
x_ℓ
L_r
x_r

(a)

(b)

Fig. (2.4) Transfer Hamiltonian model.

ψ_ℓ and one on the right as ψ_r. These states are constructed to decay exponentially into the oxide. If we now decrease the oxide thickness to the point where tunneling is possible, (Fig. (2.4b)) then ψ_r and ψ_ℓ will overlap. We may now seek a modified solution to the time dependent Schrödinger equation by taking linear combinations of ψ_ℓ and ψ_r. The transition matrix element of the Hamiltonian between states ψ_ℓ and ψ_r can then be evaluated using the usual methods of time-dependent perturbation theory.

Bardeen (1961) showed, by following this prescription, that the transition matrix element $M_{\ell r}$ between the normalized states ψ_ℓ and ψ_r is given by

$$M_{\ell r} = - \frac{\hbar^2}{2m} \int_S \{\psi_\ell^*(\underline{x}) \nabla \psi_r(\underline{x}) - \psi_r(\underline{x}) \nabla \psi_\ell^*(\underline{x})\}.d\underline{S} \quad . \tag{2.33}$$

The integral is evaluated over a lamina S parallel to, and within the barrier separating the two metals. Knowing the matrix element for tunneling between the two states, we can immediately write down (using the Fermi "golden rule" of first order time-dependent perturbation theory) the transition rate $T_{\ell \to r}$ for an electron in state ψ_ℓ to tunnel into the right hand metal

i.e. $$T_{\ell \to r} = \frac{2\pi}{\hbar} \sum_r |M_{\ell r}|^2 \, \delta(E_\ell - E_r) \quad . \tag{2.34}$$

Consider, for example, the case of a rectangular system where the left hand metal is represented by a potential well of width L_ℓ (the thickness of the metal film) and the oxide barrier is of constant height ϕ_o above the bottom of the band. The boundaries of the metal are denoted by coordinates $x_\ell - L_\ell$ and x_ℓ as in Fig. (2.4a). A simple calculation such as is given in Schiff (1955) shows that the normalized eigenstates of such a system are given by

$$\psi_{\underline{k}_\ell}(\underline{x}) = \left(\frac{2}{AL_\ell}\right)^{\frac{1}{2}} e^{i\underline{k}_{||}\cdot\underline{x}_{||}} \sin[k_x(x-x_\ell)+\beta], \quad x_\ell - L_\ell < x < x_\ell$$

$$= \left(\frac{2}{AL_\ell(\kappa_\ell^2 + k_{x_\ell}^2)}\right)^{\frac{1}{2}} k_{x_\ell} e^{i\underline{k}_{||}\cdot\underline{x}_{||}} e^{-\kappa_\ell(x-x_\ell)}, \quad x_\ell < x \tag{2.35}$$

where β is some constant phase, while the energy of the state is given by

$$E_{\underline{k}_\ell} = \frac{\hbar^2}{2m}(k_{x_\ell}^2 + \underline{k}_{||}^2) \tag{2.36}$$

relative to the bottom of the band. κ_ℓ is defined by

$$\kappa_\ell^2 = \frac{2m}{\hbar^2}[\phi_o - E_{x_\ell}], \quad \text{where} \quad E_{x_\ell} = \frac{\hbar^2 k_{x_\ell}^2}{2m} . \tag{2.37}$$

The factors in front of the wavefunction are determined by the requirements of normalization and the continuity of the wavefunction at the metal-oxide interface. For the parallel part of the wavefunction, $e^{i\underline{k}_{||}\cdot\underline{x}_{||}}$, we have

chosen to impose cyclic boundary conditions and normalization over an area A parallel to the barrier. The normalization of the x-part of the wavefunction can be restricted to the well since the thickness of the metal films is much greater than the penetration depth of the wavefunction into the oxide. The wavefunction can then be characterized by the spectrum

$$\underline{k}_\ell = \left(\frac{\pi n_{x_\ell}}{L_\ell} , \frac{2\pi n_{y_\ell}}{\sqrt{A}} , \frac{2\pi n_{z_\ell}}{\sqrt{A}} \right) \tag{2.38}$$

where n_{x_ℓ}, n_{y_ℓ} and n_{z_ℓ} take on integral values. In a completely analogous fashion, we can write down the wavefunction ψ_r which decays into the oxide from the right hand metal.

The matrix element between states $\underline{k}_\ell$ and $\underline{k}_r$, which is just the overlap integral in Eqn. (2.33), is then given by

$$M_{\underline{k}_\ell \underline{k}_r} = - \frac{\hbar^2}{2m} \delta_{\underline{k}_{||_\ell}, \underline{k}_{||_r}} \cdot \frac{4 k_{x_\ell} k_{x_r} \kappa}{\{ L_\ell L_r (\kappa^2 + \kappa_{x_\ell}^2)(\kappa^2 + \kappa_{x_r}^2)\}^{\frac{1}{2}}} e^{-\kappa (x_r - x_\ell)} \tag{2.39}$$

The conservation of parallel momentum demonstrated in the delta-function is due to the overlap integral in Eqn. (2.33), and we have imposed conservation of energy so that $\kappa_\ell = \kappa_r = \kappa$. If the bottoms of the bands are

separated by an energy E_o, then

$$E_{x_r} = \frac{\hbar^2 k_{x_r}^2}{2m} = E_o + E_{x_\ell} . \qquad (2.40)$$

Since $x_r - x_\ell = s$ (the oxide thickness), the square of the matrix element may be expressed in terms of the transmission coefficient as defined by Eqn. (2.17)

i.e. $$|M_{\underline{k}_\ell \underline{k}_r}|^2 = \left(\frac{\hbar^2}{2m}\right)^2 \delta_{\underline{k}_{||_\ell}, \underline{k}_{||_r}} P(E_{x_\ell}) \frac{k_{x_\ell} k_{x_r}}{L_\ell L_r} . \qquad (2.41)$$

This may further be expressed in terms of the one dimensional density of states normal to the barrier (i.e. the number of k_{x_ℓ} states per unit energy range). According to Eqn. (2.38) the density of states (which we denote by $\rho_{\underline{k}_\ell}$) is given by

$$\rho_{\underline{k}_\ell} = \frac{L_\ell}{\pi} \left(\frac{\partial E_{\underline{k}_\ell}}{\partial k_{x_\ell}}\right)^{-1} = \frac{1}{2\pi} \left(\frac{2m}{\hbar^2}\right) \frac{L_\ell}{k_{x_\ell}} . \qquad (2.42)$$

Thus the square of the matrix element now becomes

$$|M_{\underline{k}_\ell \underline{k}_r}|^2 = \frac{1}{4\pi^2} \delta_{\underline{k}_{||_\ell} k_{||_r}} \frac{P(E_{x_\ell})}{\rho_{\underline{k}_\ell} \rho_{\underline{k}_r}} . \qquad (2.43)$$

This result, although derived for the case of a square barrier, holds in general for arbitrary barriers such as the WKB type (Harrison (1961)).

We may now proceed to calculate the transition rate $T_{\ell\to r}$ using Eqn. (2.34). First we must modify this equation by inserting the statistical factor $f^o_{\underline{k}_\ell}(1 - f^o_{\underline{k}_r})$ into the summation to ensure that there is a state $\underline{k}_\ell$ available to make a transition into a state $\underline{k}_r$ which is vacant. Thus

$$T_{\underline{k}_\ell\to r} = \frac{2\pi}{\hbar}\sum_{\underline{k}_r} |M_{\underline{k}_\ell\underline{k}_r}|^2\, f^o_{\underline{k}_\ell}(1 - f^o_{\underline{k}_r})\,\delta(E_{\underline{k}_\ell} - E_{\underline{k}_r}) . \quad (2.44)$$

To this we must add the transition probability of the reverse process (i.e. $\underline{k}_\ell$ may be filled by a state from the right). Thus

$$T_{\underline{k}_\ell\leftarrow r} = -\frac{2\pi}{\hbar}\sum_{\underline{k}_r} |M_{\underline{k}_r\underline{k}_\ell}|^2\, f^o_{\underline{k}_\ell}(1 - f^o_{\underline{k}_r})\,\delta(E_{\underline{k}_\ell} - E_{\underline{k}_r}) . \quad (2.45)$$

The total transition rate is then

$$T_{\underline{k}_\ell} = \frac{2\pi}{\hbar}\sum_{\underline{k}_r} |M_{\underline{k}_\ell\underline{k}_r}|^2\, (f^o_{\underline{k}_\ell} - f^o_{\underline{k}_r})\,\delta(E_{\underline{k}_\ell} - E_{\underline{k}_r}) \quad . \quad (2.46)$$

The summation over $\underline{k}_{||_r}$ is done using the momentum conserving delta function in the matrix element while the summation over k_{x_r} is carried out by using the density of states and the energy conserving delta function. The result is

$$T_{\underline{k}_\ell} = \frac{1}{2\pi\hbar}\,\frac{P(E_{x_\ell})}{\rho_{\underline{k}_\ell}}\,(f^o_{\underline{k}_\ell} - f^o_{\underline{k}_r}) \quad . \quad (2.47)$$

If we use Eqn. (2.42) for the density of states and remember that the x-component of electron velocity is $v_{x_\ell} = \hbar k_{x_\ell}/m$, then we see that

$$T_{\underline{k}_\ell} = \frac{v_x P(E_{x_\ell})}{2L_\ell} (f^o_{\underline{k}_\ell} - f^o_{\underline{k}_r}) \quad . \qquad (2.48)$$

This result is exactly what we expect since the transition probability per unit time for an electron on the left to tunnel into the right is just the number of times it strikes the barrier per unit time $(v_{x_\ell}/2L_\ell)$ multiplied by the transmission probability on each approach.

The current across the barrier is just given by

$$I = 2e \sum_{\underline{k}_\ell} T_{\underline{k}_\ell} = \frac{2eA}{(2\pi)^2} \iint d\underline{k}_{||_\ell} \int dE_{\underline{k}_\ell} \rho_{\underline{k}_\ell} T_{\underline{k}_\ell} \quad . \qquad (2.49)$$

We use Eqn. (2.47) for $T_{\underline{k}_\ell}$ and remember that $E_{\underline{k}_\ell} = E_{x_\ell} + \hbar^2 k_{||}^2/2m$ to write I in the form

$$I = \frac{4\pi emA}{h^3} \int_0^\infty dE[f^o(E - \mu_\ell) - f^o(E - \mu_\ell + eV)] \int_0^\infty P(E_x) dE_x \; .$$

This is the same result for the tunneling current as we obtained in the one-electron picture in section 2.1. We note the conspicuous absence of the density of states

factors in the above result. This comes about simply because the square of the matrix element is proportional to the particle velocities [Eqn. (2.41)] or inversely proportional to the densities of states [Eqn. (2.43)]. In the case of super-conductive tunneling it will be necessary to take $|M_{\ell r}|^2$ as being constant.

CHAPTER III

THE ZERO BIAS ANOMALY

3.1 Nonequilibrium Tunneling

We noted in the last chapter (Eqn. (2.48)) that the transition rate for tunneling was given by

$$T \sim \frac{v_x P(E_x)}{2L} \quad .$$

This can be interpreted as the inverse of the time, τ_B, that it takes an electron to decide to make a transition through the oxide. Since tunneling occurs predominantly at directions normal to the barrier we can use as estimates for v_x the Fermi velocity v_f which is of the order of 10^8 cm/sec in typical metals. We saw in Section 2.3 that at the Fermi energy μ, $P(\mu) \approx 10^{-7}$. Taking the width of the metal film as $L \approx 2000$ Å, we obtain the estimate

$$\tau_B = \frac{1}{T} \sim 10^{-6} \text{ seconds} \quad . \tag{3.1}$$

In conventional treatments of the tunneling process it is always assumed that the metal electrodes are in their equilibrium state. This is accounted for by using the equilibrium Fermi-Dirac distribution functions f^o. However, it is obvious that this is not exactly the case. When an electron tunnels into the opposite metal it does

so by conserving energy and therefore finds itself at some energy above the Fermi level in the metal it has tunneled into. The electron is thus in an excited non-equilibrium state and will rapidly thermalize to the Fermi level by a number of possible relaxation processes present in the host metal. By using the equilibrium distribution functions in tunneling calculations it is then implicitly assumed that the excited state decays immediately or has a zero relaxation time. Nevertheless, for a short time, the electron is in an excited non-equilibrium state, the short time being characteristic of the relaxation times in the metal. While it is in this excited state, it will prevent any other electrons from tunneling into that same state by virtue of the Pauli exclusion principle, thereby effectively "blocking" that state for a short time.

Consider the situation if the relaxation times in the metal were of the order of the tunneling times, that is, of the order of 10^{-6} seconds. We would then expect the electrons that occupy the excited states, by virtue of their long life times, to strongly block or impede any electrons that want to tunnel into the same states. This situation would manifest itself by a strong decrease in conductance of the tunnel junction. In typical normal metals, relaxation times are of the order of 10^{-9} to 10^{-11} seconds at liquid He^4 temperatures.

Therefore we would expect to see deviations in conductance due to such blocking effects to be of the order of the ratio of the relaxation times to the tunneling times, that is to one part in 10^{+3}— 10^{+5}. Small changes in conductance such as these could easily be seen experimentally by using the derivative measurement techniques outlined in Section 1.3 which are capable of resolving changes in tunnel junction conductance to one part in 10^{+5}.

To illustrate this idea in more detail, we shall briefly consider only the interaction of the electron with the lattice. It is well known (Wilkins (1968)) that the relaxation time of an excited electron in an electron-phonon gas decreases as the excitation energy of the electron above the Fermi level increases. Consider the situation at 0°K where the Fermi levels are perfectly sharp. If our junction is biased by only a small amount, the tunneling electrons that are injected into the metal have low excitation energies above the Fermi surface, therefore their life times are relatively long and thus we expect to see the minimum conductance. As we increase the bias we increase the energy of the injected electrons above the Fermi level thus decreasing the effective relaxation time. Since the tunneling times remain essentially constant within the bias energy range we would then expect to see an increase in conductance.

Qualitatively then, an effect of this sort should manifest itself as a small dip in conductance of the order of one part in 10^{+3} to 10^{+5} and a few millivolts wide (since this is typically the order of the Debye energy). Small conductance minima with this behavior near zero bias have been seen experimentally in a number of tunnel junctions by Chen and Adler (1970) and others (see for example: Rowell, McMillan and Feldmann (1968)). In what follows, we shall attempt to justify this effect theoretically and compare it with experiment.

To treat the blocking effect quantitatively, we take the point of view that the distribution functions to be used in the tunneling current are steady state rather than equilibrium. We use a transport model based on the Boltzmann equation to find the steady state distribution functions and thus their deviations from equilibrium. The model is illustrated in Fig. (3.1) and to avoid cumbersome notation we simply refer to quantities on the right with a prime.

The rate of change of occupation $f_{\underline{k}'}$ of a state $\underline{k}'$ on the right is due to the following processes:

(1) Electrons in states $\underline{k}$ on the left can tunnel into $\underline{k}'$ on the right ((a) of Fig. (3.1)). This process serves to increase $f_{\underline{k}'}$ and the rate of change of $f_{\underline{k}'}$ is just the transition rate given by Eqn. (2.44).

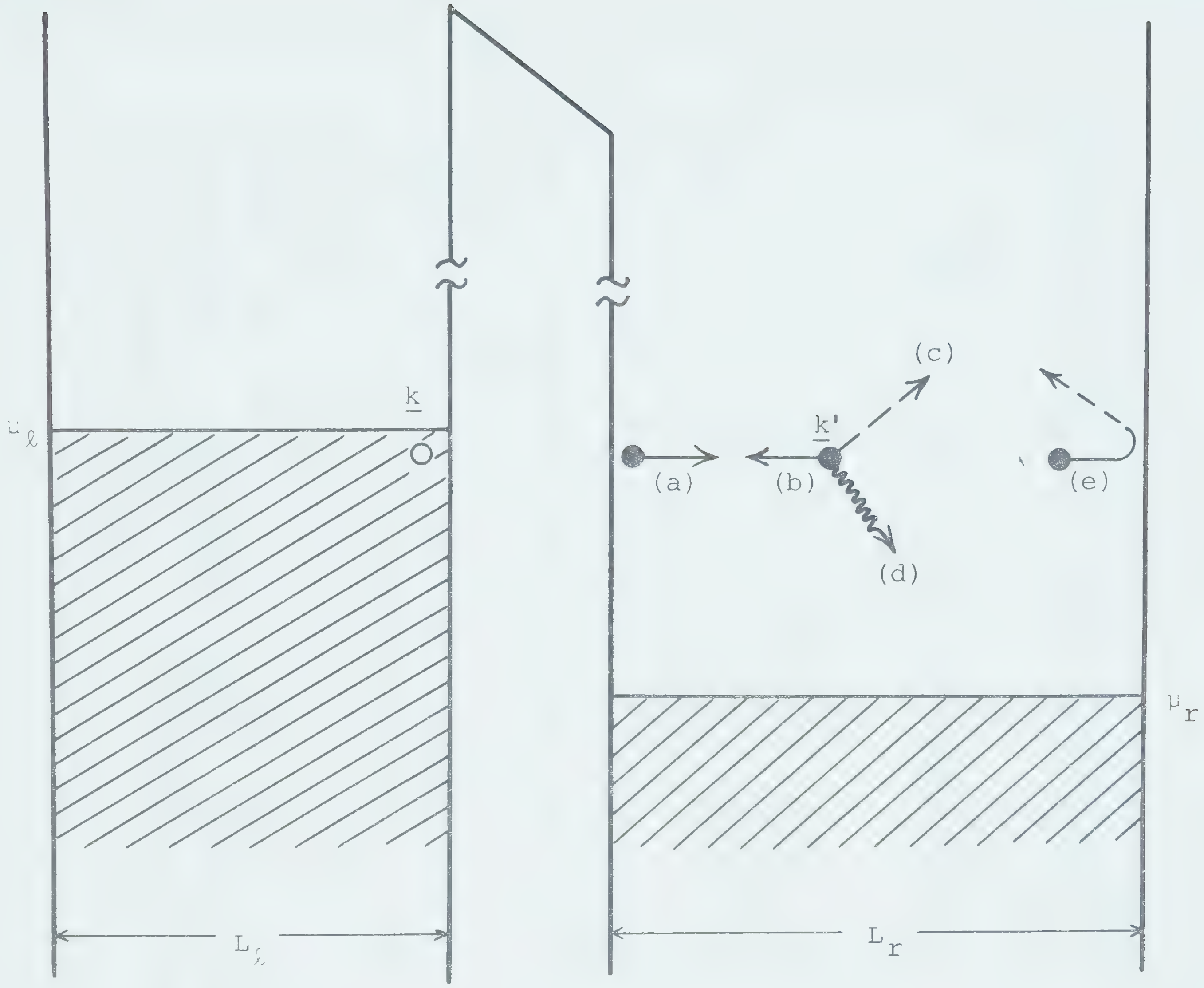
μ_ℓ
$\underline{k}$
$\underline{k}'$
(a)
(b)
(c)
(d)
(e)
μ_r
L_ℓ
L_r

Fig. (3.1) Schematic diagram of scattering processes described in text.

i.e. $$\left.\frac{\partial f_{\underline{k}'}}{\partial t}\right|_{\ell\to r} = \frac{2\pi}{\hbar}\sum_{\underline{k}} |M_{\underline{k}\underline{k}'}|^2 \; f_{\underline{k}}(1 - f_{\underline{k}'})\,\delta(E_{\underline{k}} - E_{\underline{k}'}) \quad . \tag{3.2}$$

(2) Electrons can leave the state $\underline{k}'$ by tunneling into the left as in (b) of Fig. (3.1). Thus

$$\left.\frac{\partial f_{\underline{k}'}}{\partial t}\right|_{r\to\ell} = -\frac{2\pi}{\hbar}\sum_{\underline{k}} |M_{\underline{k}\underline{k}'}|^2 \; f_{\underline{k}'}(1-f_{\underline{k}})\,\delta(E_{\underline{k}} - E_{\underline{k}'}) \quad . \tag{3.3}$$

(3) Electrons may be scattered out of $\underline{k}$ by various mechanisms. For instance, inelastic scattering with emission or absorption of a lattice phonon as in (d) of Fig.(3.1) will alter both the electron's energy and momentum. Elastic scattering by impurities and lattice defects (c) as well as non-specular boundary scattering (e) will change the electrons momentum. We must remember that we have normalized the electrons to a box of thickness L so that specular scattering at the sides is implicitly assumed. We shall account for these scattering processes by introducing a relaxation time $\tau_{\underline{k}'}$, which in general will be energy, momentum, and temperature dependent. Thus we shall assume that

$$\left.\frac{\partial f_{\underline{k}'}}{\partial t}\right|_{\text{scatt.}} = -\frac{\Delta f_{\underline{k}'}}{\tau_{\underline{k}'}} \quad , \tag{3.4}$$

where $\Delta f_{\underline{k}'}$ is the departure of $f_{\underline{k}'}$ from equilibrium. That is;

$$f_{\underline{k}'} = f^{o}_{\underline{k}'} + \Delta f_{\underline{k}'} \quad , \qquad (3.5)$$

where $f^{o}_{\underline{k}'}$ is the equilibrium Fermi-Dirac distribution function. Thus if we were to turn off the tunneling process any out of equilibrium $\Delta f_{\underline{k}'}$ would decay to zero according to

$$\Delta f_{\underline{k}'}(t) = \Delta f_{\underline{k}'}(0)\, e^{-t/\tau_{\underline{k}'}} \quad .$$

We shall discuss the relaxation times $\tau_{\underline{k}'}$ and shall justify Eqn. (3.4) in the next section.

At steady state, Boltzmann's equation simply says that the net rate of change of $f_{\underline{k}'}$ is zero for any value of $\underline{k}'$. That is;

$$\frac{\partial f_{\underline{k}'}}{\partial t} = \left.\frac{\partial f_{\underline{k}'}}{\partial t}\right|_{\ell\to r} + \left.\frac{\partial f_{\underline{k}'}}{\partial t}\right|_{\ell\leftarrow r} + \left.\frac{\partial f_{\underline{k}'}}{\partial t}\right|_{\text{scatt.}} = 0 \quad . \qquad (3.6)$$

If we substitute the relevant quantities into Eqn. (3.6) we obtain the equation

$$\frac{\Delta f_{\underline{k}'}}{\tau_{k'}} = \frac{2\pi}{\hbar} \sum_{\underline{k}} |M_{\underline{kk}'}|^2 (f_{\underline{k}} - f_{\underline{k}'})\,\delta(E_{\underline{k}} - E_{\underline{k}'}) \quad , \qquad (3.7)$$

which simply says that the rate at which electrons tunnel

into state $\underline{k}'$ is equal to the rate at which $\underline{k}'$ relaxes. A similar equation may be immediately written, by symmetry, for a state $\underline{k}$ in the left hand side. That is;

$$\frac{\Delta f_{\underline{k}}}{\tau_{\underline{k}}} = \frac{2\pi}{\hbar} \sum_{\underline{k}'} |M_{\underline{kk}'}|^2 (f_{\underline{k}'} - f_{\underline{k}}) \delta(E_{\underline{k}} - E_{\underline{k}'}) \qquad (3.8)$$

which just expresses the particle-hole symmetry of the problem. Eqns. (3.7) and (3.8) may be reduced by carrying out the summations as in Eqn. (2.47). We obtain

$$\frac{\Delta f_{\underline{k}'}}{\tau_{\underline{k}'}} = \frac{2\pi}{\hbar} \rho_{\underline{k}} |M|^2 (f_{\underline{k}} - f_{\underline{k}'}) \quad ,$$

$$\frac{\Delta f_{\underline{k}}}{\tau_{\underline{k}}} = \frac{2\pi}{\hbar} \rho_{\underline{k}'} |M|^2 (f_{\underline{k}'} - f_{\underline{k}}) \quad , \qquad (3.9)$$

where

$$|M|^2 = \frac{1}{4\pi^2} \frac{P(E_x)}{\rho_{\underline{k}}\rho_{\underline{k}'}} \quad . \qquad (3.10)$$

Making the substitutions $f_{\underline{k}} = f^o_{\underline{k}} + \Delta f_{\underline{k}}$ and $f_{\underline{k}'} = f^o_{\underline{k}'} + \Delta f_{\underline{k}'}$, we are able to solve Eqns. (3.9) algebraically to obtain the difference of steady state distribution functions, $f_{\underline{k}} - f_{\underline{k}'}$, which we shall use to determine the tunneling current. The result is given by

$$f_{\underline{k}} - f_{\underline{k}'} = \frac{f^o_{\underline{k}} - f^o_{\underline{k}'}}{1 + \frac{2\pi}{\hbar}|M|^2 \{\rho_{\underline{k}}\tau_{\underline{k}'} + \rho_{\underline{k}'}\tau_{\underline{k}}\}} \quad . \qquad (3.11)$$

Consider the term

$$\frac{2\pi}{\hbar} |M|^2 \rho_{\underline{k}}$$

appearing in the denominator of Eqn. (3.11). Using the definition given by Eqn. (3.10) and expressing the density of states in terms of the x-component of velocity, we have

$$\frac{2\pi}{\hbar} |M|^2 \rho_{\underline{k}} = \frac{1}{2\pi\hbar} \frac{P(E_x)}{\rho_{\underline{k}'}} = \frac{v_x' P(E_x)}{2L'}$$

$$= \frac{1}{\tau_B'} \qquad (3.12)$$

where τ_B' is just the tunneling time for an electron in the right hand metal. Eqn. (3.11) may now be rewritten as

$$f_{\underline{k}} - f_{\underline{k}'} = \frac{f^o_{\underline{k}} - f^o_{\underline{k}'}}{1 + \frac{\tau_{\underline{k}'}}{\tau_B'} + \frac{\tau_{\underline{k}}}{\tau_B}} \quad . \qquad (3.13)$$

Since the tunneling current is proportional to $f_{\underline{k}} - f_{\underline{k}'}$, we can see from Eqn. (3.13) that the deviation from the ideal current will be of the order of $\tau_{\underline{k}}/\tau_B$, the ratio of relaxation times in the metal to tunneling times. We now turn to a discussion of the relaxation times and their behavior with temperature and energy.

3.2 Relaxation Times

We shall describe the scattering due to lattice defects, impurities or non-specular boundary scattering by a constant relaxation time τ_i. We suspect these processes are elastic in nature and should therefore be temperature and energy independent. Since we lack detailed data about the structure or impurity composition of the evaporated metallic films that make up the tunnel junctions, we make no a priori estimates of τ_i except to say that it is probably comparable to the electron-phonon relaxation time in order of magnitude. We shall therefore treat τ_i as a constant to be extracted, if possible, from our model.

In contrast, we expect that the electron-phonon relaxation times will be sensitive functions of both excitation energy and temperature. The reasons are statistical in nature. At 0°K, an increase in the energy of an excited state means an increase in the number of empty states that it may make a transition into. Therefore the probability of a transition increases while the relaxation time decreases. An increase in temperature will smear the Fermi level and increase the number of states. Therefore we also expect the relaxation time to decrease with increasing temperature. The phonons, obeying bose statistics can be

created in any number. A detailed calculation of the electron-phonon relaxation time is therefore in order since by changing the junction bias, we are effectively changing the excitation energy of the tunneling electrons that are injected into the metal. The temperature dependence is also important because at a few degrees Kelvin the thermal energy k_BT becomes comparable to the energy width of the zero bias anomalies.

We shall calculate the relaxation time of an excited electron in the presence of a lattice (phonon gas) by using Fermi's golden rule and considering only first order scattering processes in the square of the electron-phonon matrix element. In Fig. (3.2) we consider the four processes that alter the occupancy of the excited state $\underline{p}$. $E_{\underline{p}}$ is the energy of the excited state with momentum $h\underline{p}$ while $E_{\underline{k}}$ is the energy of the final state with momentum $h\underline{k}$. The phonon has momentum $\pm\hbar\underline{q}$ (where $\underline{q} = \underline{p}-\underline{k}$) and energy $\hbar\omega(\underline{q},\lambda)$ where λ is the polarization index. The processes in the first column lead to a decrease in occupancy of $\underline{p}$ by absorption or emission of a phonon while those in the second column lead to a decrease. The rate of change of $f_{\underline{p}}$, the occupancy of the state $\underline{p}$, can be written down by inspection of the diagrams and by noting that an initial electron or phonon has the occupancy factors f and N,

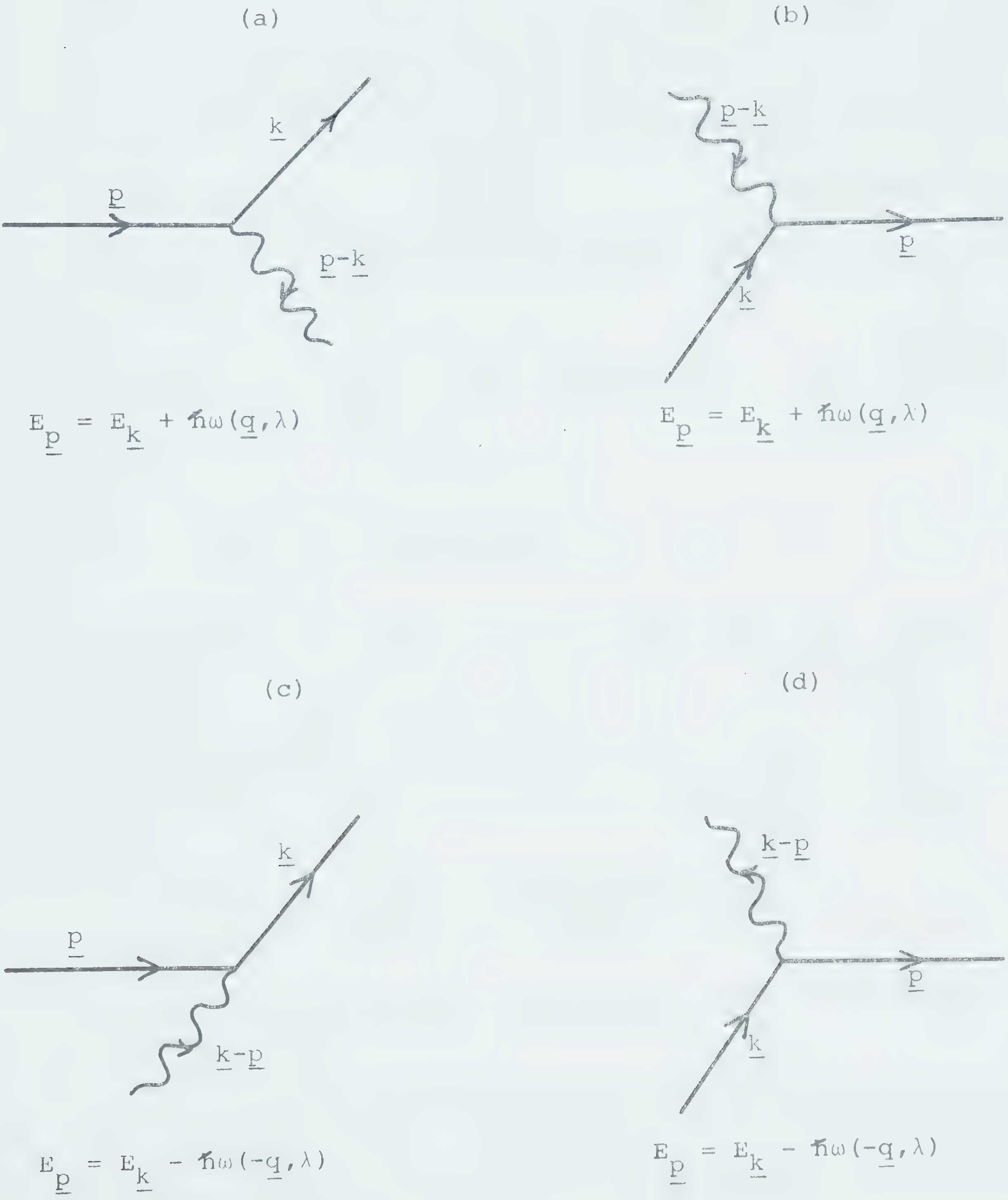
(a)
k
p
p-k
E_p = E_k + ħω(q,λ)
(b)
p-k
p
k
E_p = E_k + ħω(q,λ)
(c)
k
p
k-p
E_p = E_k - ħω(-q,λ)
(d)
k-p
p
k
E_p = E_k - ħω(-q,λ)

Fig. (3.2). Processes that lead to a decay of an excited electron state.

respectively, while the final state factors are (1-f) and (1+N) respectively. N is the Bose statistical factor for phonons. As an example the first process in Fig. (3.2a) contributes the following term

$$\left.\frac{\partial f_{\underline{p}}}{\partial t}\right|_{(a)} = -\frac{2\pi}{\hbar}\sum_{\underline{k},\lambda}|G(\underline{q},\lambda)|^2 f_{\underline{p}}(1-f_{\underline{k}})(1+N_{\underline{q}})\,\delta(E_{\underline{p}}-E_{\underline{k}}-\hbar\omega(q,\lambda)) \tag{3.14}$$

The electron-phonon matrix element, $G(\underline{q},\lambda)$, has the form (see Bardeen (1937))

$$G(\underline{q},\lambda) = -i\left(\frac{\hbar}{2\omega(\underline{q},\lambda)MN}\right)^{\frac{1}{2}} \underline{q}\cdot\underline{\xi}_\lambda \; v(\underline{q}) \tag{3.15}$$

where MN is the mass density of the lattice and $\underline{\xi}_\lambda$ is the phonon polarization vector. $v(\underline{q})$ is the Fourier transform of the ion pseudopotential. When all four processes in Fig. (3.2) are taken into account we have

$$\begin{aligned}\frac{\partial f_{\underline{p}}}{\partial t} = -\frac{2\pi}{\hbar}\sum_{\underline{k},\lambda}|G(\underline{q},\lambda)|^2\{&\delta(E_{\underline{p}}-E_{\underline{k}}-\hbar\omega(\underline{q},\lambda))\times\\ &\times[f_{\underline{p}}(1-f_{\underline{k}})(1+N_{\underline{q}}) - f_{\underline{k}}N_{\underline{q}}(1-f_{\underline{p}})] + \\ &+\delta(E_{\underline{p}}-E_{\underline{k}}+\hbar\omega(\underline{q},\lambda))[f_{\underline{p}}N_{\underline{q}}(1-f_{\underline{k}})-f_{\underline{k}}(1-f_{\underline{p}})(1+N_{\underline{q}})]\}.\end{aligned} \tag{3.16}$$

The above expression is identically zero if f and N are the equilibrium statistical functions. As in the

previous section we let the departure of the state $\underline{p}$ from equilibrium be $\Delta f_{\underline{p}}$, where $\Delta f_{\underline{p}} = f_{\underline{p}} - f^{o}_{\underline{p}}$. We shall use the equilibrium distribution functions for $f_{\underline{k}}$ and $N_{\underline{q}}$. Thus we are assuming that the electron that has tunneled into an excited state $\underline{p}$ is scattered by the lattice into the equilibrium distribution. With these considerations Eqn. (3.16) now becomes

$$\frac{\partial f_{\underline{p}}}{\partial t} = - \frac{\Delta f_{\underline{p}}}{\tau_{\underline{p}}} \quad . \tag{3.17}$$

where the relaxation time $\tau_{\underline{p}}$ is given by

$$\frac{1}{\tau_{\underline{p}}} = \frac{2\pi}{\hbar} \sum_{\underline{k},\lambda} |G(\underline{q},\lambda)|^2 \{ (N^{o}_{\underline{q}}+1-f^{o}_{\underline{k}})\,\delta(E_{\underline{p}}-E_{\underline{k}}-\hbar\omega(\underline{q},\lambda)$$

$$+ (N^{o}_{\underline{q}}+f^{o}_{\underline{k}})\,\delta(E_{\underline{p}}-E_{\underline{k}}+\hbar\omega(\underline{q},\lambda))\} \quad . \tag{3.18}$$

This expression may be simplified by defining the excitation energy $\varepsilon_{\underline{p}} = E_{\underline{p}} - \mu$ above the Fermi level μ. The summation over $\underline{k}$ states becomes

$$\sum_{\underline{k}} \longrightarrow \frac{V}{(2\pi)^3} \int d\Omega_{\underline{k}} \int_0^\infty |\underline{k}|^2 \, d|\underline{k}|$$

$$\longrightarrow \frac{V}{\hbar(2\pi)^3} \int \frac{dS(\underline{k})}{v(\underline{k})} \int_{-\mu}^{\infty} d\varepsilon_{\underline{k}} \tag{3.19}$$

where $dS(\underline{k}) = |\underline{k}|^2 \, d\Omega_{\underline{k}}$ is an element of $\underline{k}$ space area on

the energy surface defined by $E_{\underline{k}} = \hbar^2 \underline{k}^2/2m$, and $v(\underline{k})$ is the velocity defined by $v(\underline{k}) = |\nabla_{\underline{k}} E_{\underline{k}}|/\hbar = \hbar|\underline{k}|/m$. Since $\omega(\underline{q},\lambda)$ is of the order of the Debye frequency ω_D, the dominant contribution in the $\varepsilon_{\underline{k}}$ integration comes from $\varepsilon_{\underline{k}} \gtrless \hbar\omega_D << \mu$. Hence we can extend the lower limit in Eqn. (3.19) to infinity and evaluate the surface integral on the Fermi surface. If we make these changes and carry out the $\varepsilon_{\underline{k}}$ integration over the energy conserving delta function, we obtain

$$\frac{1}{\tau(\varepsilon_{\underline{p}},\underline{p})} = \frac{2\pi}{\hbar} \cdot \frac{V}{(2\pi)^3} \int \frac{dS_F(\underline{k})}{\hbar v_F(\underline{k})} \sum_{\lambda} |G(\underline{q},\lambda)|^2 \times$$

$$\times \{2N^o(\omega(\underline{q},\lambda))+1+f^o(\varepsilon_{\underline{p}}+\hbar\omega(\underline{q},\lambda))-f^o(\varepsilon_{\underline{p}}-\hbar\omega(\underline{q},\lambda))\}. \tag{3.20}$$

We can separate out the phonon contribution in a convenient manner by inserting a delta function in (3.20).

i.e. $$\frac{1}{\tau(\varepsilon_{\underline{p}},\underline{p})} = \frac{2\pi}{\hbar} \int_0^\infty d(\hbar\omega)\, \alpha_{\underline{p}}(\hbar\omega) F_{\underline{p}}(\hbar\omega) \times$$

$$\times [2N^o(\hbar\omega) + 1 + f^o(\varepsilon_{\underline{p}}+\hbar\omega) - f^o(\varepsilon_{\underline{p}}-\hbar\omega)] \tag{3.21}$$

where by definition

$$\alpha^2_{\underline{p}}(\hbar\omega) F_{\underline{p}}(\hbar\omega) = \frac{V}{(2\pi)^3} \int \frac{dS_F(\underline{k})}{\hbar v_F(\underline{k})} \sum_{\lambda} |G(\underline{q},\lambda)|^2 \delta(\hbar\omega - \hbar\omega(\underline{q},\lambda)) . \tag{3.22}$$

We are tunneling into an evaporated film which is probably polycrystalline and characteristic of an isotropic material. Therefore, we do not expect to see lattice anisotropy in the relaxation time and consequently we average the inverse life time over the Fermi surface. Eqn. (3.21) becomes

$$\frac{1}{\tau(\varepsilon)} = \frac{2\pi}{\hbar}\int_0^\infty d(\hbar\omega)\,\alpha^2(\hbar\omega)F(\hbar\omega)\,[2N^{O}(\hbar\omega)+1+f^{O}(\varepsilon+\hbar\omega)-f^{O}(\varepsilon-\hbar\omega)] \tag{2.23}$$

where

$$\alpha^2(\hbar\omega)F(\hbar\omega) = \frac{\displaystyle\int\frac{dS_F(\underline{p})}{v_F(\underline{p})}\int\frac{dS_F(\underline{k})}{v_F(\underline{k})}\,\frac{V}{(2\pi)^3\hbar}\sum_\lambda |G(\underline{q},\lambda)|^2\,\delta(\hbar\omega-\hbar\omega(\underline{q},\lambda))}{\displaystyle\int\frac{dS_F(\underline{p})}{v_F(\underline{p})}} \tag{2.24}$$

The quantity α^2F is dimensionless and while difficult to calculate from first principles, can be extracted from tunneling experiments in superconductors and is presently known for Pb, Hg, Sn and In (see McMillan and Rowell (1969)). The awkward notation $\alpha^2(\hbar\omega)F(\hbar\omega)$ was invented with the following intent: the phonon density of states in a metal is given by

$$F(\hbar\omega) = \sum_\lambda \frac{V}{(2\pi)^3}\int d^3\underline{q}\;\;\delta(\hbar\omega - \hbar\omega(\underline{q},\lambda)) \quad . \tag{3.25}$$

Thus $\alpha^2(\hbar\omega)$ is taken to be a measure of the strength of the electron-phonon coupling. For convenience we replace

$\hbar\omega$ by ω and refer to ω as the phonon energy (typically of the order of meV). We shall now proceed to discuss the properties of the relaxation time $\tau(\varepsilon)$ given by

$$\frac{1}{\tau(\varepsilon)} = \frac{2\pi}{h} \int_0^\infty d\omega\ \alpha^2 F(\omega)\,[2N^o(\omega)+1+f^o(\varepsilon+\omega)-f^o(\varepsilon-\omega)] \tag{3.26}$$

where $N^o(\omega) = \dfrac{1}{e^{\omega/k_BT} - 1}$ and $f^o(\varepsilon) = \dfrac{1}{1+e^{\varepsilon/k_BT}}$. (3.27)

We first note that the relaxation time at any temperature is an even function of excitation energy ε. This follows directly from the above definitions. At T=0, $N^o(\omega) = 0$, and the statistical factor in the integrand of Eqn. (3.26) is just a step function

$$\begin{aligned} 1 + f^o(\varepsilon+\omega) - f^o(\varepsilon-\omega) &= 1 \qquad -\varepsilon < \omega < \varepsilon \\ &= 0 \qquad \text{otherwise.} \end{aligned}$$

Therefore at T = 0,

$$\frac{1}{\tau(\varepsilon)} = \frac{2\pi}{h} \int_0^{|\varepsilon|} d\omega\ \alpha^2 F(\omega) \quad , \tag{3.28}$$

where the absolute value on the upper limit ensures that the relaxation time is both positive and even. At finite temperatures the cut-off in the step function is smeared by the thermal energy k_BT but is still fairly

sharp if $k_BT << \varepsilon$. Physically this just means that an electron of excitation energy ε cannot decay to equilibrium by emitting a phonon of energy ω greater than ε. Since the excitation energies will be of the order of or less than the bias energy we can therefore disregard $\alpha^2F(\omega)$ for $\omega > eV_{max}$. The maximum voltage we deal with in the zero-bias anomalies is ~ 5 mV, therefore we can disregard any information in $\alpha^2F(\omega)$ beyond ω ~ 5 meV. In order to facilitate calculations, we shall make use of this fact by assuming that the metals we deal with may be represented, up to ω ~ 5 meV, by a power law behavior of the form

$$\alpha^2(\omega)F(\omega) = a_n\, \omega^n \, . \tag{3.29}$$

The relaxation time then becomes

$$\frac{1}{\tau(\varepsilon)} = \frac{2\pi a^n}{\hbar} \int_0^\infty \omega^n \left(\frac{2}{e^{\omega/k_BT} - 1} + \frac{1}{1 + e^{\varepsilon+\omega/k_BT}} + \frac{1}{1+e^{\varepsilon-\omega/k_BT}} \right) d\omega \, . \tag{3.30}$$

Eqn. (3.30) may be simplified somewhat to yield

$$\frac{1}{\tau(\varepsilon)} = \frac{2\pi a_n}{\hbar} (k_BT)^{n+1} \{2\Gamma(n+1)\zeta(n+1) + F_n(\frac{\varepsilon}{k_BT}) + F_n(-\frac{\varepsilon}{k_BT})\} \tag{3.31}$$

where $$F_n(z) = \int_0^\infty \frac{x^n dx}{e^{x-z} + 1} \tag{3.32}$$

and Γ and ζ are the Gamma and Riemann Zeta functions respectively. Rhodes (1950) has studied the functions $F_n(z)$ and has tabulated their properties and values for integral values of n. We shall consider only the cases n = 1 and 2. For n = 1, $\tau(\varepsilon)$ can be evauated in closed form to give

$$\frac{1}{\tau(\varepsilon)} = \frac{\pi a_1}{\hbar} [\varepsilon^2 + (\pi k_B T)^2] \quad . \tag{3.33}$$

The relaxation time for the case n = 2 cannot be evaluated in close form. However, Rhodes gives convenient expansions for $F_2(z)$ with which the life-time may be approximately evaluated. For the case n = 2, we have

$$\frac{1}{\tau(\varepsilon)} = \frac{2\pi a_2}{\hbar} (k_B T)^3 \, \Omega(\frac{\varepsilon}{k_B T}) \tag{3.34}$$

where

$$\Omega(z) = 7\zeta(3) + (2\mathrm{Ln}2)z^2 + \frac{z^4}{4!} - \frac{1}{2}\frac{z^6}{6!} + \frac{z^8}{8!} - \ldots \quad (|z| \leq 1) \tag{3.35}$$

$$= 4\{\zeta(3) + \frac{|z|^3}{12} + \frac{\pi^2 |z|}{12} + \sum_{r=1}^{\infty} (-1)^{r+1} \frac{e^{-r|z|}}{r^3}\}; \quad (|z| \geq 1) \tag{3.36}$$

From the above expansions, we obtain the following limits

$$\frac{1}{\tau(\varepsilon)} \xrightarrow[\varepsilon\to 0]{} \frac{2\pi a_2}{\hbar} \cdot 7\zeta(3)(k_BT)^3$$

$$\frac{1}{\tau(\varepsilon)} \xrightarrow[T\to 0]{} \frac{2\pi a_2}{\hbar} \frac{\varepsilon^3}{3} \quad . \tag{3.37}$$

The Debye frequency spectrum F(ω) defined in Eqn. (3.25) varies quadratically with ω at small frequencies. The model with n = 2 then simply states that the electron-phonon coupling, α^2, is constant at low frequencies. With this behavior, the relaxation time should, according to Eqns. (3.37), vary inversely as the temperature and energy cubed. Measurements of the relaxation frequency in lead and indium by cyclotron resonance (see Goy and Castaing (1972)) indicate that this cubic behavior is observed. However, theoretical one-OPW calculations by Allen and Cohen (1970) and Carbotte and Dynes (1968) indicate the possibility that $\alpha^2F(\omega)$ behaves linearly with ω at low frequencies due to Umklapp processes. We shall not attempt to resolve this question here but shall calculate the zero-bias anomaly with both models.

3.3 Calculation of the Current, Conductance and Derivative of Conductance Due to the Blocking Effect

In order to calculate the tunneling current, we shall assume that the only relaxation processes of

importance are the ones described in the previous section. We characterize the relaxation times for elastic scattering and inelastic electron-phonon collisions by τ_i (constant) and τ_{ep} (energy and temperature dependent) respectively. Since the rates of change of occupation of a state due to these two processes are additive, the total or combined relaxation time τ is given by

$$\frac{1}{\tau} = \frac{1}{\tau_i} + \frac{1}{\tau_{ep}} \tag{3.38}$$

for any state $\underline{k}$.

The tunneling current is simply given by summing over all transition rates from left to right (see Eqn. (2.46))

$$\text{i.e.} \quad I = 2e \sum_{\underline{k}} \frac{2\pi}{\hbar} \sum_{\underline{k}'} |M_{\underline{kk}'}|^2 (f_{\underline{k}} - f_{\underline{k}'}) \delta(E_{\underline{k}} - E_{\underline{k}'}) \tag{3.39}$$

where $f_{\underline{k}}$ and $f_{\underline{k}'}$ are now the steady state distribution functions on left and right sides respectively. Their difference is given by Eqn. (3.11)

$$\text{i.e.} \quad f_{\underline{k}} - f_{\underline{k}'} = \frac{f^o_{\underline{k}} - f^o_{\underline{k}'}}{1 + \frac{2\pi}{\hbar} |M|^2 (\rho_{\underline{k}} \tau_{\underline{k}'} + \rho_{\underline{k}'} \tau_{\underline{k}})} \tag{3.40}$$

where $\tau_{\underline{k}}$ and $\tau_{\underline{k}'}$ are the total relaxation times on the left and right hand sides respectively. Since we expect

the change from equilibrium to be small, we expand Eqn. (3.40) to obtain

$$f_{\underline{k}}-f_{\underline{k}'} = (f^{o}_{\underline{k}}-f^{o}_{\underline{k}'})\{1 - \frac{2\pi}{\hbar}|M|^2(\rho_{\underline{k}}\tau_{\underline{k}'} + \rho_{\underline{k}'}\tau_{\underline{k}})\}. \qquad (3.41)$$

The tunneling current may now be represented by

$$I = I_o + \delta I \qquad (3.42)$$

where

$$I_o = \frac{4\pi e}{\hbar} \sum_{\underline{k}} \sum_{\underline{k}'} |M_{\underline{kk}'}|^2 (f^{o}_{\underline{k}}-f^{o}_{\underline{k}'})\delta(E_{\underline{k}}-E_{\underline{k}'}) \qquad (3.43)$$

is the conventional tunneling current calculated with equilibrium distribution on both sides and discussed in Sections 2.1 and 2.4. δI is the small negative correction to the tunneling current due to the blocking effect and is given by

$$\delta I = -\frac{4\pi e}{\hbar} \sum_{\underline{k}} \sum_{\underline{k}'} |M_{\underline{kk}'}|^2 (f^{o}_{\underline{k}}-f^{o}_{\underline{k}'}) \frac{2\pi}{\hbar}|M|^2(\rho_{\underline{k}}\tau_{\underline{k}'} + \rho_{\underline{k}'}\tau_{\underline{k}})$$

$$\times\ \delta(E_{\underline{k}}-E_{\underline{k}'}) \quad . \qquad (3.44)$$

The summation in Eqn. (3.44) may be done in the usual way. That is;

$$\sum_{\underline{k}} \sum_{\underline{k}'} |M_{\underline{kk}'}|^2 \longrightarrow \frac{A}{(2\pi)^2} \int dE_{\underline{k}} \int dE_{\underline{k}'} \int d^2\underline{k}_{||}\ \rho_{\underline{k}}\rho_{\underline{k}'}|M|^2 \qquad (3.45)$$

where

$$|M|^2 = \frac{1}{4\pi^2}\frac{P(E_x)}{\rho_k\rho_{k'}} \quad .$$

We must also remember that the relaxation times depend only upon the excitation energies, i.e. $\tau_{\underline{k}} = \tau(E_{\underline{k}}-\mu)$ and $\tau_{\underline{k}'} = \tau(E_{\underline{k}'}-\mu')$. Since the Fermi levels are separated by a bias eV (i.e. $\mu-\mu'=eV$), the expression for the blocking current reduces to

$$\delta I = \frac{4\pi emA}{h^3}\int_0^\infty dE[f^o(E-\mu)-f^o(E+eV-\mu)]\int_0^E P^2(E_x)$$

$$\times \left(\frac{\tau'(E+eV-\mu)}{2\pi\hbar\rho'(E_x)} + \frac{\tau(E-\mu)}{2\pi\hbar\rho(E_x)}\right) dE_x \quad . \qquad (3.46)$$

In contrast to the conventional current I_o the blocking current δI explicitly depends upon the densities of state in both left and right hand metals. Clearly, if the relaxation times become very small, the blocking current δI vanishes as we expect. We may note that the blocking current depends upon the square of the transmission coefficient and should therefore be a sensitive function of oxide barrier thickness. Eqn. (3.46) may be simplified by making use of the fact that tunneling occurs predominantly with velocities normal to the barrier. Therefore we replace the quantity $P(E_x)/2\pi\hbar\rho(E_x)$ by its value at the Fermi energy

i.e. $$\frac{P(E_x)}{2\pi\hbar\rho(E_x)} \rightarrow \frac{P(\mu)v_F}{2L} = \frac{1}{\tau_B} \tag{3.47}$$

where v_F is the Fermi velocity and τ_B is the tunneling time for an electron as defined in Section 3.1.

Therefore Eqn. (3.46) becomes

$$\delta I = -\frac{\sigma_o}{e}\int_0^{\infty} dE\{f^o(E-\mu)-f^o(E+eV-\mu)\}.\{\frac{\tau'(E+eV-\mu)}{\tau_B} + \frac{\tau(E-\mu)}{\tau_B}\} \tag{3.48}$$

where

$$\sigma_o = \frac{4\pi e^2 m}{h^3}\int_0^{\mu} P(E_x)dE_x$$

is the ideal zero-bias conductance defined in Eqns.(2.20) and (2.21). Eqn. (3.48) may be written in a more compact form by making use of the variable $\varepsilon = E-\mu$ to obtain

$$\delta I(V) = -\frac{\sigma_o}{e}\int_{-\infty}^{+\infty} d\varepsilon[f^o(\varepsilon)-f^o(\varepsilon+eV)].[\frac{\tau'(\varepsilon+eV)}{\tau_B'} + \frac{\tau(\varepsilon)}{\tau_B}] .$$

We can simplify the above equation still more by noting that the energy dependence of the effective life times comes from their electron-phonon parts which are even functions of their arguments. Using this fact and the identity

$$f^o(\varepsilon)-f^o(\varepsilon+eV) = -f^o(-\varepsilon-eV)-f^o(-\varepsilon) \tag{3.49}$$

the blocking current may be written as

$$\delta I(V) = -\frac{\sigma_o}{e}\int_{-\infty}^{\infty} d\varepsilon\,[f^o(\varepsilon)-f^o(\varepsilon+eV)]\,(\frac{\tau'(\varepsilon)}{\tau_B'} + \frac{\tau(\varepsilon)}{\tau_B}) . \tag{3.50}$$

The conductance of a junction, normalized to zero bias is given by

$$\frac{\sigma(V)}{\sigma_o} = \frac{1}{\sigma_o}\frac{dI_o(V)}{dV} + \frac{\delta\sigma(V)}{\sigma_o} \tag{3.51}$$

where $\delta\sigma(V) \equiv \frac{d}{dV}(\delta I(V))$ is the blocking conductance. Using Eqn. (3.50) we find

$$\frac{\delta\sigma(V)}{\sigma_o} = -\int_{-\infty}^{+\infty} d\varepsilon\,(-\frac{df^o(\varepsilon)}{d\varepsilon}).(\frac{\tau'(\varepsilon+eV)}{\tau_B'} + \frac{\tau(\varepsilon+eV)}{\tau_B}) . \tag{3.52}$$

This is the basic form that we use to compute the characteristics of the zero-bias anomaly. It may easily be verified from Eqn. (3.52) that the blocking conductance $\delta\sigma(V)$ is an even function of V and hence it is symmetric about zero bias. In subsequent work we shall simply use V in place of eV and define the bias in units of energy (typically meV).

Zero Temperature

In order to observe the behavior of the blocking conductance $\delta\sigma(V)$, we set T = 0 since in this case we

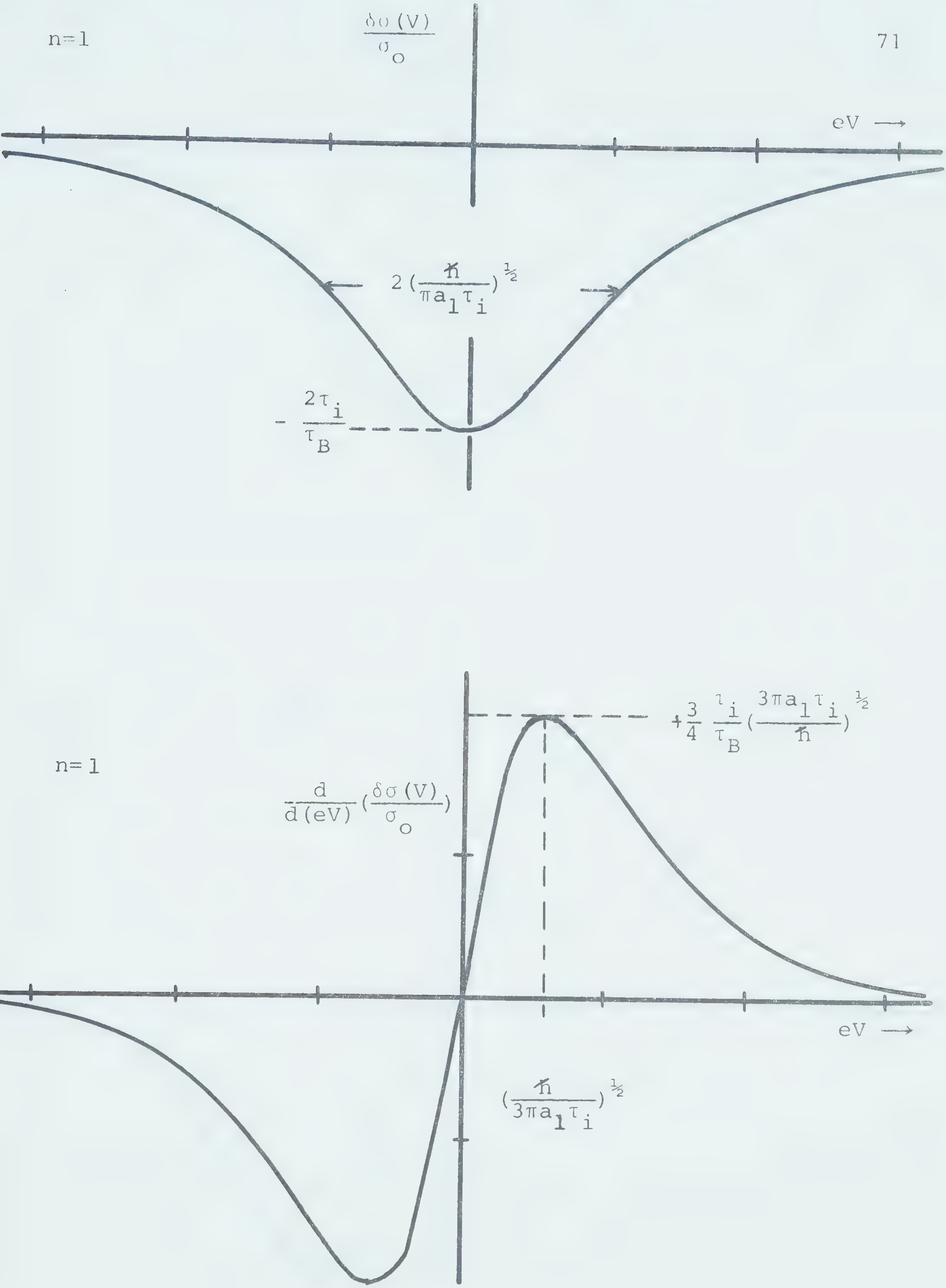

Fig. (3.3). Conductance and derivative conductance for n=1.

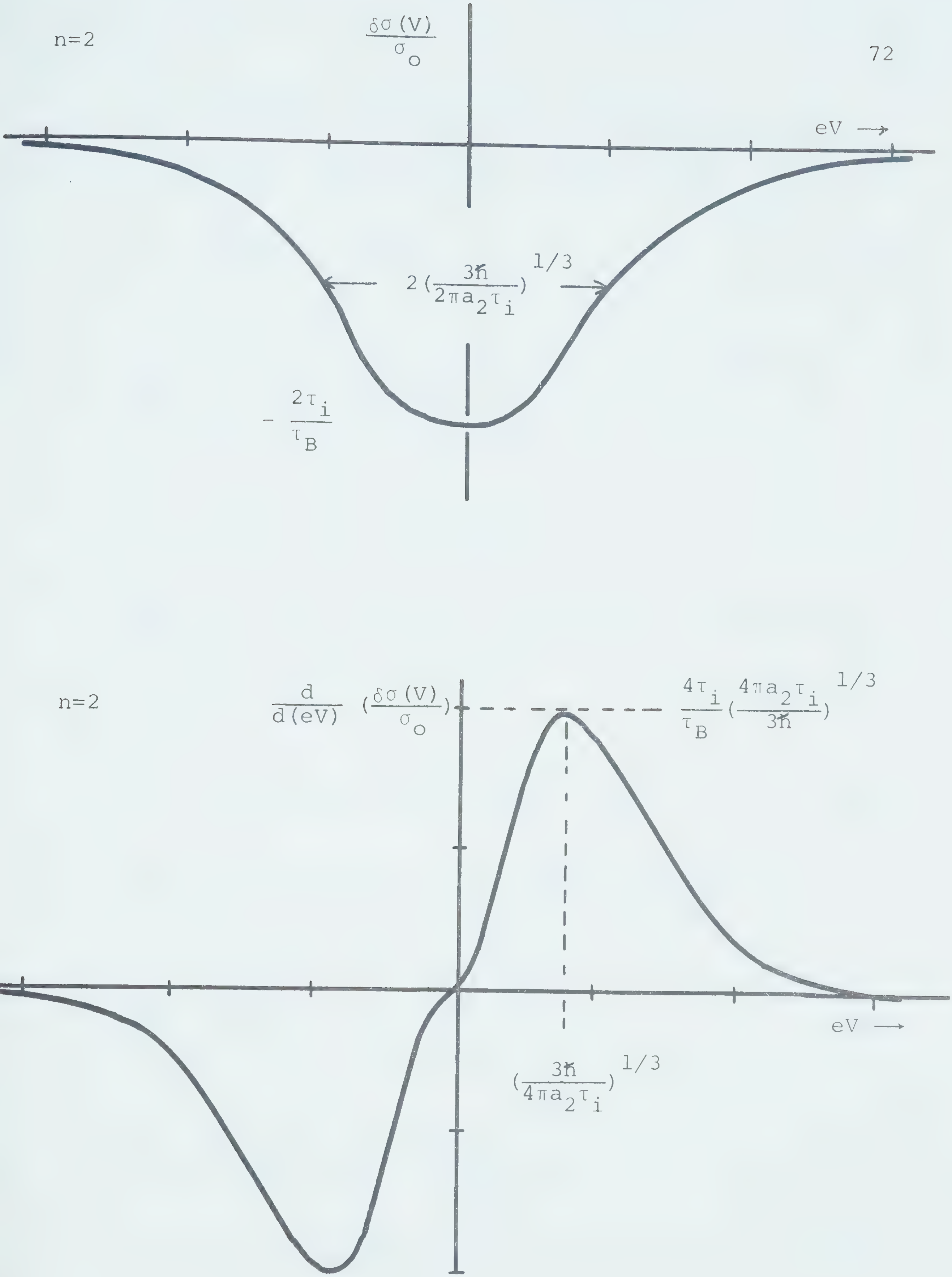

Fig. (3.4). Conductance and derivative conductance for n=2.

can evaluate it in closed form. At zero temperature, $-df^{o}(\varepsilon)/d\varepsilon = \delta(0)$, and Eqn. (3.52) becomes

$$\frac{\delta\sigma(V)}{\sigma_o} = -\frac{2\tau(V)}{\tau_B} \qquad (3.53)$$

where for convenience we have assumed a symmetric tunnel junction so that $\tau'(V) = \tau(V)$, and $\tau_B' = \tau_B$. The effective relaxation time $\tau(V)$ is given by

$$\frac{1}{\tau(V)} = \frac{1}{\tau_i} + \frac{1}{\tau_{ep}(V,T=0)} \qquad (3.54)$$

where τ_i and τ_{ep} are the impurity and electron-phonon relaxation times respectively. At T = 0, τ_{ep} is given by Eqn. (3.28),

$$\text{i.e.} \quad \frac{1}{\tau_{ep}(V,T=0)} = \frac{2\pi a_n}{\hbar} \frac{|V|^{n+1}}{n+1} \qquad (3.55)$$

where n corresponds to the power law behavior of $\alpha^2F(\omega) = a_n\omega^n$. For the case n=1 and n=2, we find

$$n=1: \quad \frac{\delta\sigma(V)}{\sigma_o} = -\frac{2/\tau_B}{\frac{1}{\tau_i} + \left(\frac{\pi a_1}{\hbar}\right) V^2} \,, \qquad (3.56)$$

$$n=2: \quad \frac{\delta\sigma(V)}{\sigma_o} = -\frac{2/\tau_B}{\frac{1}{\tau_i} + \left(\frac{2\pi a_2}{3\hbar}\right) |V|^3} \,. \qquad (3.57)$$

The features of the conductance and its derivative are plotted in Fig. (3.3) for n=1 and in Fig. (3.4) for n=2.

3.4 Comparison of Theory with Experiment

In Fig. (3.5), we show the experimental conductance of an Al-Al junction at biases up to 5 meV for several different temperatures. The dip in conductance about zero voltage is what we commonly refer to as the zero-bias anomaly. The sharpness of the anomaly broadens considerably with increases in temperature. However, we notice that the conductance over the range of ±5 meV is not symmetric about the region. We assume that this asymmetry arises from the ideal background conductivity discussed in Section 2.4. Therefore we suppose that the experimental conductance in Fig. (3.5) may be represented by an expression of the form

$$\sigma(V) = \sigma_o + \sigma_1 V + \sigma_2 V^2 + \delta\sigma(V,T) \tag{3.58}$$

where the first three terms constitute the ideal background conductance (see Rowell, McMillan and Feldmann (1968)) with σ_1 and σ_2 being small constants. One possible way to test this conjecture is to use the fact that the ZBA conductance given by $\delta\sigma(V,T)$ is an even function of bias. Therefore if we take the odd part of Eqn. (3.58) we obtain simply

$$\frac{\sigma_{odd}(V)}{\sigma_o} = \frac{\sigma(V) - \sigma(-V)}{\sigma_o} = \frac{\sigma_1}{\sigma_o} V \tag{3.59}$$

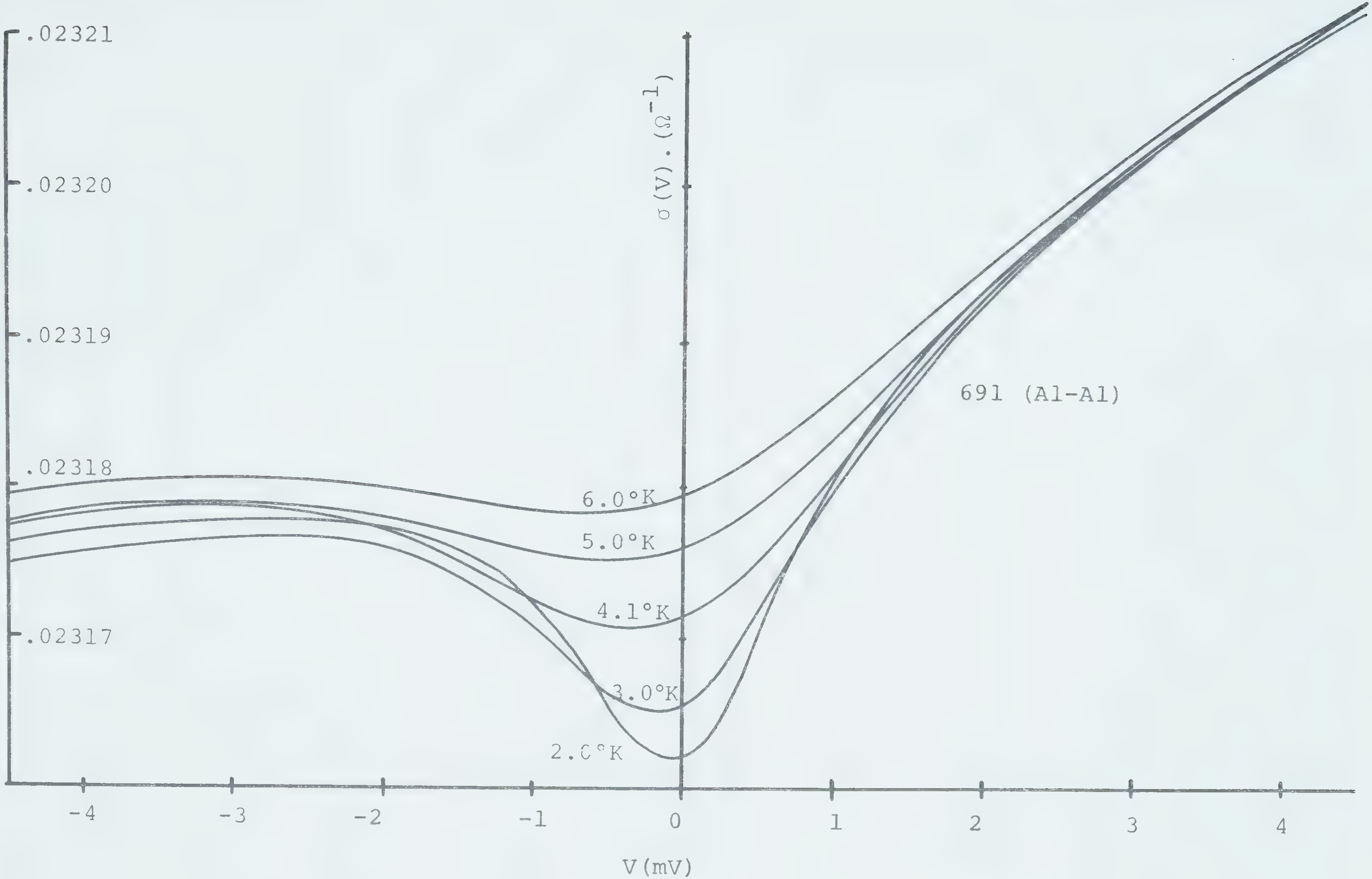

Fig. (3.5). Experimental conductance of an Al-Al junction.

and so theoretically the odd conductance is directly proportional to bias. The experimental odd conductance obtained by using the data in Fig. (3.5) is shown in Fig. (3.6). We note that it is proportional to bias up to 5 meV to about one part in 10^5 thus agreeing with theory.

In principle then, we can effectively compare theory to experiment by taking the even part of the theoretical conductance

$$\text{i.e.}\quad \sigma_e(x) = \sigma_o + \sigma_2 V^2 + \delta\sigma(V,T) \qquad (3.60)$$

and comparing it to the even part of the experimental conductance. Unfortunately we do not have sufficient data to isolate the background part $\sigma_2 V^2$. Certainly it should be smaller than the linear term $\sigma_1 V$ and we shall therefore neglect it. However it may be troublesome in the sense that it masks the asymptotic behavior of the ZBA conductance.

In practice, a more sensitive and accurate measure of the ZBA conductance is given by its experimentally determined derivative as outlined in Section 1.3. Therefore in the rest of this chapter we prefer to test the theory by comparing the theoretical derivative of even conductance

$$\text{i.e.}\quad \frac{d\sigma_e(V)}{dV} = \frac{d}{dV}\,\delta\sigma(V,T) \qquad (3.61)$$

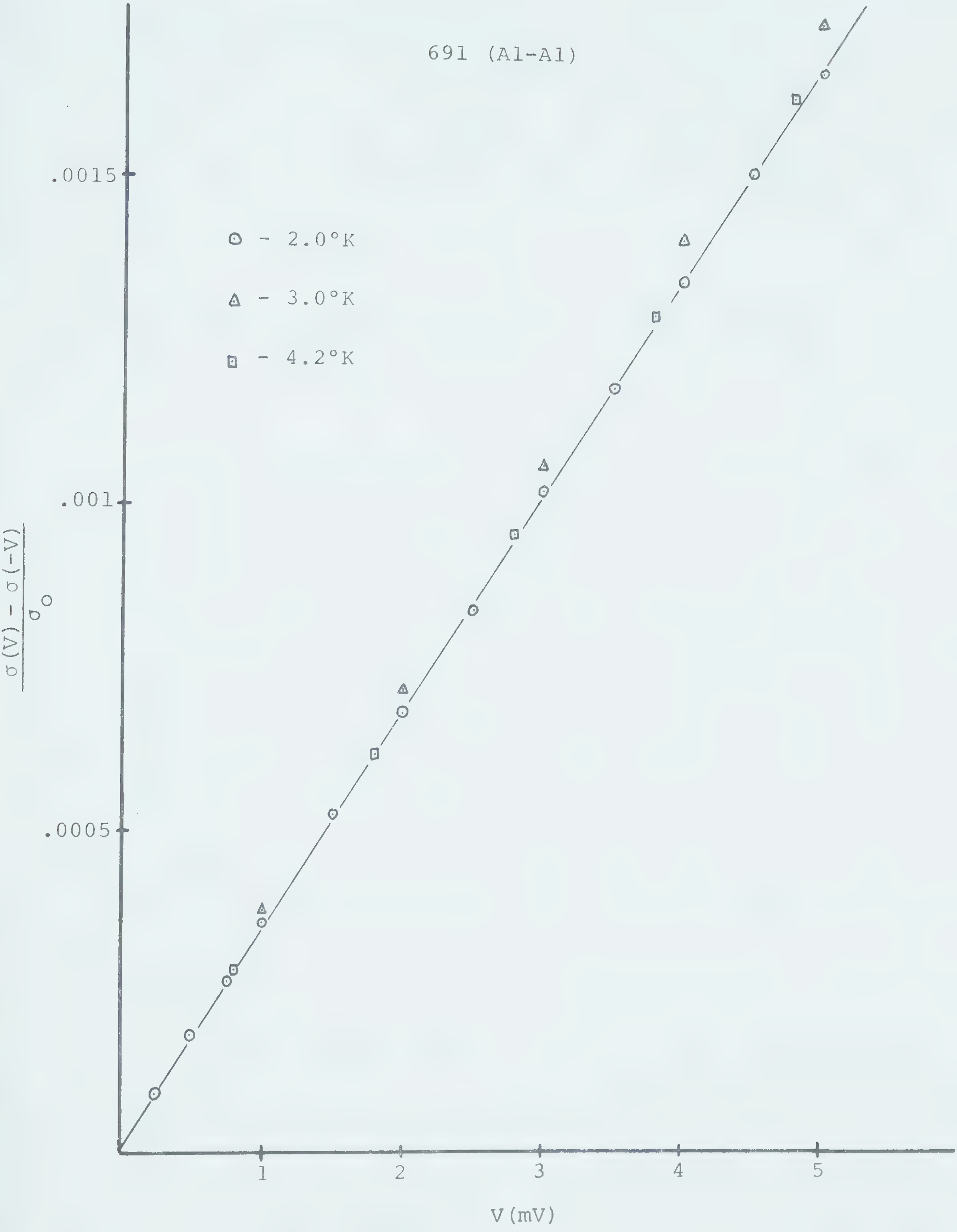

Fig. (3.6). Experimental odd conductance.

with its experimental counterpart. We assume at the outset that the two electrodes making up the Al-Al junction are similar in nature and have the same τ_i, τ_{ep} and τ_B. Therefore the even derivative of conductivity is given by

$$\frac{1}{\sigma_o}\frac{d\sigma_e(V)}{dV} = \frac{d}{dV}\left(\frac{\delta\sigma(V)}{\sigma_o}\right) = -2\int_{-\infty}^{+\infty} d\varepsilon\left(-\frac{\partial f^o(\varepsilon)}{\partial\varepsilon}\right)\frac{d}{dV}\left[\frac{\tau(\varepsilon+V)}{\tau_B}\right] . \tag{3.62}$$

For finite temperatures the integral in the above expression must be done numerically. The reason is simply that the half-width of the distribution $-\partial f^o(\varepsilon)/\partial\varepsilon$ is about 3.53 k_BT so that at 2°K, the thermal smearing is of the order of half a meV. This is comparable to the width of the ZBA conductance as may be seen in Fig.(3.5). For numerical calculations it is convenient to cast Eqn. (3.63) into the form

$$\frac{1}{\sigma_o}\frac{d\sigma_e(V)}{dV} = \int_0^{\infty}\frac{dx}{(1+e^x)(1+e^{-x})}\{S(V-xk_BT)+S(V+xk_BT)\} \tag{3.63}$$

where

$$S(\varepsilon) \equiv -2\frac{d}{d\varepsilon}\left[\frac{\tau(\varepsilon)}{\tau_B}\right] .$$

The effective relaxation time is given by

$$\frac{1}{\tau(\varepsilon)} = \frac{1}{\tau_i} + \frac{1}{\tau_{ep}(\varepsilon,T)}$$

where the electron-phonon relaxation time $\tau_{ep}(\varepsilon,T)$ is given by Eqn. (3.33) for the case where $n=1$ and by Eqn. (3.34) for the case where $n=2$.

Fig. (3.7) shows the experimental $d\sigma_e/dV$ vs V curves for the same Al-Al junction measured at $T=3.0$, 4.1, 5.0 and 6.0°K. The dashed line is the theoretical curve given by Eqn. (3.63) for the case where $n=1$ (i.e. $\alpha^2F(\omega) = a_1\omega$). The theoretical curve was fitted to the 3°K experimental data and yields the values

$$\tau_B = 1.4 \times 10^{-7} \text{ sec.}$$

$$\tau_i = 3.5 \times 10^{-10} \text{ sec.}$$

The electron-phonon coupling constant a_1 was chosen to agree with the calculation of $\alpha^2(\omega)F(\omega)$ by Carbotte and Dynes (1968) and was given the value $a_1 = .003/\text{meV}$. The overall shape of the theoretical curves is not extremely sensitive to temperature. Accordingly, the theoretical and experimental peak positions and heights are compared in Fig. (3.8) for the same set of values τ_i, τ_B and a_1. Excellent agreement is found for the peak positions as a function of temperature. The theory predicts a stronger temperature dependence for the peak heights than experimentally observed. The behavior of the theoretical curves are found to be quite insensitive to the choice of τ_i. Fig. (3.9) depicts the temperature dependence of

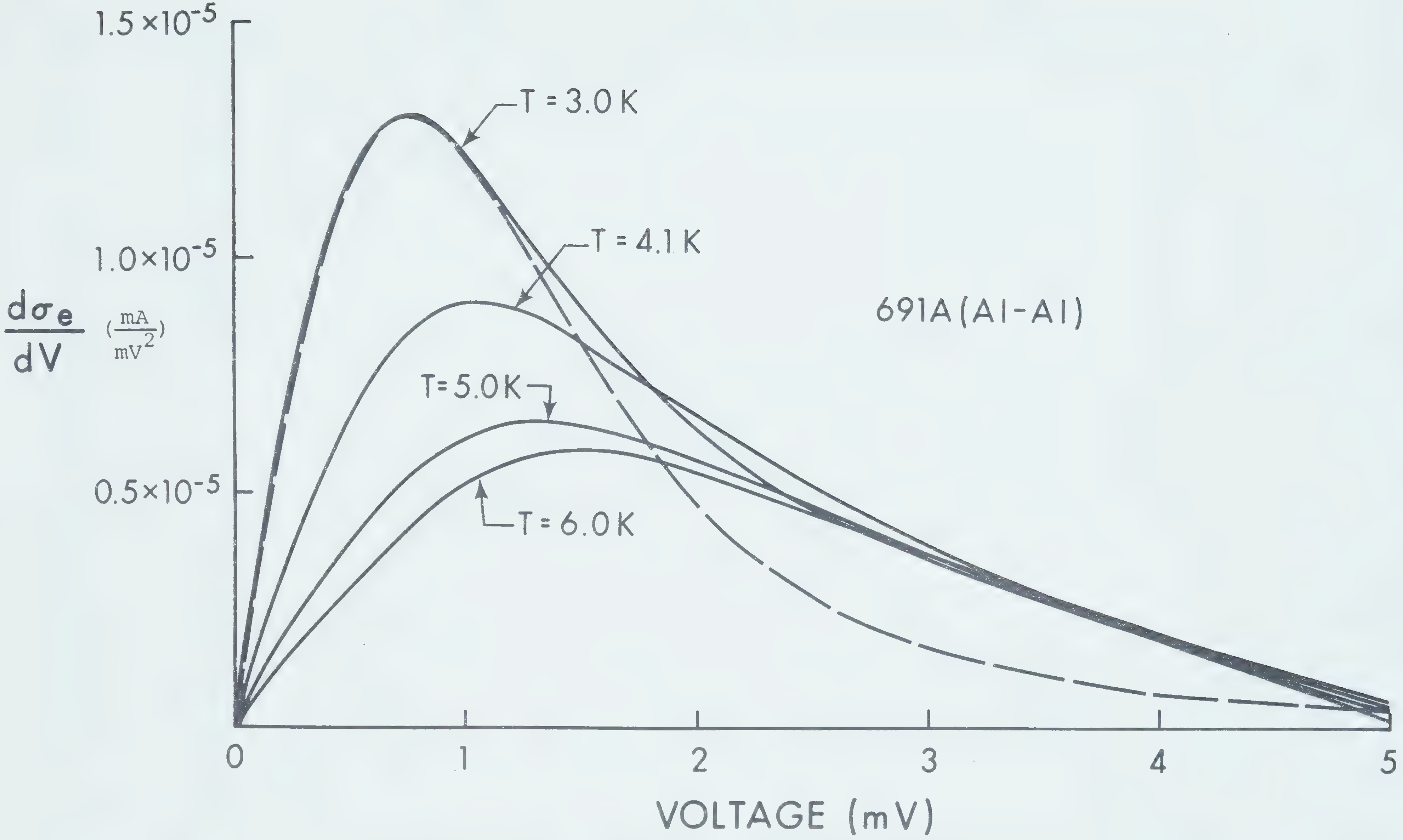

Fig. (3.7). $d\sigma_e/dV$ vs V. (expt. ——— ; theory — — —).

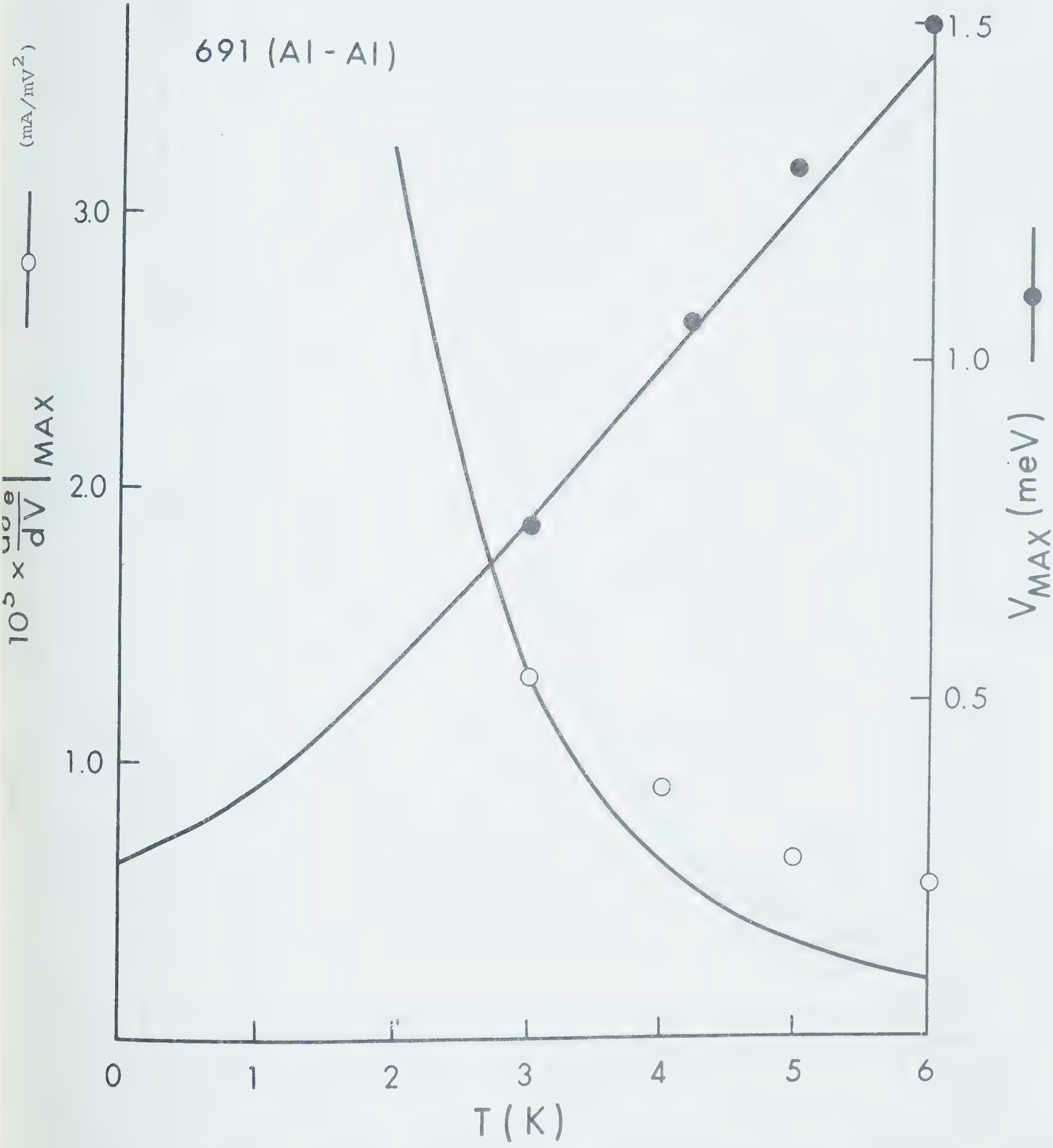

Fig. (3.8). Peak height and position vs temperature (expt. O ● ; theory ——).

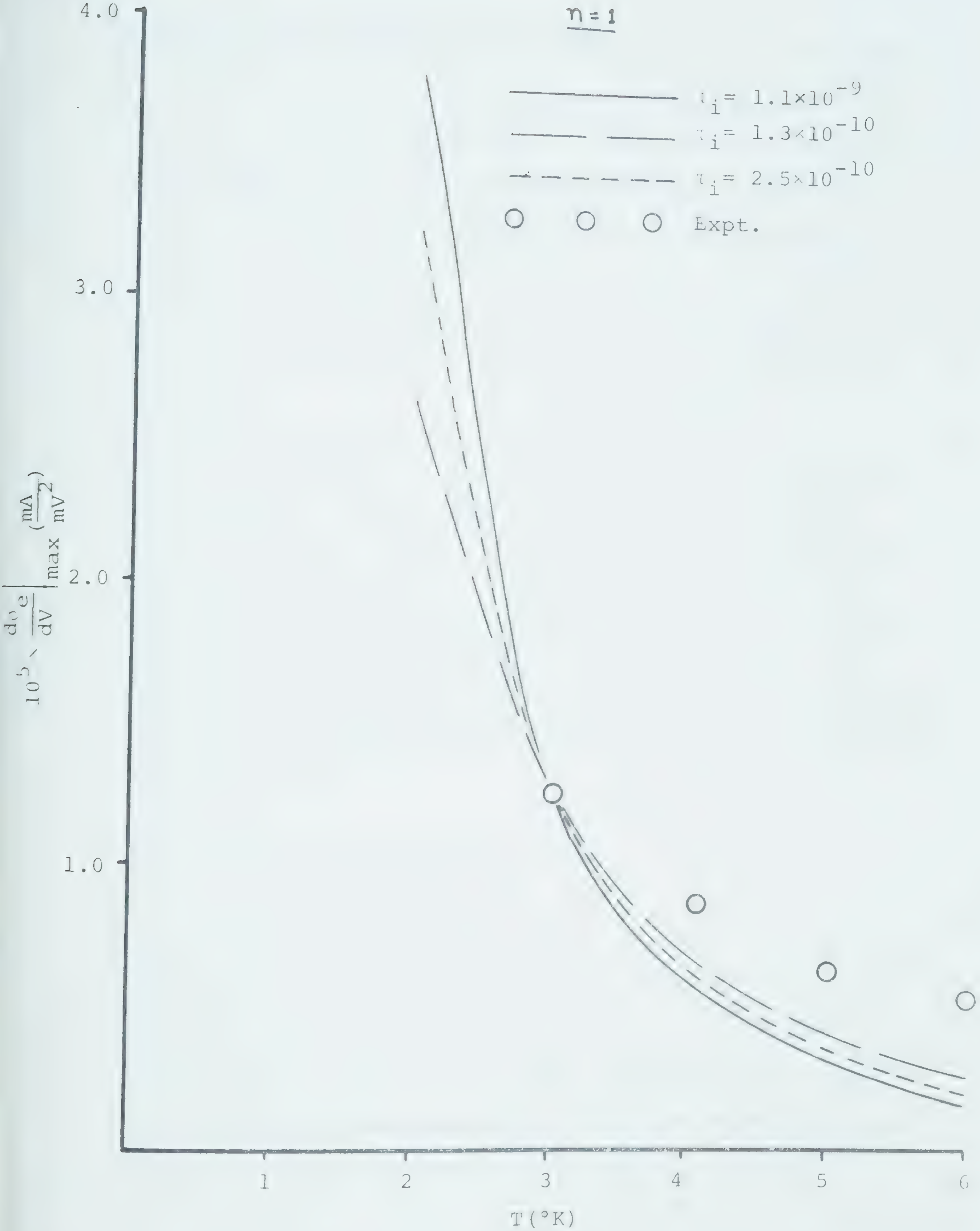

Fig. (3.9). Dependence of peak position on τ_i.

the peak amplitudes with different τ_i's. We have fixed the theoretical amplitude to agree with experiment at 3°K. Fig. (3.10) shows how the peak position behaves with changing τ_i. We note that there is relatively little change in the characteristics when the impurity time τ_i is varied over an order of magnitude. We may conclude that the zero-bias anomaly shape depends weakly upon the nature of the elastic scattering mechanisms in the film.

We have also calculated the behavior of the zero-bias anomaly for the case where $n = 2$ (i.e. $\alpha^2(\omega)F(\omega) = a_2 \omega^2$). In Fig. (3.11) we show the second derivative of current for $n = 2$ at 3°K. For comparison we also show the experimental data as well as the $n = 1$ result that was illustrated in Fig. (3.7). The $n = 2$ model curve was fitted to the experimental data as shown and yielded the values

$$\tau_i = 3.5 \times 10^{-9} \text{ sec}$$

$$\tau_B = 2.7 \times 10^{-6} \text{ sec}$$

where the electron-phonon coupling constant $a_2 = .0003/\text{meV}^2$ was again chosen to agree with the calculation of Carbotte and Dynes (1968). The theoretical and experimental peak heights and positions of the second derivative are compared in Fig. (3.12) and Fig. (3.13)

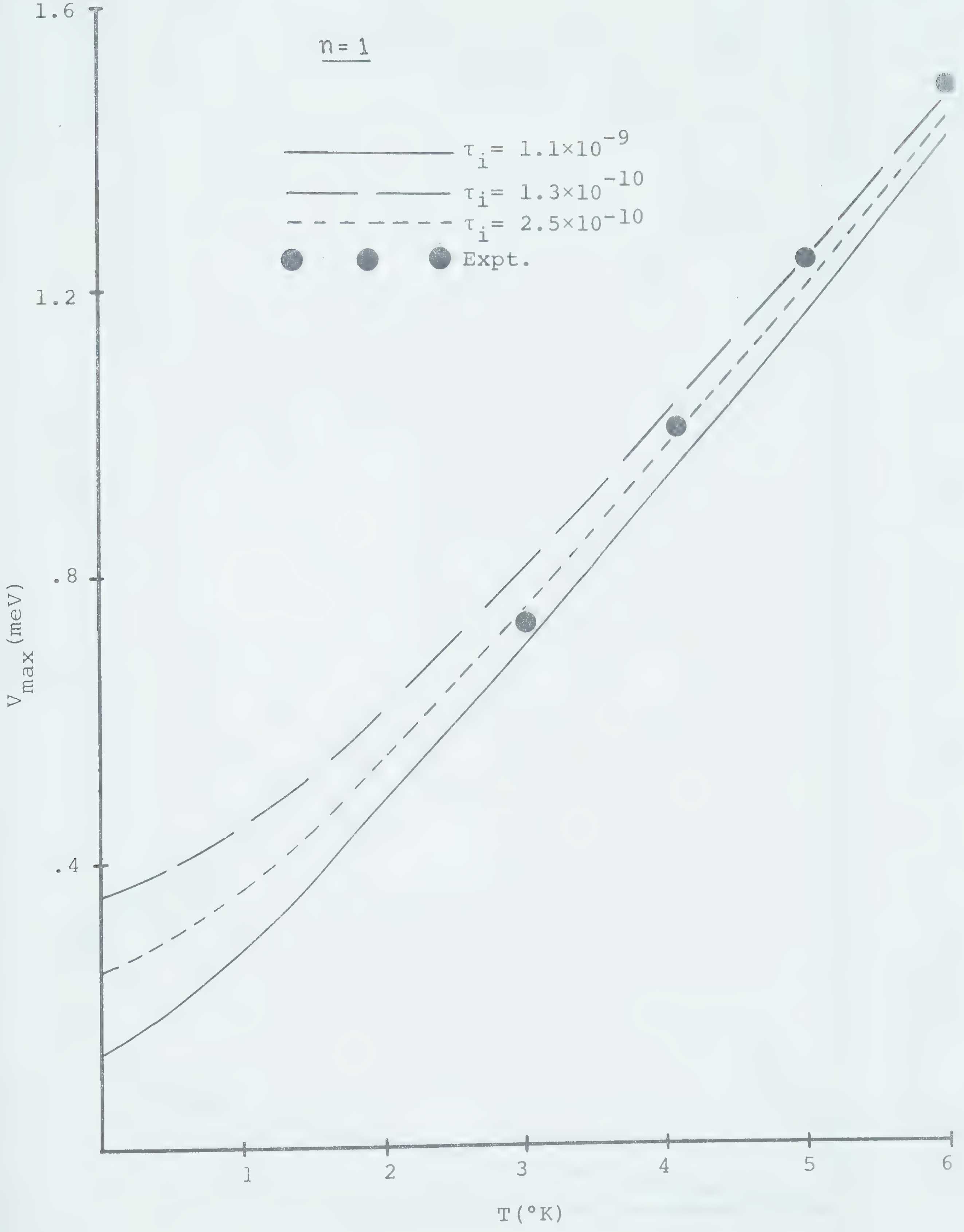

Fig. (3.10). Dependence of peak position on τ_i.

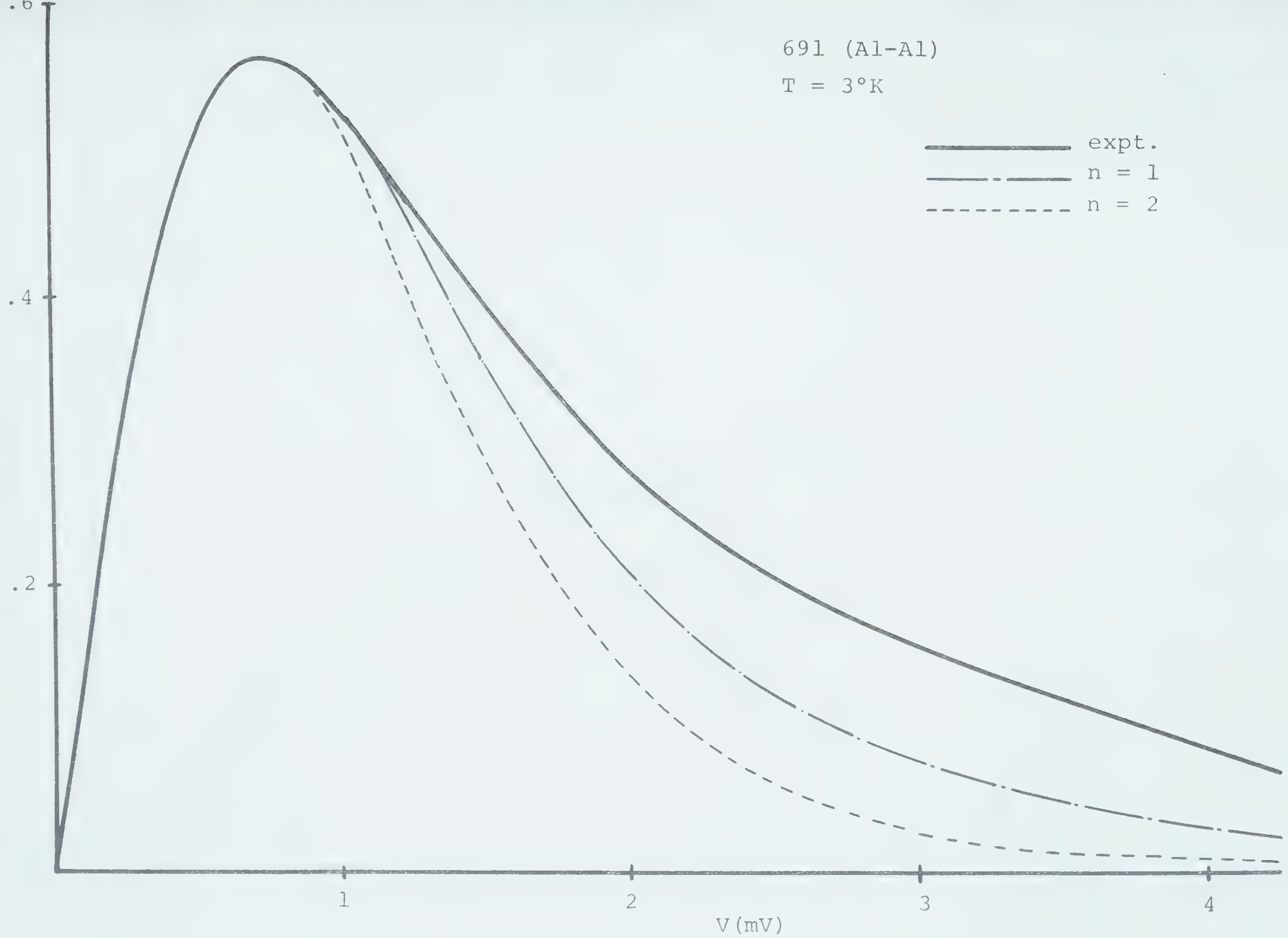

Fig. (3.11). Model dependence of ZBA.

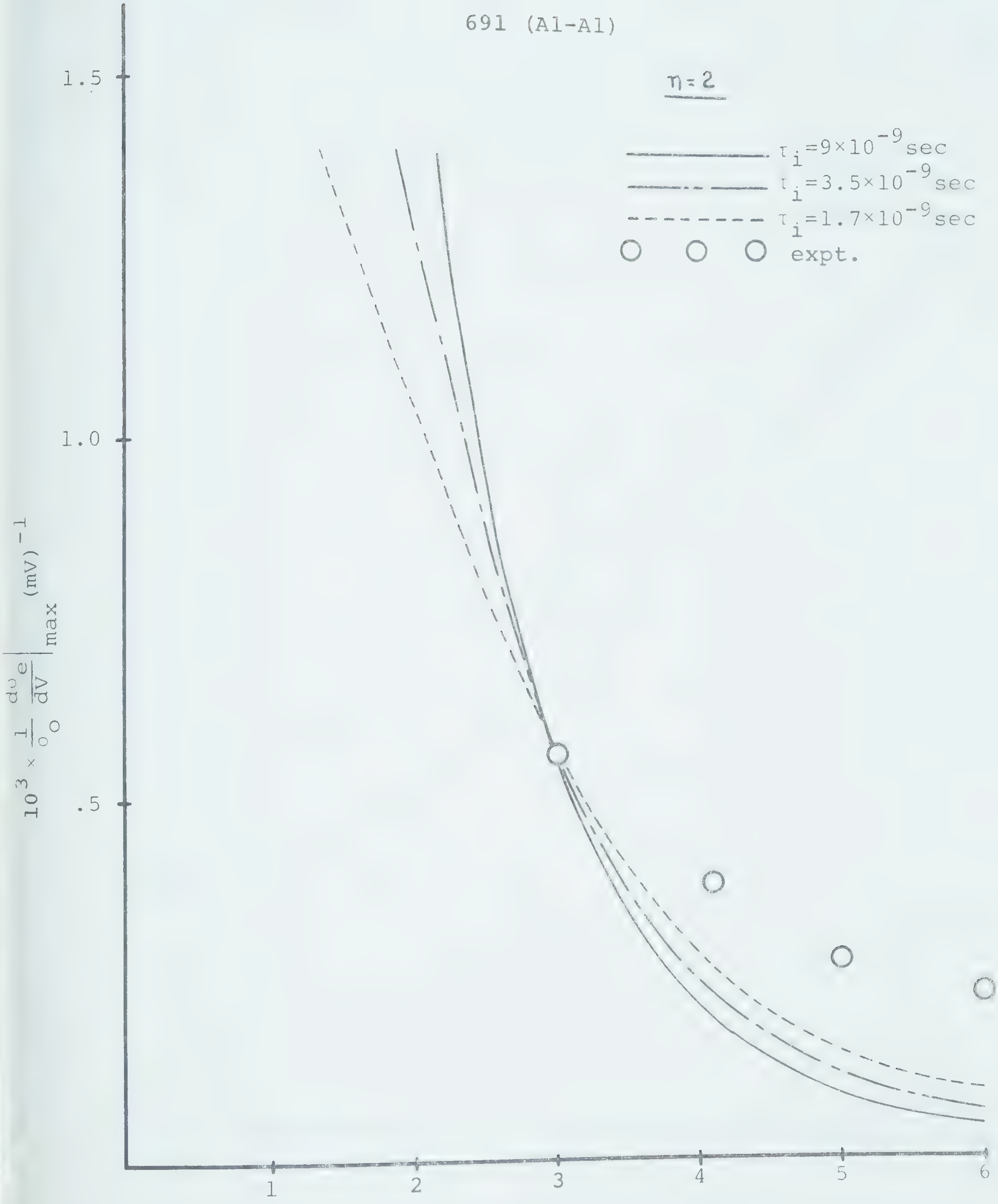

Fig. (3.12). Dependence of peak height on τ_i(n=2).

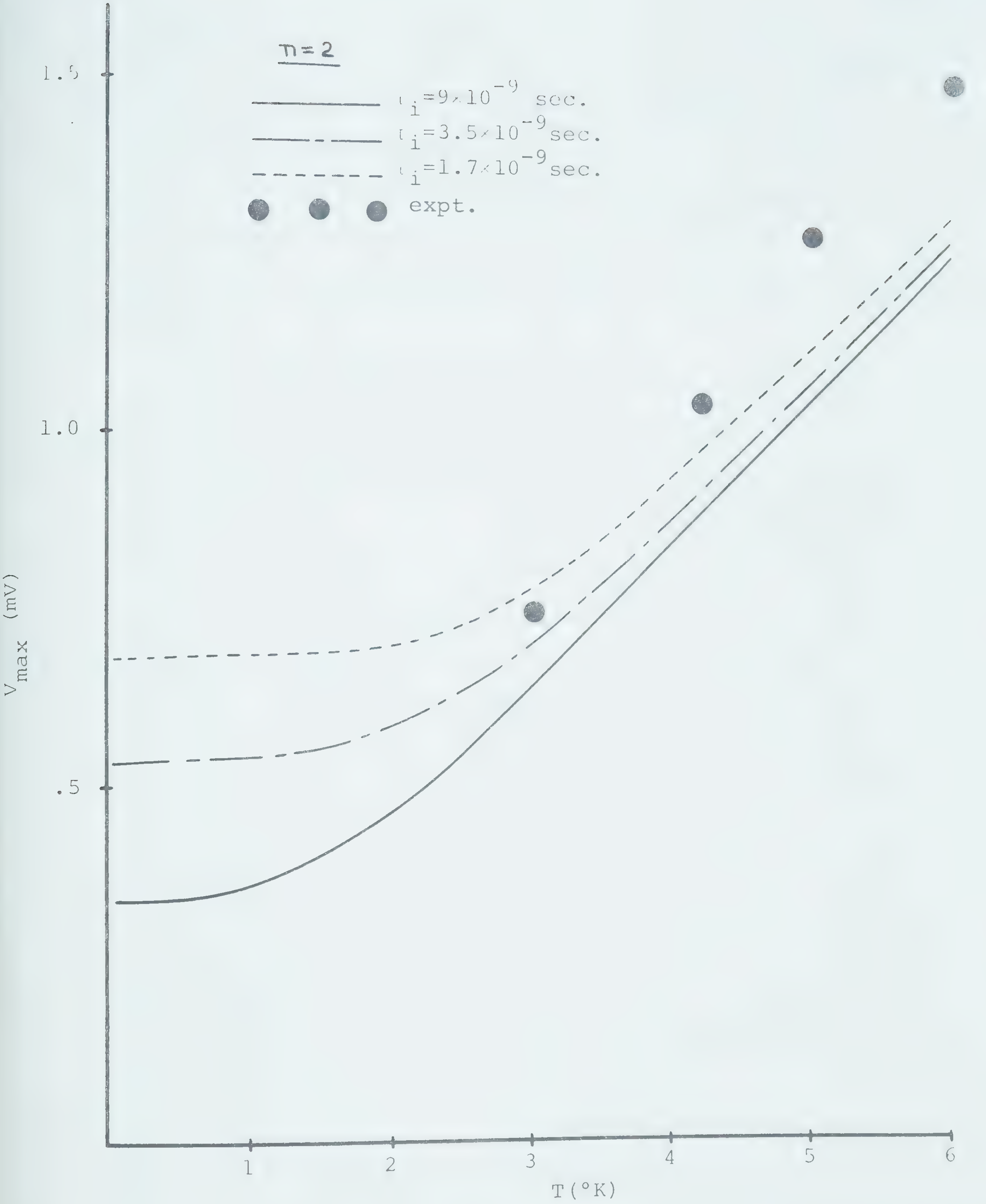

Fig. (3.13). Dependence of peak position on τ_i (n=2).

respectively for different choices of τ_i. The results again show that the peak heights and positions are relatively insensitive to τ_i. In general it may be noted that the overall behavior of the n=2 model is very similar to that of the n=1 model, although the agreement with experiment is poorer in the case of the former.

An additional example of a tunnel junction that displays the ZBA behavior is that of a Pb-PbO-Au junction whose experimental derivative of even conductance is shown in Fig. (3.14). Although the ZBA structure is clearly in evidence at low bias, it is masked to some extent by a rising background. This is probably due to inelastic tunneling of electrons at the lead-oxide interface. In order to account for this in a theoretical calculation, we have simply fitted a linear background to obtain agreement with the experimental data at 1.13°K. The theoretical curves at higher temperatures were then generated with the same set of parameters. The calculation was done using an n=1 model. We find that although the shapes of the curves agree at higher temperatures, theory predicts a stronger temperature dependence of the amplitude than is measured experimentally.

In conclusion, the observed structure near zero bias in the conductance and its derivative $d\sigma/dV$ for

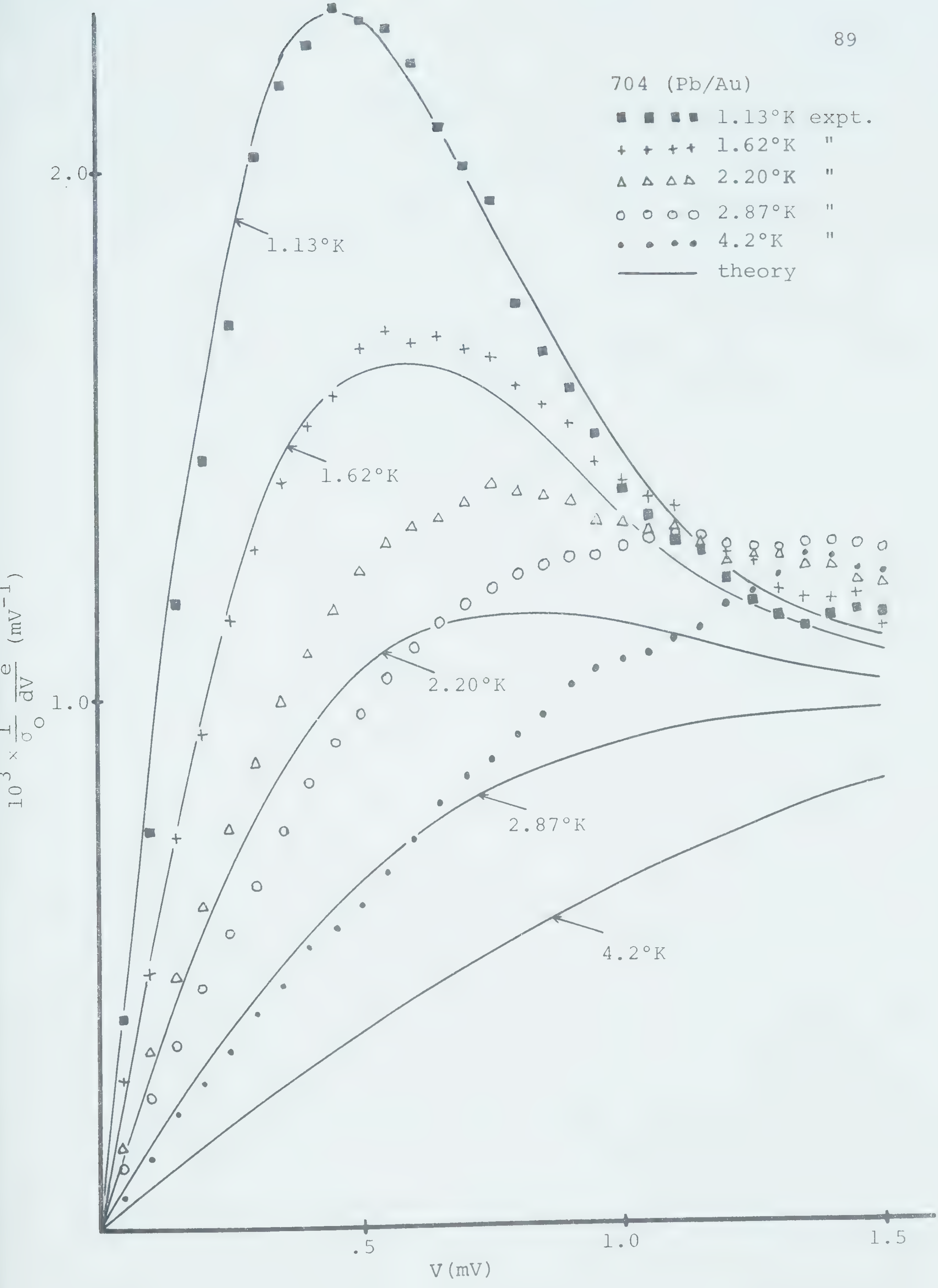

Fig. (3.14). Theoretical fit to Pb/Au ZBA

normal metal-insulator-metal tunneling junctions has been accounted for by including the effects of finite electron relaxation rates in the junction electrodes. The non-zero life-times lead to an observable blocking of otherwise available electron tunneling states at low bias. The fit to our data suggests that $\alpha^2(\omega)F(\omega)$ behaves nearly linearly at low energies rather than quadratically.

CHAPTER IV

INELASTIC ELECTRON TUNNELING

4.1 The Inelastic Current

In our treatment of the zero-bias anomaly we assumed the oxide barrier is without structure and provides essentially a homogeneous forbidden region to the electrons as would a vacuum. However tunneling measurements have shown that a considerable amount of non-ideal behavior is present in I-V characteristics which may be directly attributed to the presence of the barrier. A typical example is the Pb-PbO-Pb junction whose experimental second derivative of current is shown in Fig. (4.1) as a function of bias voltage. We note the large amount of structure present in the second derivative up to 60 meV. This behavior is due to the fact that electrons may lose energy as they tunnel through the barrier. The oxide is host to a number of mechanisms that may cause the electron to tunnel inelastically. The oxide may have bulk phonon structure as well as ever present impurities that provide molecular rotational and vibrational excited states. The metal-oxide interface may also provide additional degrees of freedom.

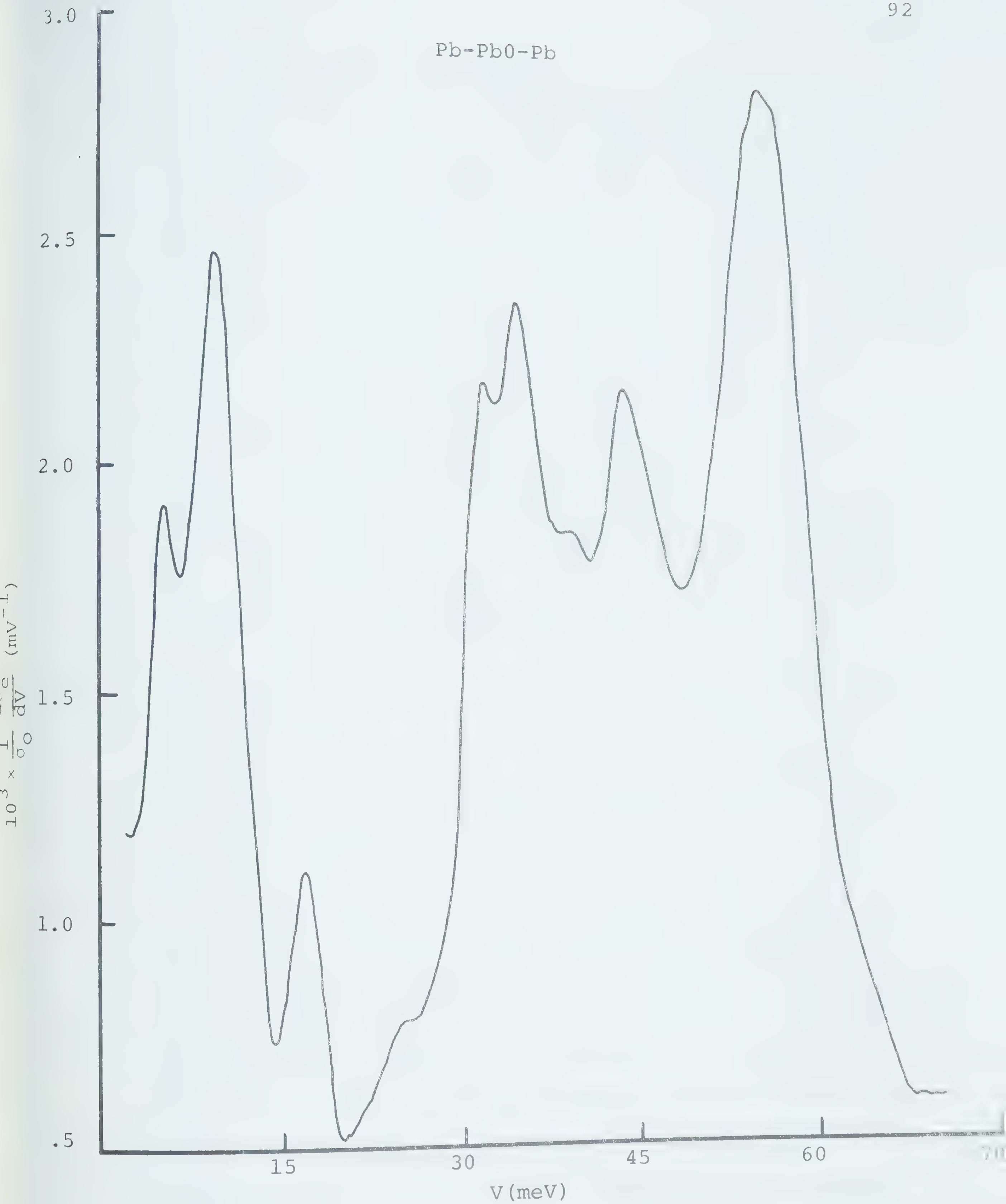

Fig. (4.1). Second derivative of current vs voltage for a Pb-Pb0-Pb junction.

If a voltage V is applied to a junction, the tunneling is elastic to a first approximation and the I-V relationship is linear. However, suppose that at T = 0 there is a system in its ground state that requires an energy $\hbar\omega_o$ to be excited. If the bias energy eV is less than $\hbar\omega_o$, the electron cannot tunnel inelastically by exciting this system because there are no available states in the other metal. When $eV = \hbar\omega_o$, the electron may now tunnel inelastically. Thus an electron in a definite energy state E has more than one available energy state into which it may make a transition. The opening of this new threshold will result in an additional current and therefore a small change of slope in the I-V curve at $eV = \hbar\omega_o$. Consequently there will be a step in the conductance and a spike in the derivative of conductance at this bias. In practice a finite temperature will smear the Fermi surface of both metals and will thus smear the spike although it will be centered about $eV = \hbar\omega_o$. In general a continuous excitation spectrum will be present in the oxide. The second derivative of current will then mime the frequency spectrum of the barrier. In principle the tunnel junction will then act as a spectroscopic probe of the barrier and any impurities within it. Lambe and Jacklevic (1968) confirmed in a series of well prepared experiments that this was true in practice. They showed

that one could observe and identify molecular vibrations in doped M-I-M junctions. They also showed how one could estimate the effect of temperature on the line-width of a spectral peak due to the smearing of the Fermi surfaces in the metals. We shall obtain their result here in a slightly different fashion.

The mechanism whereby coupling occurs between the tunneling electrons and internal states of the barrier may be thought of as a perturbation of the barrier potential. Consider the transmission coefficient for the WKB barrier given by Eqn. (2.19). If $\delta(x)$ is some small perturbation to the barrier potential $\phi(x)$ we have

$$P(E_x) = \exp\left(-\int_{x_\ell}^{x_r} \{\frac{2m}{\hbar^2}[\phi(x)-\delta(x)-E_x]\}^{\frac{1}{2}} dx\right).$$

If $\delta(x)$ is small we can make an expansion to first order in $\delta(x)$ to obtain

$$P(E_x) = \exp\left(-\int_{x_\ell}^{x_r} \{\frac{2m}{\hbar^2}[\phi(x)-E_x]\}^{\frac{1}{2}} dx\right)\left(1 + \frac{1}{2}\int_{x_1}^{x_2} \{\frac{2m}{\hbar^2}(\frac{\delta^2(x)}{\phi(x)-E_x})\}^{\frac{1}{2}} dx\right)$$

The first term will give rise to the elastic current while the second term will give the inelastic contribution. However, this is a very over-simplified view of the inelastic process. The perturbation potential will be the result of a superposition of potentials which

depend upon the positions of the oxide atoms, the impurity molecules and perhaps the positions of the metallic atoms diffused into the oxide. As these positions are a function of time, they will contain factors like $\exp(i\omega_{\underline{q}}t)$ where $\omega_{\underline{q}}$ is the frequency of the normal modes of wave vector $\underline{q}$ of the system. Thus if one were to do the problem in the context of a time dependent perturbation expansion one would obtain energy and momentum conservation equations of the form

$$E_{\underline{k}}-E_{\underline{k}'} = \hbar\omega_{\underline{q}} \quad ; \quad \hbar\underline{k} - \hbar\underline{k}' = \hbar\underline{q}$$

where $E_{\underline{k}}$ and $h\underline{k}$ are the energy and momentum of the electron in the left hand metal and $E_{\underline{k}'}$ and $h\underline{k}'$ are the energy and momentum of the electron after it has tunneled through the barrier into the right hand metal. With this in mind we can treat the process of inelastic tunneling in exactly the same way as we determined the electron-phonon relaxation time in Section 3.2. That is, we suppose there exists, a matrix element $M_{\underline{kk}'}$ that connects the states $\underline{k}$ and $\underline{k}'$ on either side of the barrier inelastically. If we make use of Fig. (3.2) and imagine that a barrier separates the initial and final states $\underline{k}$ and $\underline{k}'$ respectively then we can write the transition rate for the process whereby an electron in state $\underline{k}$ on the left tunnels inelastically into the

right hand metal. That is,

$$T_{\underline{k}} = \frac{2\pi}{\hbar} \sum_{\underline{k}'} |M_{\underline{kk}'}|^2 \{\delta(E_{\underline{k}}-E_{\underline{k}'}-\hbar\omega_{\underline{q}})[f^0_{\underline{k}}(1-f^0_{\underline{k}'})(1+N^0_{\underline{q}})-f^0_{\underline{k}'}(1-f^0_{\underline{k}})N_{\underline{q}}]$$

$$+\ \delta(E_{\underline{k}}-E_{\underline{k}'}+\hbar\omega_{\underline{q}})[f^0_{\underline{k}}(1-f^0_{\underline{k}'})N^0_{\underline{q}}-f^0_{\underline{k}'}(1-f^0_{\underline{k}})(1+N_{\underline{q}})]\} \tag{4.1}$$

where $f^0_{\underline{k}}$ and $f^0_{\underline{k}'}$ are the equilibrium distributions in the left and right hand metals respectively. $N^0_{\underline{q}}$ is the equilibrium distribution function for the internal degrees of freedom in the barrier, and we assume that $N_{\underline{q}}$ depends only on $\omega_{\underline{q}}$. We assume that the left hand side is at bias energy eV above the right hand side. Therefore

$$f^0_{\underline{k}} = \frac{1}{1 + e^{E_{\underline{k}}-\mu-eV/k_BT}} \qquad f^0_{\underline{k}'} = \frac{1}{1 + e^{E_{\underline{k}'}-\mu/k_BT}} \tag{4.2}$$

We define $\Delta f_{\underline{k}} = f^0_{\underline{k}}-f^0_{\underline{k}}$ (V=0) and make use of the fact that the transition rate is zero for zero bias. Therefore Eqn. (4.1) becomes

$$T_{\underline{k}} = \frac{2\pi}{\hbar} \Delta f_{\underline{k}} \sum_{\underline{k}'} |M_{\underline{kk}'}|^2 \{\delta(E_k-E_{\underline{k}'}-\hbar\omega_{\underline{q}})[1+N^0_{\underline{q}}-f^0_{\underline{k}'}]$$

$$+\ \delta(E_{\underline{k}}-E_{\underline{k}'}+\hbar\omega_{\underline{q}})[f^0_{\underline{k}'}+N^0_{\underline{q}}]\}\ . \tag{4.3}$$

Now

$$\sum_{\underline{k}'} = \frac{AL'}{\pi(2\pi)^2} \int d^2\underline{k}'_{||} \int_0^\infty \frac{dE_{\underline{k}'}}{\hbar v'_x} \tag{4.4}$$

according to our density of states and box normalization scheme presented in Section 2.5. Carrying out the summation in Eqn. (4.3) we find

$$T_{\underline{k}} = \frac{2\pi}{\hbar}\,\Delta f_{\underline{k}} \int_0^\infty d(\hbar\omega)\,\alpha_{\underline{k}}^2(\hbar\omega)\,F_{\underline{k}}(\hbar\omega)\,[2N^{o}(\hbar\omega)+1+f^{o}(E_{\underline{k}}+\hbar\omega-\mu) - f^{o}(E_{\underline{k}}-\hbar\omega-\mu)] \qquad (4.5)$$

where we have defined

$$\alpha_{\underline{k}}^2(\hbar\omega)\,F_{\underline{k}}(\hbar\omega) = \frac{AL'}{4\pi^3}\int \frac{d^2\underline{k}'_{||}}{v'_x}\,|M_{\underline{kk}'}|^2\,\delta(\hbar\omega-\hbar\omega_{\underline{q}}) \qquad (4.6)$$

The inelastic tunneling current is simply given by $\delta I = 2e \sum_{\underline{k}} T_{\underline{k}}$. Therefore

$$\delta I = \frac{4\pi emA}{h^3}\int_0^\infty dE\,\Delta f_E \int_0^\infty d(\hbar\omega)\,[2N^{o}(\hbar\omega)+1+f^{o}(E+\hbar\omega-\mu) - f^{o}(E-\hbar\omega-\mu)]\;G_{\underline{k}}(\hbar\omega) \qquad (4.7)$$

where

$$G(\hbar\omega) \equiv \frac{4LAL'}{m(2\pi)^3}\int\frac{d^2\underline{k}_{||}}{v_x}\int\frac{d^2\underline{k}'_{||}}{v'_x}\,\delta(\hbar\omega-\hbar\omega_{\underline{q}})\,|M_{\underline{kk}'}|^2 \;. \qquad (4.8)$$

If we use the variable $\varepsilon = E-\mu-eV$ in Eqn. (4.7) we obtain

$$\delta I = c \int_{-\infty}^{+\infty} d\varepsilon\,[f^{o}(\varepsilon)-f^{o}(\varepsilon+eV)] \int_{0}^{\infty} d\omega\; G(\omega)\,[2N^{o}(\omega)+f^{o}(\varepsilon+\omega) + f^{o}(\omega-\varepsilon)] \tag{4.9}$$

where

$$c = \frac{4\pi emA}{h^3} .$$

We have expressed the current in terms of the dimensionless function $G(\omega)$ defined in Eqn. (4.8). We note that $G(\omega)$ is defined in a fashion analogous to the function $\alpha^2F(\omega)$ as in Eqn. (3.24). As such $G(\omega)$ may be thought of as the product of the spectral density of states of the barrier multiplied by an effective frequency dependent coupling constant. It is not our intent here to attempt a calculation of $G(\omega)$ from Eqn. (4.8). However it will essentially be dependent upon the transmission coefficient and the dynamics of the coupling of electrons to internal degrees of freedom of the barrier.

We shall now assume that $N^{o}(\omega)$ is the equilibrium Bose factor as defined in Eqn. (3.27). Thus Eqn. (4.9) would describe the inelastic tunneling current due to the bulk oxide phonons in the barrier. We note that because of the properties of the statistical factors in Eqn. (4.9) the inelastic tunneling current is an odd function of bias voltage. Thus the conductance due to

it will be an even function of bias. This has been established experimentally in the case of Pb-Pb0-Pb junctions by Rowell, McMillan and Feldmann (1969) and is true in general for any junction where the oxide phonons may be identified easily. We also note that the T = 0 limit of the inelastic tunneling current as given by Eqn. (4.9) becomes

$$\delta I = c \int_0^V d\varepsilon \int_0^\varepsilon d\omega \; G(\omega) \quad . \tag{4.10}$$

Therefore the inelastic zero temperature conductivity is given by

$$\delta\sigma = c \int_0^V d\omega \; G(\omega) \tag{4.11}$$

and thus

$$\frac{d}{dV} (\delta\sigma) = c \; G(V) \; . \tag{4.12}$$

For finite temperatures, Eqn. (4.9) may be simplified considerably by reversing the order of integration. The integration over the statistical factors may then be carried out analytically and yields

$$\delta I = c \int_0^\infty d\omega \; G(\omega) \{ (V-\omega) [N^o(V-\omega) - N(-\omega)] - (V+\omega) [N^o(V+\omega) - N(\omega)] \} \; . \tag{4.13}$$

Physically, the interesting quantity is the second derivative of current and is given by

$$\frac{d^2}{dV^2}(\delta I) = c\int_0^\infty d\omega\; G(\omega)\cdot\frac{1}{k_BT}\left[K\left(\frac{V-\omega}{k_BT}\right) - K\left(\frac{V+\omega}{k_BT}\right)\right] \qquad (4.14)$$

where the kernel function K(x) is defined by

$$K(x) = \frac{e^{2x}(x-2) + e^{x}(x+2)}{(e^{x}-1)^{3}} \qquad (4.15)$$

and is an even function of x. In Eqn. (4.14) the term $K((V-\omega)/k_BT)$ represents inelastic current flow by emission of a phonon of energy $\hbar\omega$ whereas the term $K((V+\omega)/k_BT)$ refers to inelastic current flow with absorption of a phonon of energy $\hbar\omega$ (anti-Stokes flow). If we have an extremely narrow spectral line such that it may be approximated by a delta function distribution (i.e. $G(\omega) \sim \delta(\omega-\omega_o)$), then the second derivative of current due to this resonance is given by

$$\frac{d^2}{dV^2}(\delta I) \propto \frac{c}{k_BT}\left[K\left(\frac{V-\omega_o}{k_BT}\right) - K\left(\frac{V+\omega_o}{k_BT}\right)\right] \quad . \qquad (4.16)$$

If the position of the resonance is much greater than the thermal energy (i.e. $\hbar\omega_o >> k_BT$) the absorption or anti-Stokes term is negligible and we are left with

$$\frac{d^2}{dV^2}(\delta I) \propto \frac{c}{k_BT}K\left(\frac{V-\omega_o}{k_BT}\right) \quad . \qquad (4.17)$$

Using Eqn. (4.15) we find that the response in the second derivative takes the form of a distribution of

height proportional to $c/6k_BT$ and linewidth 5.44 k_BT centered at $eV = \hbar\omega_o$. This is precisely the behavior that Lambe and Jacklevic (1968) found experimentally and justified theoretically. This analysis describes the linewidth expected for a sharp resonance due to the thermal smearing of the Fermi levels in both normal metal electrodes. Although there may be other sources of linewidth broadening in the actual phonon spectra of the barrier or the molecular vibrational and rotational levels of impurities, nevertheless this treatment illustrates that there is a lower limit on the resolving power of a tunneling spectrometer using normal metals.

It is interesting to study the behavior of the total area or intensity of the second derivative of current vs voltage curves. Thus

$$\int_0^\infty \left[\frac{d^2}{dV^2}(\delta I)\right]dV = c\int_0^\infty d\omega\ G(\omega)\int_0^\infty dV.\frac{1}{k_BT}\left[K\left(\frac{V-\omega}{k_BT}\right)-K\left(\frac{V+\omega}{k_BT}\right)\right]. \tag{4.18}$$

The second integral in Eqn. (4.18) can be done exactly and we find

$$\int_0^\infty \left[\frac{d^2}{dV^2}(\delta I)\right]dV = c\int_0^\infty d\omega\ G(\omega)\left[1+\frac{2e^{\omega/k_BT}(1-\omega/k_BT)-1}{(e^{\omega/k_BT}-1)^2}\right]. \tag{4.19}$$

If the spectra occur at frequencies ω such that $\omega \gg k_BT$, the second term in the integrand above is very small

compared to unity and we obtain

$$\int_0^\infty [\frac{d^2}{dV^2} (\delta I)]dV = c \int_0^\infty d\omega \; G(\omega) = \text{constant} \; . \qquad (4.20)$$

Therefore for spectra located far above thermal energies the intensity or total area of the second derivative of current should be constant as a function of temperature. This was also verified experimentally by Lambe and Jacklevic in the same paper.

4.2 Inversion for G(ω) in Terms of the Second Derivative of Inelastic Tunneling Current

Let us consider Eqn. (4.14) for the moment as an integral equation for $G(\omega)$ in terms of the second derivative of inelastic current which we shall denote by

$$I''(V) = \frac{1}{c} \frac{d^2}{dV^2} (\delta I) \quad . \qquad (4.21)$$

For a fixed temperature T we shall assume that $I''(V)$ is absolutely integrable, allowing us to define its Fourier transform by

$$I''(s) = \frac{1}{\sqrt{2\pi}} \int_{-\infty}^{\infty} I''(V) \; e^{-isV} \; dV \quad . \qquad (4.22)$$

Since the kernel function $K(x)$ is even Eqn. (4.14) may be cast into the form

$$\frac{I''(s)}{\kappa(sk_BT)} = -\frac{4i}{\sqrt{2\pi}}\int_0^\infty G(\omega)\ \sin(s\omega)d\omega \quad , \tag{4.23}$$

where

$$\kappa(s) \equiv \int_0^\infty \cos(sx)\cdot K(x)\ dx \quad . \tag{4.24}$$

Making use of the identity

$$\int_0^\infty \frac{\sin(ax)\cos(bx)}{x}dx = \frac{\pi}{2}\ \theta(a-b) \quad , \tag{4.25}$$

we obtain

$$G(\omega) = \frac{i}{\sqrt{2\pi}}\int_0^\infty \frac{I''(s)}{\kappa(sk_BT)}\ \sin(\omega s)ds \quad . \tag{4.26}$$

$\kappa(s)$ may be evaluated in close form to yield

$$\kappa(s) = 2\ (\pi s)^2\ \frac{1}{(e^{\pi s} - e^{-\pi s})^2} \quad . \tag{4.27}$$

Therefore the barrier function $G(\omega)$ may be determined from $I''(V)$ by means of the formula

$$G(\omega) = \frac{2}{\pi}\int_0^\infty \frac{\sin(s\omega)\sinh^2(s\pi k_BT)}{(s\pi k_BT)^2}\int_0^\infty I''(V)\ \sin(sV)dV \tag{4.28}$$

The zero temperature limit is easily obtained making use of Eqn. (4.25) and we note that

$$G(\omega) \xrightarrow[T\to 0]{} I''(V)$$

in accordance with Eqn. (4.12). Eqn. (4.28) represents a valid inversion for the spectral quantity $G(\omega)$ in principle. In practice the experimental noise and background inherent in measurements of $I''(V)$ would severely limit its applicability. However, given the measured quantity $I''(V,T')$ at some temperature T', it allows us to deduce the corresponding $I''(V,T)$ at some higher temperature $T > T'$. If we substitute Eqn. (4.28) into Eqn. (4.19) a long calculation yields the following relationship

$$I''(V,T) = \frac{1}{k_B T} \int_0^\infty I''(V',T') \left[K\left(\frac{V-V'}{k_B T}; \frac{2\pi T'}{T}\right) - K\left(\frac{V+V'}{kT}; \frac{2\pi T'}{T}\right) \right] dV' \tag{4.29}$$

where the modified kernel function $K(x;y)$ is defined by

$$K(x;y) = \frac{2}{y^2} \left(\frac{e^{2x}(x - x\cos y - y\sin y) + e^{x}(x + y\sin y - x\cos y)}{(e^{2x} - 2e^{x}\cos y + 1)(e^{x} - 1)} \right) \tag{4.30}$$

In the zero temperature limit this reduces to the familiar form;

$K(x;0) = K(x)$, (previously defined in Eqn.(4.15)).

It may be noted that for certain values of the ratio T'/T the kernel $K(x;y)$ is quite simple. For example, if $T'/T = 1/2$ then

$$K(x,\pi) = \frac{4xe^{x}}{\pi^{2}(e^{2x}-1)} = \frac{2x}{\pi^{2}\sinh x} \quad . \qquad (4.31)$$

$K(x,\pi)$ corresponds to a distribution of height $2/\pi^2$ and linewidth $4.4k_BT$. Eqn. (4.29) may be of use to workers in low temperature tunneling spectroscopy who wish to isolate the natural linewidth broadening in sharp spectra due to the thermal smearing of the Fermi levels in the electrodes from other sources of broadening inherent in the barrier.

CHAPTER V

TUNNELING IN SUPERCONDUCTORS

5.1 The Semiconductor Picture

The subject of electron tunneling can be discussed in varying degrees of sophistication. The simplest method is that used by Giaever (1960) to explain his original experiments in superconductive tunneling. In this method the superconductor is treated in terms of single particle excitations only (quasi-particles) since they are the ones involved in the tunneling process. The quasi-particle density of states is drawn with an energy gap of 2Δ centered at the Fermi energy as in Fig. (5.1a). At $T = 0°K$ all states below the gap are filled and those above the gap are empty. At finite temperatures particle-hole pairs are created, the particles existing above the gap while the holes lie below the gap. Tunneling into the gap region is not allowed and this leads to structure in the I-V curve which gives a measure of the energy gap as well as of the quasi-particle density of states. In this approach to superconductive tunneling the superconductor is treated much like a semiconductor and consequently it is called the semiconductor model

of a superconductor. Giaever was able to obtain a good fit to experimental data by using this simple model.

Following Giaever, we make the following assumptions in deriving the tunneling current.

1) The quasi-particles of both superconductors are independent particles satisfying Fermi-Dirac statistics and have an occupation probability given by

$$f^{o}(\varepsilon) = \frac{1}{1 + e^{\varepsilon/k_B T}} \tag{5.1}$$

where ε is measured from the Fermi energy.

2) The difference in Fermi energies between the two superconductors is given by the applied voltage V.

3) There exists a matrix element $M_{\underline{kk}'}$ connecting the states $\underline{k}$ and $\underline{k}'$ on opposite sides of the barrier. This matrix element is considered constant when the energy is varied in the region of interest.

4) The density of quasi-particle states is considered to be constant when the metal is in its normal state

$$\rho_{\underline{k}}(\varepsilon) = \rho_N \tag{5.2}$$

and is given by

$$\rho_{\underline{k}}(\varepsilon) = \rho_N \, n(\varepsilon) \qquad (5.3)$$

when the metal is superconducting. $n(\varepsilon)$ is the reduced density of states and according to BCS is given by

$$n(\varepsilon) = \frac{|\varepsilon|}{\sqrt{\varepsilon^2 - \Delta^2}} \quad , \qquad |\varepsilon| > \Delta \qquad (5.4)$$

$$= 0 \qquad\qquad |\varepsilon| < \Delta \qquad (5.5)$$

where Δ is the energy gap considered to be independent of energy but not temperature.

With these assumptions we can write down the expression for the tunneling current in terms of transition probabilities in exactly the same way as we obtained Eqn. (3.39).

$$\text{i.e.} \quad I = \frac{4\pi e}{\hbar} \sum_{\underline{k}} \sum_{\underline{k}'} |M_{\underline{k}\underline{k}'}|^2 (f^o_{\underline{k}} - f^o_{\underline{k}'}) \, (E_{\underline{k}} - E_{\underline{k}'}) \quad . \qquad (5.6)$$

In section 2.5 the matrix element was evaluated for the case of normal electrodes and it was found to contain density of states factors that cancelled the densities of states in the summations over right and left hand states. In superconductors it can be argued (Bardeen (1961) and Harrison (1961)) that the density of states factors in $|M_{\underline{k}\underline{k}'}|^2$ are the same as in the normal metal. In superconductive tunneling it is necessary to make this assumption to obtain agreement with experiment. Thus we simply take

$$|M_{\underline{k}\underline{k}'}|^2 = \delta_{\underline{k}_{||}\underline{k}'_{||}} \; |M|^2 \tag{5.7}$$

and Eqn. (5.6) becomes

$$I = \frac{4\pi e}{h} \sum_{\underline{k}_{||}} \int_0 dE_{\underline{k}} [f^o(E_{\underline{k}}-\mu) - f^o(E_k-\mu+V)]\,|M|^2 \quad \rho_{\underline{k}}\rho_{\underline{k}'} \tag{5.8}$$

If we now make the replacements as in Eqn. (5.3) we find

$$I = \sigma_o \int_{-\infty}^{\infty} d\varepsilon \;\; [f^o(\varepsilon) - f^o(\varepsilon+V)]n(\varepsilon)n'(\varepsilon+V) \tag{5.9}$$

where

$$\sigma_o = \frac{4\pi e}{\hbar} \sum_{\underline{k}_{||}} |M|^2 \;\; \rho_N \;\rho_N' \quad . \tag{5.10}$$

In the limit that both metals are normal $n(\varepsilon) = n'(\varepsilon+V)=1$ and

$$I_{nn} = \sigma_o V \; .$$

Therefore σ_o is just the conductivity of the junction in the normal state. Using the definitions of the densities of states given by Eqn. (5.4) we obtain

$$I(V) = \sigma_o \int_{-\infty}^{+\infty} d\varepsilon \cdot \frac{|\varepsilon|}{\sqrt{\varepsilon^2-\Delta_\ell^2}} \cdot \frac{|\varepsilon+V|}{\sqrt{(\varepsilon+V)^2-\;\Delta_r^2}} \cdot [f^o(\varepsilon)-f^o(\varepsilon+V)] \tag{5.11}$$

where (ℓ,r) denotes (left, right). We shall not pursue

the quantitative aspects of Eqn. (5.11) as these are given in a number of excellent reviews (e.g. see Douglass and Falicov (1964) or Solymar (1972)). Rather, we simply present the results in diagramatical fashion and discuss the results qualitatively.

Fig. (5.1a) shows a semiconductor type of energy diagram for the case of tunneling between a normal metal and a superconductor. The density of states functions, according to BCS, are also included. At T = 0°K there are no excited quasi-particles in the superconductor and no excited electrons in the normal metal. Under these conditions it is easy to see that there is no current until a voltage of $V = \pm\Delta(0)$ is reached as in Fig. (5.1b). At $V = \pm\Delta(0)$ the current rises rapidly due to the sharp Fermi energy in the normal metal and also the very high density of states in the superconductor at the gap edge. As V is increased further the current continues to rise and approaches the curve for normal-normal (N-N) tunneling, coinciding with it for $V \gg \Delta(0)$. This is due to the fact that the superconducting density of states returns to that of the normal metal for energies $\varepsilon \gg \Delta(0)$ (Eqn. 5.4).

For finite temperatures there are excited quasi-particles above the gap as well as quasi-holes below

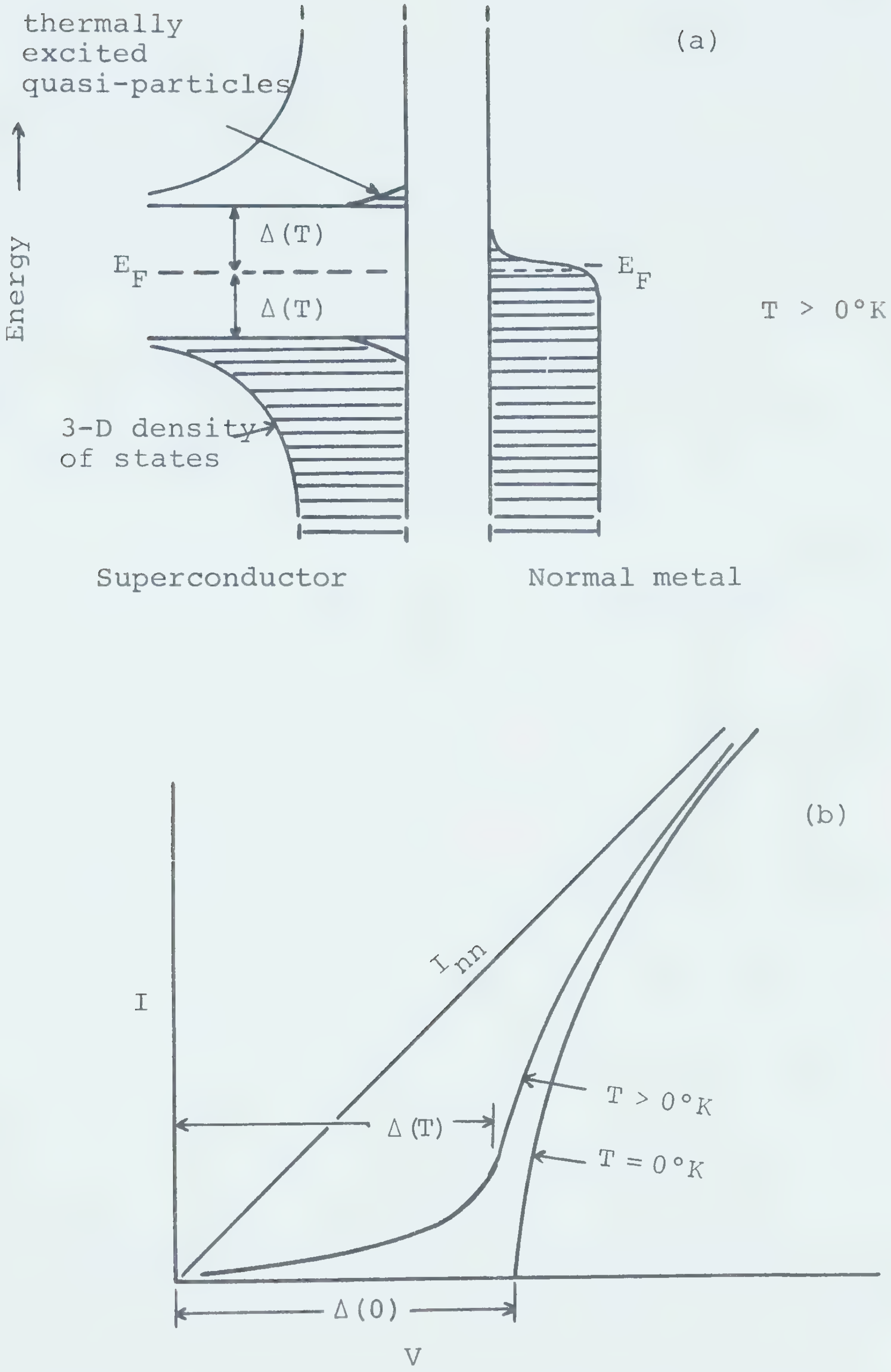
thermally
excited
quasi-particles
(a)
Energy
$\Delta(T)$
E_F
$\Delta(T)$
E_F
T > 0°K
3-D density
of states
Superconductor
Normal metal
(b)
I
I_{nn}
$\Delta(T)$
T > 0°K
T = 0°K
$\Delta(0)$
V

Fig. (5.1). (a) Energy level diagram for tunneling between a superconductor and a normal metal. (b) I-V curves expected on the basis of simple theory.

the gap in the superconductor. In the normal metal the Fermi level becomes smeared. Thus when V is increased from zero, current immediately begins to flow and continues to rise gradually until $V = \pm\Delta(T)$ is reached. At that point the density of states in the superconductor becomes large and the current increases more rapidly and approaches I_{nn} for $V >> \Delta(T)$.

The tunneling between two superconductors ($\Delta_r \neq \Delta_\ell$) is depicted in Fig. (5.2). At T = 0°K there are no excited states and tunneling does not occur until a voltage of $V = \pm(\Delta_\ell(0)+\Delta_r(0))$ is reached. At this point the current rises discontinuously because the density of states on both sides of the barrier is infinite at the gap edge. For $V >> (\Delta_\ell(0)+\Delta_r(0))$ the current approaches the n-n curve for tunneling as before.

At finite temperatures and for $V < (\Delta_r(T)-\Delta_\ell(T))$ the current increases gradually because the number of quasi-particles available for tunneling is increasing. However in the range $(\Delta_r(T)-\Delta_\ell(T) < V < (\Delta_r(T)+\Delta_\ell(T))$, the number of quasi-particles available for tunneling remains constant while, at the same time, the density of states in the right decreases. This leads to a decreasing current and thus negative resistance as shown in Fig. (5.2b). According to Eqn. (5.11) at $V=\Delta_r(T)-\Delta_\ell(T)$ there is a logarithmic singularity in the current. At

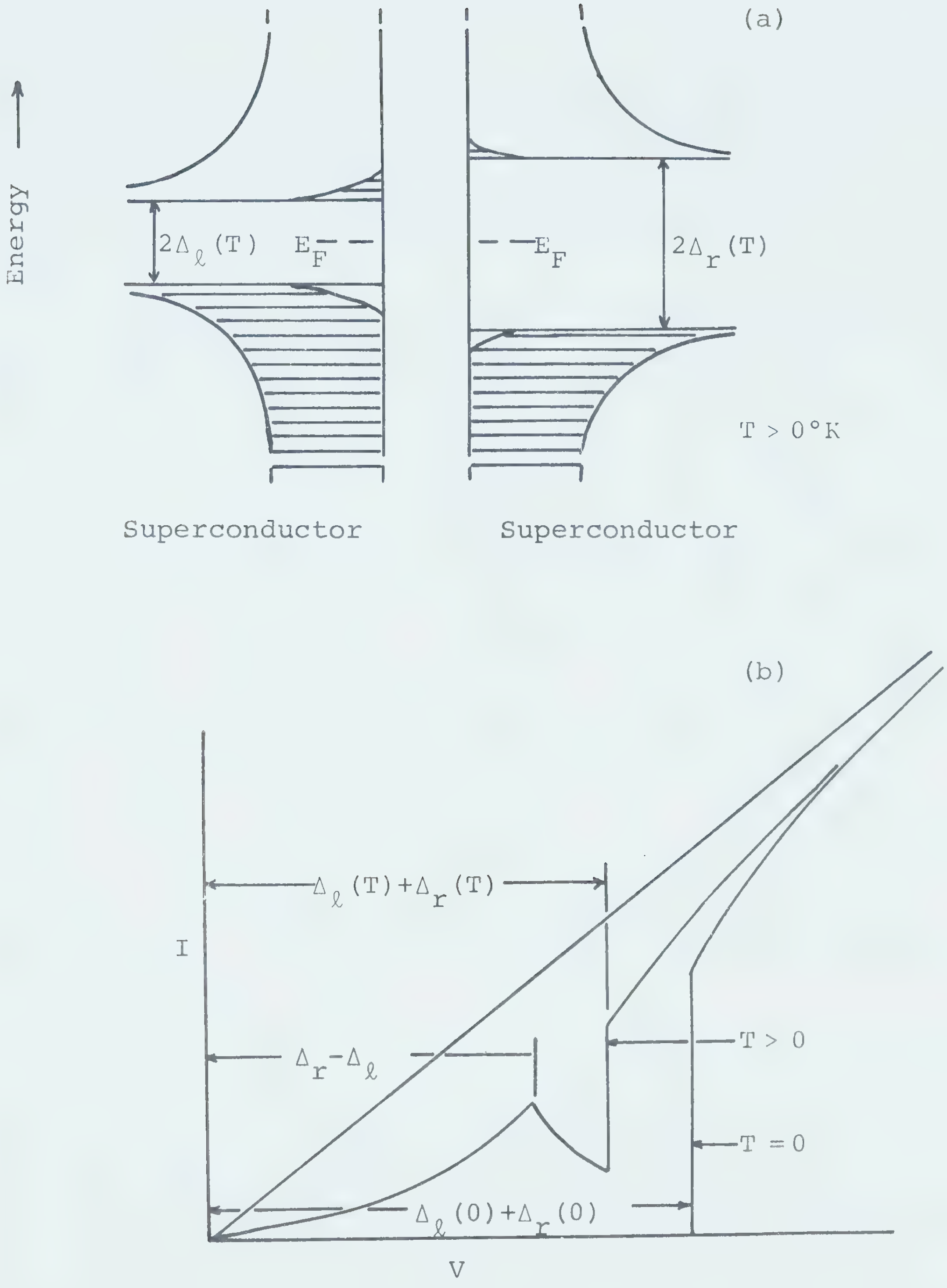
(a)
Energy
2Δℓ(T)
E_F
E_F
2Δr(T)
T > 0°K
Superconductor
Superconductor
(b)
Δℓ(T)+Δr(T)
I
Δr−Δℓ
T > 0
T = 0
Δℓ(0)+Δr(0)
V

Fig. (5.2). (a) Energy level diagram for tunneling between two different superconductors. (b) I-V curves expected on the basis of simple theory.

$V = \Delta_{\ell}(T) + \Delta_{r}(T)$ we again have an infinite density of states on both sides of the barrier and there is a discontinuous rise in current even for finite temperatures.

The special case of tunneling between identical superconductors is shown in Fig. (5.3). At $T = 0°K$ there is no current until $V = 2\Delta(0)$ is reached, whereupon because of the infinite density of states on both sides, there is a discontinuous rise in current. At finite temperatures, as the bias is slowly increased the current slowly increases until the point where there can be no back current flow from the lower biased electrode. At this point the current remains nearly constant. At low reduced temperatures ($T/T_c \ll 1$) a slight decrease in current is expected because the quasiparticles from the left face a slowly decreasing density of states on the right.

In real tunnel junctions the discontinuous current jump at $V = 2\Delta(T)$ has never been observed. There are several possible reasons normally given why perfect agreement should not be expected. First, the prediction is based on BCS theory and it is unlikely that an ideal BCS superconductor really exists. Second, most of the reported experiments have been done on thin films where tunneling occurs into many randomly oriented crystallites,

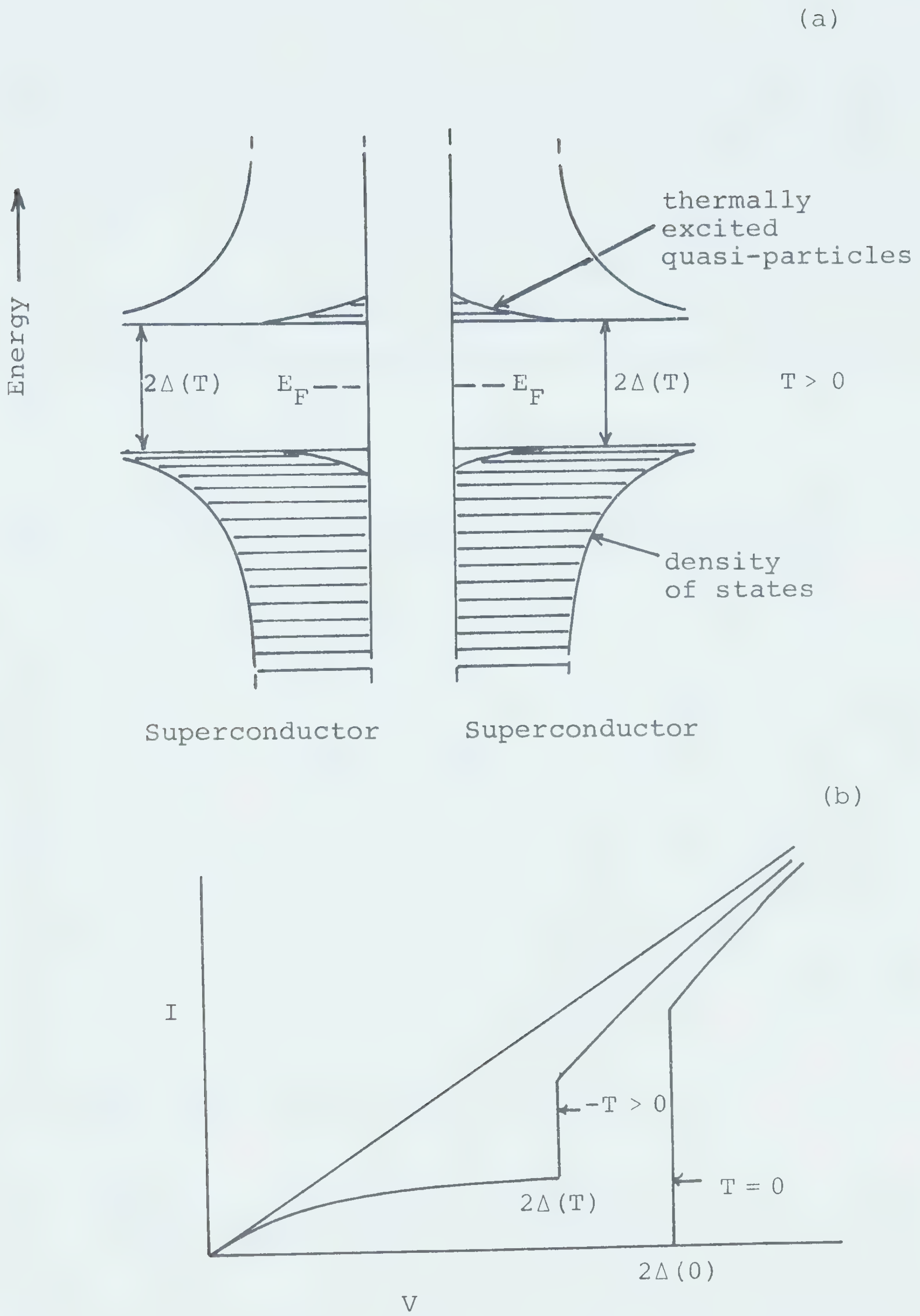
(a)
Energy
thermally
excited
quasi-particles
2Δ(T)
E_F
E_F
2Δ(T)
T > 0
density
of states
Superconductor
Superconductor
(b)
I
T > 0
2Δ(T)
T = 0
2Δ(0)
V

Fig.(5.3). (a) Energy level diagram for tunneling between identical superconductors. (b) I-V curves expected on the basis of simple theory.

giving a gap that is probably averaged over many directions. For an anisotropic superconductor this would result in a smeared current rise. Another likely cause for this is the smearing of the gap due to a non-uniform strain across the tunnel junction. In the next section we show that this smearing may be partially explained by life time effects.

5.2 Non-Equilibrium Tunneling in Superconductors

In Chapter III, we showed that the zero bias anomalies in conductance seen experimentally were the result of blocking effects due to the finite relaxation times of the electrons. It is then natural to ask what effect finite relaxation times have on the tunneling of quasi-particles in superconductors. To calculate these effects, we use the semiconductor picture of a superconductor and proceed according to the assumptions in Section 5.1. However, we now write the expression for the tunneling current in the form

$$I = \frac{4\pi e}{\hbar} \sum_{\underline{k}} \sum_{\underline{k}'} |M_{\underline{kk}'}|^2 (f_{\underline{k}} - f_{\underline{k}'})^2 (E_{\underline{k}} - E_{\underline{k}'}) \tag{5.12}$$

where it is understood that the distribution functions in the above equations are steady state rather than the equilibrium ones. We may now proceed to define effec-

tive relaxation times for the quasi-particles in both superconductors and derive the deviations of the steady state distribution functions from equilibrium as in Section 3.1. However, in that section the deviations from equilibrium were derived for a system of independent particles (electrons) satisfying Fermi statistics and having in general an unspecified density of states. This is in accordance with our assumptions about the behavior of quasi-particles and we can simply take over the results of Eqn. (3.40)

$$\text{i.e.}\quad f_{\underline{k}}-f_{\underline{k}'} = \frac{f^{o}_{\underline{k}}-f^{o}_{\underline{k}}}{1+\frac{2\pi}{\hbar}|M|^{2}(\rho_{\underline{k}}\tau_{\underline{k}'}+\rho_{\underline{k}'}\tau_{\underline{k}})} \tag{5.13}$$

where $\tau_{\underline{k}}$ and $\rho_{\underline{k}}$ are the effective relaxation times and densities of state respectively for the quasi-particles in a superconductor. The summations in Eqn. (5.12) are then done in the standard fashion

$$I = \frac{4\pi e}{h}\sum_{\underline{k}_{||}}\int_{0}^{\infty}\frac{dE_{\underline{k}}[f^{o}_{\underline{k}}(E_{\underline{k}}-\mu)-f^{o}(E_{\underline{k}}-\mu+V)]\rho_{\underline{k}}\rho_{\underline{k}'}|M|^{2}}{1+\frac{2\pi}{\hbar}|M|^{2}(\rho_{\underline{k}}\tau_{\underline{k}'}+\rho_{\underline{k}'}\tau_{\underline{k}})}\,. \tag{5.14}$$

We assume the superconducting quasi-particle relaxation times $\tau_{\underline{k}}$ depend only upon their excitation energies above the Fermi surfaces in the respective metals. Furthermore the densities of state are as given in

Eqn. (5.2). The integral in Eqn. (5.14) may then be replaced by one over the range of excitation energies ε and we obtain

$$I = \sigma_o \int_{-\infty}^{\infty} \frac{d\varepsilon[f^o(\varepsilon) - f^o(\varepsilon+V)]n(\varepsilon)\ n'(\varepsilon+V)}{1 + \frac{2\pi}{\hbar}\ |M|^2(\rho_N\ n(\varepsilon)\tau'(\varepsilon+V) + \rho_N' n'(\varepsilon+V)\tau(\varepsilon))} \tag{5.15}$$

where the primes refer to different sides of the junction and $|M|^2$ and ρ_N are the averaged matrix element and normal density of states at the Fermi surface. We note that if the relaxation times are zero then Eqn. (5.15) reduces to the conventional superconducting tunnel current given by Eqn. (5.9). Likewise,if both sides of the junction are normal, the reduced densities of states are unity and we obtain the normal ZBA current as in Eqn. (3.42). We shall now proceed to discuss the superconducting relaxation times to be used in Eqn. (5.15).

5.3 Superconducting Relaxation Times

Bardeen, Richayzen and Tewordt (1959) in the course of an investigation on the thermal conductivity of superconductors calculated the life times of quasiparticles due to elastic scattering processes. They found that the elastic scattering relaxation time of

a quasi-particle of excitation energy ε above the Fermi surface in a superconductor is given by

$$\tau_s = \frac{|\varepsilon|}{\sqrt{\varepsilon^2 - \Delta^2}} \tau_N \tag{5.16}$$

where τ_s is the relaxation time in the superconductor while τ_N is the relaxation time in the normal metal. For $\varepsilon >> \Delta$ the quasi-particles behave essentially like normal electrons in the sense that they have the same scattering times. However near the gap edge ($\varepsilon = \Delta$) the life times are infinite. This is not as serious as it sounds, for in the same paper, they showed that the speed or group velocity of the excitations or quasi-particles v_s is given by

$$v_s = \frac{\sqrt{\varepsilon^2 - \Delta^2}}{|\varepsilon|} v_N \tag{5.17}$$

where v_N is the Fermi velocity of the normal electrons. Thus the mean free paths of the quasi-particles due to elastic scattering is given by

$$\ell = \tau_s v_s = \tau_N v_N \tag{5.18}$$

so that the mean free paths of the quasi-particles are the same as those of the normal electrons. Nevertheless, the fact that the life time is infinite is a measure of the

correlation the quasi-particle feels due to the presence of the condensate although the elastic scattering processes do not allow it to lose energy and thus recombine into the ground state.

In the case of a quasi-particle in the presence of a lattice or phonon gas, Tewordt (1962) showed that the relaxation time of a quasi-particle of excitation energy ε above the Fermi energy is given by the lengthy formula:

$$\frac{1}{\tau_s(\varepsilon)} = \frac{2\pi}{\hbar}[f^{o}(-\varepsilon)]^{-1} \Bigg\{ \int_0^{\varepsilon-\Delta} \frac{\alpha^2(\omega)F(\omega)d\omega}{[(\varepsilon-\omega)^2-\Delta^2]^{\frac{1}{2}}} \cdot (\varepsilon-\omega)$$

$$\times \left(1 - \frac{\Delta^2}{\varepsilon(\varepsilon-\omega)}\right) f^{o}(\omega-\varepsilon)[1 + N^{o}(\omega)]$$

$$+ \int_0^{\infty} \frac{\alpha^2(\omega)F(\omega)d\omega}{[(\varepsilon+\omega)^2-\Delta^2]^{\frac{1}{2}}} \cdot (\varepsilon+\omega)\left(1-\frac{\Delta^2}{\varepsilon(\varepsilon+\omega)}\right) f^{o}(-\varepsilon-\omega)N^{o}(\omega)$$

$$+ \int_{\varepsilon+\Delta}^{\infty} \frac{\alpha^2(\omega)F(\omega).(\omega-\varepsilon)}{[(\omega-\varepsilon)^2-\Delta^2]^{\frac{1}{2}}} \left(1 + \frac{\Delta^2}{\varepsilon(\omega-\varepsilon)}\right) f^{o}(\omega-\varepsilon)(1+N^{o}(\omega))\Bigg\} \tag{5.19}$$

Physically, the first term corresponds to a quasi-particle state scattering into another quasi-particle state with emission of a phonon of energy ω. The second term is the same process except that a phonon of energy ω is absorbed. The third term is the recombination

term and corresponds to the destruction of a pair of quasi-particle states of opposite momenta and spin with the creation of a phonon of energy ω. It may be easily shown that in the limit of a normal metal ($\Delta = 0$) Eqn. (5.19) reduces to the expression for the life time obtained for a normal electron in Eqn. (3.26). The quasi-particle-phonon relaxation time given by Eqn. (5.19) is not infinite at the gap edge as in the case of elastic scattering because of the presence of the recombination time.

5.4 The Nonequilibrium Tunneling Current

In order to calculate the nonequilibrium tunneling current we take our effective quasi-particle relaxation time $\tau(\varepsilon)$ to be given by

$$\frac{1}{\tau(\varepsilon)} = \frac{1}{\tau_i n(\varepsilon)} + \frac{1}{\tau_{ep}(\varepsilon)} \tag{5.20}$$

where τ_i is the normal metal elastic scattering time and the factor $n(\varepsilon)$ comes from the definition of its superconducting counterpart in Eqn. (5.16). $\tau_{ep}(\varepsilon)$ is the quasi-particle-phonon relaxation time. If we substitute Eqn. (5.20) into the expression for the superconducting tunnel current given by Eq. (5.15) we obtain

$$I = \sigma_o \int_{-\infty}^{\infty} \frac{d\varepsilon\,[f^o(\varepsilon) - f^o(\varepsilon+V)].n(\varepsilon)n'(\varepsilon+V)}{1 + n(\varepsilon)n'(\varepsilon+V)\left[\dfrac{\tau_i'/\tau_B'}{1 + \dfrac{\tau_i' n'(\varepsilon+V)}{\tau_{ep}'(\varepsilon+V)}} + \dfrac{\tau_i/\tau_B}{1 + \dfrac{\tau_i' n(\varepsilon)}{\tau_{ep}(\varepsilon)}}\right]}$$

(5.21)

where the primes refer to the opposite side of the junction and τ_B is defined by

$$\frac{1}{\tau_B} = \frac{2\pi}{\hbar}\,|M|^2\,\rho_N'$$

as in Eqn. (3.47). We may note that the tunneling current given above is an odd function of bias since $\tau_{ep}(\varepsilon)$ is an even function of its argument. Eqn. (5.21) may be written in a simpler way by assuming that we have identical superconductors on both sides of the barrier. In this case

$$I = \sigma_o \int_{-\infty}^{\infty} dt\, \frac{f^o(\varepsilon) - f^o(\varepsilon+V)}{\dfrac{1}{n(\varepsilon)n(\varepsilon+V)} + \dfrac{\tau_i}{\tau_B}\left[\dfrac{1}{1+\dfrac{\tau_i n(\varepsilon+V)}{\tau_{ep}(\varepsilon+V)}} + \dfrac{1}{1+\dfrac{\tau_i n(\varepsilon)}{\tau_{ep}(\varepsilon)}}\right]} .$$

(5.22)

The above expression for the superconducting tunneling current exhibits a new feature which is not present in the conventional current given by Eqn. (5.9).

That is, the tunneling current does not have a discontinuous jump at $V = 2\Delta(T)$. Rather, if the ratio τ_i/τ_B is small, it starts increasing at $V = 2\Delta(T)$ with a large but finite slope. For $V >> 2\Delta(T)$, we know from the behavior of the ZBA in normal tunneling that the factor in the denominator above is very small and hence the tunneling current reverts back to the conventional BCS current. The reason we do not get a discontinuous jump in the tunneling current at $V = 2\Delta(T)$ is due to the fact that the life time factor in the denominator of Eqn. (5.22) can never be zero. Therefore the infinite density of states at the gap edge which causes the jump in current is not felt.

We shall now consider the case in which the electron-phonon interaction is weak (i.e. the recombination time is large compared to the elastic scattering time). Thus the term given by

$$\frac{1}{1 + \frac{\tau_i n(\varepsilon+V)}{\tau_{ep}(\varepsilon+V)}} + \frac{1}{1 + \frac{\tau_i n(\varepsilon)}{\tau_{ep}(\varepsilon)}} \qquad (5.23)$$

is of the order of unity and the tunneling current takes the form

$$\frac{I(V)}{\sigma_o} \cong \int_{-\infty}^{\infty} d\varepsilon \, \frac{f^o(\varepsilon) - f^o(\varepsilon+V)}{\frac{2\tau_i}{\tau_B} + \frac{\sqrt{\varepsilon^2-\Delta^2}}{|\varepsilon|} \; \frac{\sqrt{(\varepsilon+V)^2-\Delta^2}}{|\varepsilon+V|}} \; . \qquad (5.23)$$

The T = 0°K tunneling current is plotted in Fig. (5.4) for various values of the ratio τ_i/τ_B and compared to the conventional BCS tunneling current. We may remark that the fit for the value of $\tau_i/\tau_B \approx .001$ corresponds closely to the experiments in superconducting Al-Al junctions by Giaever, Hart and Megerle (1962). Assuming that the nominal resistance of their junctions is of the order of 50Ω so that the tunneling time τ_B can be taken as $\tau_B \approx 10^{-7}$ sec., we obtain the value

$$\tau_i \approx 10^{-10} \text{ seconds} \quad . \tag{5.24}$$

This life time agrees with our ZBA results in Chapter III. It is interesting to note that in the same paper Giaever et al attempted to account for the finite slope of the current rise by assuming that the energy gap was smeared. They find that if they attribute the smearing to a life time, they obtain a lower limit of 10^{-11} seconds.

The smearing of the current rise as given by Eqn. (5.22) or Eqn. (5.23) depends upon the magnitude of the ratio τ_i/τ_B. Since τ_B is a measure of the resistance of the junction we disregard it in the following discussion. The elastic scattering time τ_i should depend strongly on the properties of the metallic films. In practice we expect the amount of elastic scattering

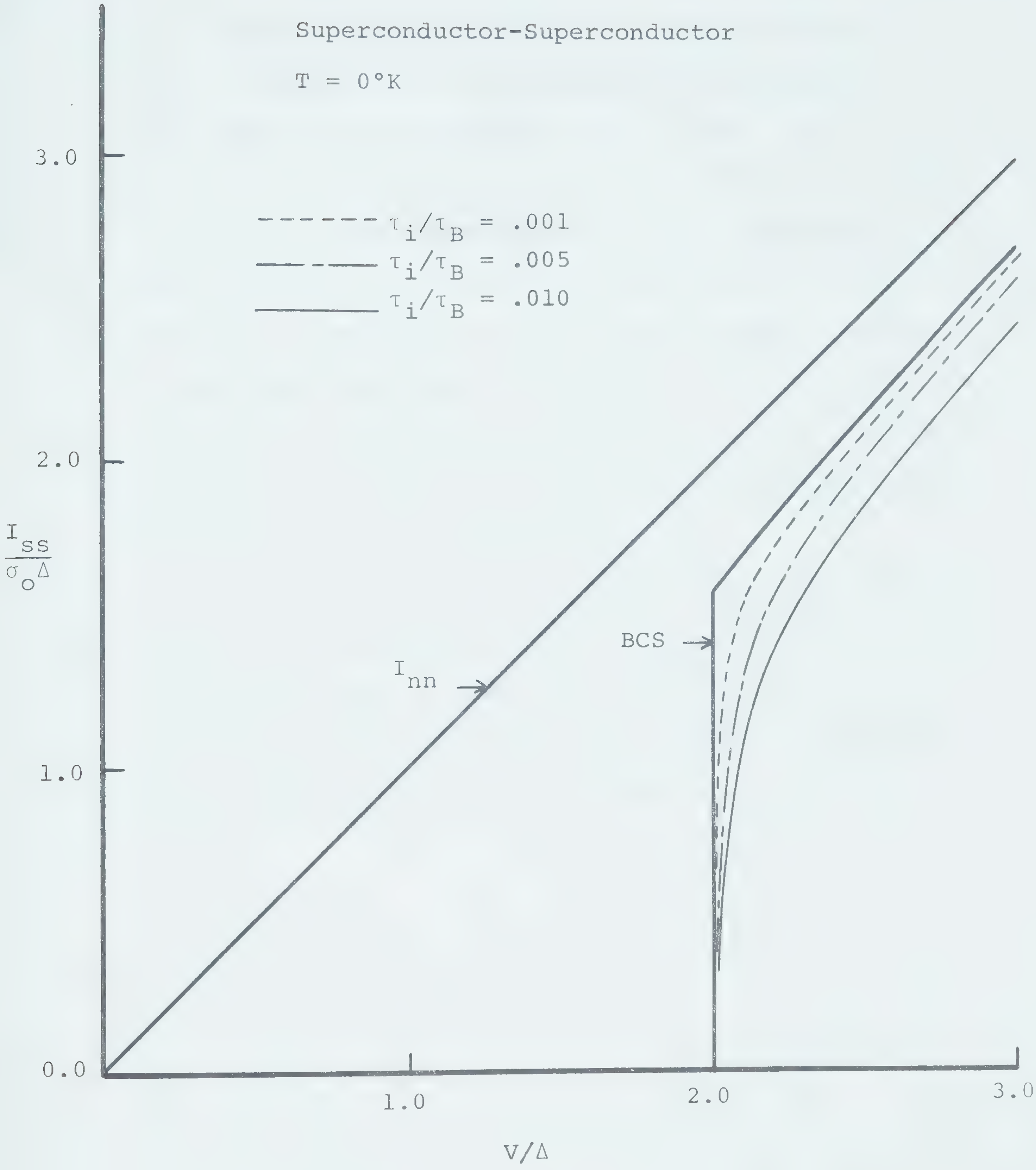

Fig. (5.4). Tunneling current due to life time effects.

to increase significantly as we either decrease the film thickness of the electrodes or else increase the impurity concentration of the films. Thus τ_i/τ_B should decrease accordingly. The width of the current rise should then decrease as the film thickness is decreased and the impurity concentration is increased. This is in agreement with the observations of Rowell (1969) who found that the width of the current rise in Pb junctions decreased as the film thickness was reduced from 2000 to 1000 Å, and the current rise became very sharp when In was alloyed into the Pb.

In the case of finite temperatures, the calculation of the tunneling current is numerically much more complicated when we take into account the relaxation time due to the lattice and the temperature dependent gap. This work is still in progress at this time.

CHAPTER VI

GEOMETRICAL EFFECTS IN TUNNEL JUNCTIONS AND CONCLUSION

6.1 Structure of the Tunnel Junction and Splitting of the ZBA

In previous chapters we treated the tunnel junction under the assumption that it was a homogeneous sandwich of the two electrodes and the insulator. In reality, tunneling occurs only at certain portions of the cross strip area of the junction. This was conclusively shown by Adler and Kreuzer (1972). They alternately passed a large current in the top film (I_y) and the bottom film of the junction (I_x) while simultaneously measuring the tunnel current (i_t) and its derivatives (Fig. (6.2a)). Fig. (6.2) shows a typical set of conductance curves that they obtained in an Al-Al junction at 4.2°K. When the conductance was measured in a conventional fashion without any additional currents flowing in either the top or bottom film, the solid curve in Fig. (6.1) was obtained. The ZBA dip in conductance is seen very clearly. When a large current (I_y) was passed along the top film, the ZBA split into two minima as shown in the dashed curve. However, upon passing a large current (I_x) along

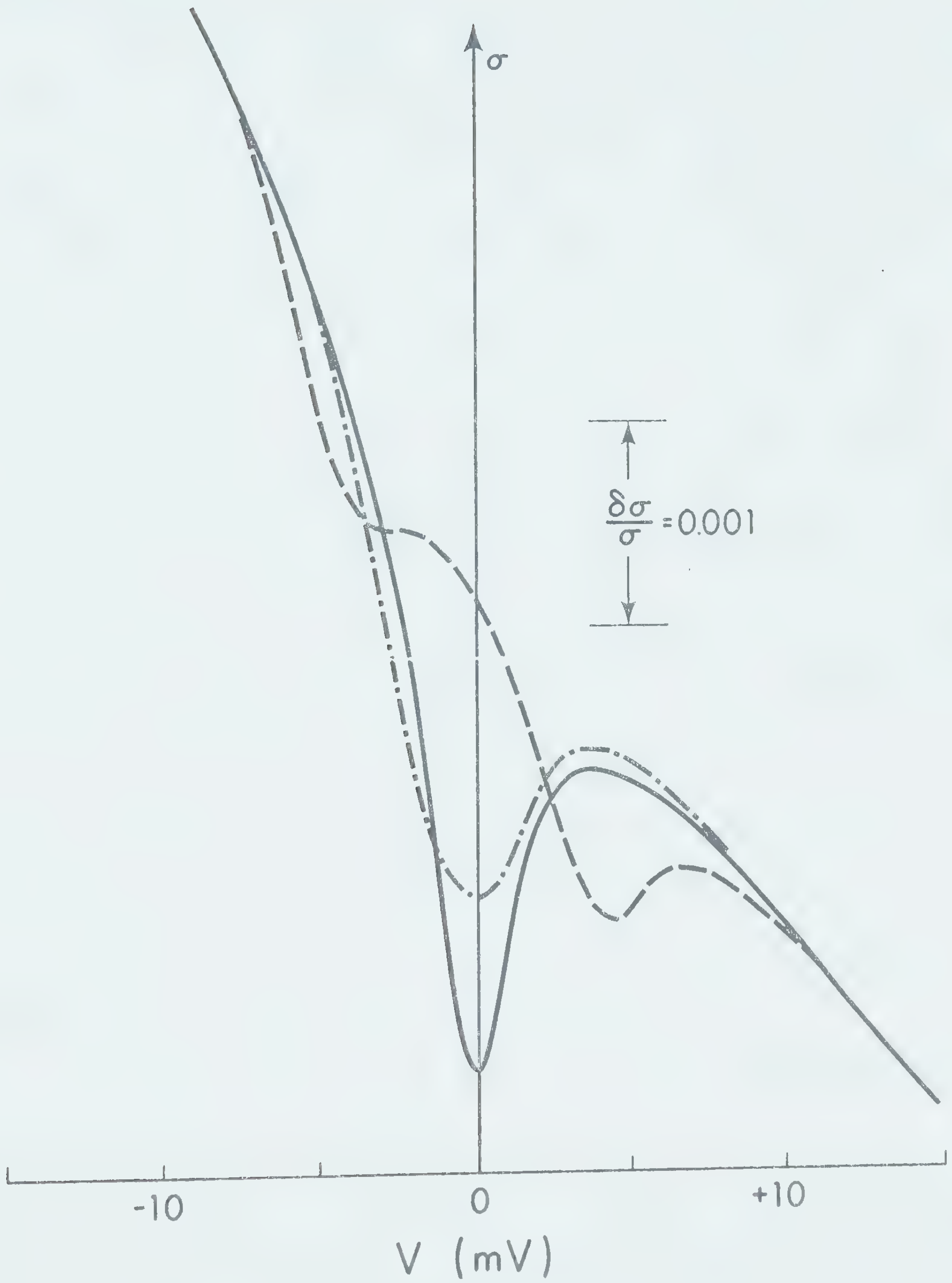

Fig. (6.1). Conductance as a function of bias for an Al-Al junction at 4.2°K: (——, no current through either electrode); (— — —, .5 A along the top film); (—. —. —, .5 A along the bottom film).

the bottom film, it was found that the ZBA characteristic smeared out as shown by the dotted curve.

This experimental result may be easily explained if one assumes that tunneling occurs only along the edges of the bottom film. Thus when the current I_y is passed along the top film, there is a potential drop along the film and the two effective areas for tunneling differ in potential. This causes the ZBA characteristics to now have two minima whose centers are separated by the potential drop along the top film. On the other hand when a current I_x is passed along the bottom film, there is a continuous potential drop along the edges and the ZBA becomes smeared out. Adler and Kreuzer summarized their results as follows:

1) Splitting of the ZBA is only observed with a current I_y (this has been tested with currents in excess of .5 A). Similar results have been obtained using Ag, In, Sn, and Pb electrodes.

2) In all cases the current I_y splits the ZBA minimum into exactly 2 minima.

3) The shift of the minima to either side is always a linear function of I_y. This ohmic behavior was found to occur over the whole range of metal film thickness used (200-4000 Å). Such ohmic behavior was also tested in several triple junctions having a common bottom

film and oxide while the top films varied in thickness by a ratio of 1:2:4.

The above results clearly suggest that the oxide barrier has two thin regions along opposite sides of the bottom film. The fact that no splitting arises from the current I_x in the bottom film then indicates a rather uniform barrier parallel to the bottom film. The junction may then be idealized by the geometry shown in Fig. (6.2b). The presence of a current I_y along the top film may then be represented by two thin regions at $y = \pm b$ being biased at two different potentials $\pm V_o$ as in Fig. (6.2c). The magnitude of the potential difference V_o is then determined by the current I_y and the film resistance. When a current I_x is passed along the bottom film, there would be a continuous potential drop along the constant thickness tunneling region as indicated in Fig. (6.2d). Adler and Kreuzer assumed that the tunneling conductance per unit area of the thin regions was given by

$$\tilde{\sigma}(V) = \tilde{\sigma}_o + \delta\tilde{\sigma}(V)$$

where $\delta\tilde{\sigma}(V)$ is the negative contribution to the conductance due to the blocking effect and is given by Eqn. (3.52). For simplicity, they considered $\delta\tilde{\sigma}(V)$ to be given by the $T = 0°K$ limit as in Eqn. (3.56)

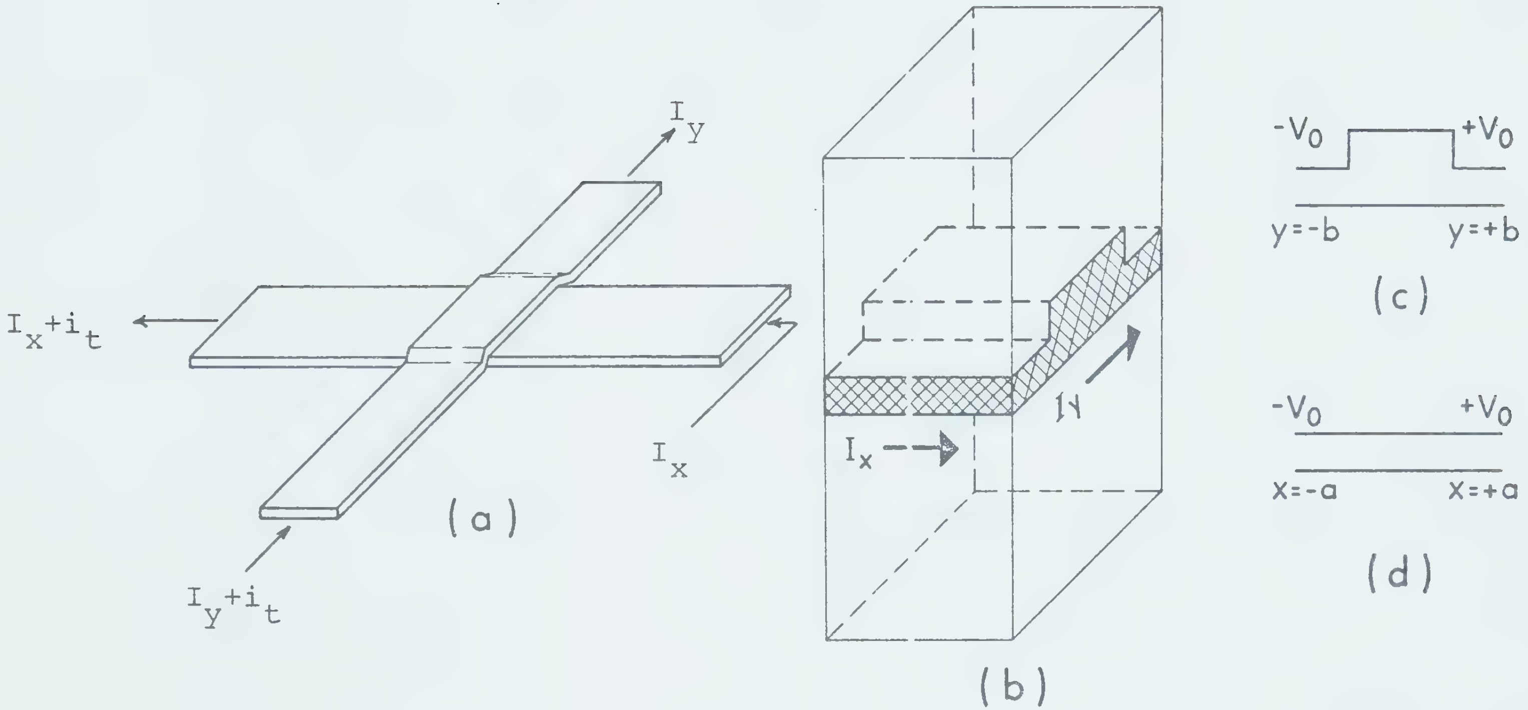
I_y
I_x+i_t
I_x
I_y+i_t
(a)
I_x
H
(b)
$-V_0$
$+V_0$
$y=-b$
$y=+b$
(c)
$-V_0$
$+V_0$
$x=-a$
$x=+a$
(d)

Fig. (6.2) Schematic of the junction geometry as described in the text.

and showed that both the smearing and splitting of the ZBA characteristic could be accounted for by using the idealized geometry in Fig. (6.2).

It follows that tunneling occurs predominantly near the edges of the junction and we are justified in assuming that the effective area for tunneling is a small fraction of the cross strip area as indicated in evaluating Eqn. (2.22). The method of introducing potential drops across the metal films by external currents may be used to probe the structure of the oxide. In principle it should be possible to obtain the conductance per unit area as a function of position in the junction by carrying out an exhaustive set of measurements with varying I_x and I_y. By using superconductor in the bottom film the resolution of such measurements with I_y may be improved by using the gap edge as a potential probe rather than the ZBA in the normal metal.

6.2 Conclusion and Discussion

In normal metals, we have shown that the observed structure near zero bias in the conductance σ and its derivative $d\sigma/dV$ can be accounted for by including the effects of the finite electron relaxation rates in the

junction electrodes. The non-zero life times then lead to an observable blocking of otherwise available electron tunneling states at low bias.

The dependence of the conductance minima on the properties of the junction may conveniently be summarized with reference to the T = 0°K diagrams in Figs. (3.3) and (3.4) for the models n=1 and n=2 respectively. We note that the amplitude of the conductance minimum is proportional to the ratio τ_i/τ_B. Hence by increasing the amount of elastic scattering in the electrodes we would decrease this ratio. Similarly, making the oxide thicker would increase the tunneling time τ_B and again make this ratio smaller. A possible experiment to test the dependence of the size of the conductance dip would be to construct a multiple junction with the same base metal film and oxide. The films deposited on top could then be alloyed with a suitable metal in increasing concentration. If our conjecture is correct, then the size of the conductance dip should decrease with increasing concentration of the alloy material in the top film. To test the dependence on oxide thickness would be more difficult. However, by carefully examining the structure of the oxide as described in Section 6.1 one should be able to, in principle, also test this aspect of the theory.

The width of the conductance dip as indicated in Figs. (3.3) and (3.4) is proportional to the quantity $(a_n \tau_i)^{-1/n+1}$ where n=1 or 2 according to which model we choose for the electron-phonon coupling. Thus as we increase the coupling strength of the electrodes or else the elastic scattering time τ_i the width of the conductance dip should decrease accordingly. A much more difficult experiment to perform would be to construct a tunnel junction with a crystal on one side. In this case τ_i should be very large compared to its value in the evaporated film and one should be able to observe a fairly deep and sharp conductance dip. Also by tunneling into single crystals one should be able to probe, in principle, the anisotropy of the electron-phonon relaxation times. These considerations can likewise be carried through for the derivative of conductance.

The agreement of theory with experiment seems to indicate that the model $\alpha^2(\omega)F(\omega) \propto \omega$ is a more reasonable choice to make. However a better test to differentiate between the two models should be possible at low temperatures. Fig. (3.4) indicates that for $\alpha^2(\omega)F(\omega) \propto \omega^2$, there is a kink in the derivative of conductance at zero bias and zero temperature. This feature rapidly disappears at higher temperatures but calculations indicate that it should become noticeable below about .5°K. This may serve as a sensitive test

for the two models although modulation problems may become severe in this low bias regime. We have no physical explanation for this kink except to say that it is a result of the fact that $d\sigma/dV$ goes like V^2 at very low bias and at zero temperature. Although we have not done so, a more complicated version of $\alpha^2(\omega)F(\omega)$ may probably exist to fit the theory in a more suitable fashion. However, there seems to be little precedent in present unrelated theoretical or experimental work to justify this.

In the work we have done on superconductive tunneling, the nonequilibrium tunneling of quasiparticles seems to indicate that the tunneling current between two identical superconductors does not have a discontinuous rise. This is in agreement with experiment. However, we have used the semiconductor picture of a superconductor both in the derivation of the transport equations for nonequilibrium tunneling and the tunneling current itself. A more rigorous treatment using the microscopic many-body theory of superconductive tunneling in the presence of relaxation processes would be in order. Nevertheless, it is encouraging that the same choice of life time parameters used to explain the normal ZBA also serve to give qualitative agreement with experiment in the case of superconductors.

REFERENCES

Adler, J.G., Chen, T.T. and Strauss, J., Rev. Sci. Instr. 42, 362 (1971).

Adler, J.G. and Kreuzer, H.J., Can.J.Phys.22, 2842 (1972).

Allen, P.B. and Cohen, M.L., Phys. Rev. 1, 1329B (1970).

Anderson, P.W. and Rowell, J.M., Phys. Rev. Lett. 10, 230 (1963).

Bardeen, J., Phys. Rev. 49, 653 (1936).

Bardeen, J., Cooper, L. N. and Schrieffer, J.R.,
Phys. Rev. 106, 162 (1957);
Phys. Rev. 108, 1175 (1957).

Bardeen, J., Phys. Rev. Lett. 6, 57 (1961).

Bardeen, J., Rickayzen, G. and Tewordt, L., Phys. Rev. 113, 982 (1959).

Carbotte, J.P. and Dynes, R.C., Phys. Rev. 172, 476 (1968).

Chen, T.T. and Adler, J.G., Solid State Comm.8, 1965 (1970).

Cohen, M.H., Falicov, L.M. and Phillips, J.C., Phys. Rev. Lett. 8, 316 (1962).

Davidov, A.S., "Quantum Mechanics", p. 71, Pergamon Press, 1965.

Douglass, D.H. Jr. and Falicov, L.M. in "Progress in Low Temp. Physics", (C.J. Gorter, ed.) Vol. 4, p.97, North Holland Publishing Co. (1964).

Fan, H.Y., Phys. Rev. 61, 365 (1942).

Fisher, J.C. and Giaever, I., J. Appl. Phys. 32, 172 (1961).

Fowler, R.H. and Nordheim, L., Proc. Roy. Soc. (London) A119, 173 (1928).

Frenkel, J., Z. Physik 51, 232 (1928).

Frenkel, J., Phys. Rev. 36, 1604 (1930).

Giaever, I., Phys. Rev. Lett. 5, 147 (1960);
Phys. Rev. Lett. 5, 464 (1960).

Giaever, I., Hart, H.R. and Megerle, K., Phys. Rev. 126, 941 (1962).

Goy, P. and Castaing, B., (Preprint).

Harrison, W.A., Phys. Rev. 123, 85 (1961).

Hartman, T.E., J. Appl. Phys. 35, 3283 (1964).

Holm, R., J. Appl. Phys. 22, 569 (1951).

Josephson, B.D., Phys. Lett. 1, 251 (1962).

Kohn, W. and Hohenberg, P., Phys. Rev. 136, 864 (1964).

Kohn, W. and Sham, L.J., Phys. Rev. 140, 1133 (1965).

Kohn, W. and Lang, N.D., Phys. Rev. B 1, 4555 (1970).

Kohn, W. and Lang, N.D., Phys. Rev. B 3, 1212 (1971).

Lambe, J. and Jaklevic, R.C., Phys. Rev. 165, 821 (1968).

McMillan, W.L. and Rowell, J.M., in "Superconductivity" Vol. 1 (R.D. Parks, ed.) Marcel Dekker, Inc., New York (1969).

Miller, S.C. and Good, R.H., Phys. Rev. 91, 174 (1953).

Rhodes, P., Proc. Roy. Soc. (London) A201, 396 (1950).

Rowell, J.M., in "Tunneling Phenomena in Solids" (E. Burstein and S. Lundqvist, ed.) [p.273 and p.385] Plenum Press, New York (1969).

Rowell, J.M., McMillan, W.L. and Feldmann, W.L., Phys. Rev. 180, 658 (1969).

Schiff, L.I., "Quantum Mechanics" 2nd ed., McGraw-Hill Book Co., Inc. (1955).

Simmons, J.G. in "Tunneling Phenomena in Solids" (E. Burstein and S. Lundqvist, ed.) p. 135, Plenum Press, New York (1969).

Sommerfeld, A. and Bethe, H.A. in "Handbuch der Physik" (S. Flügge, ed.), Vol. 24, p.150, Springer, Berlin (1933).

Stratton, R., J. Phys. Chem. Solids 23, 1177 (1962).

Tewordt, L., Phys. Rev. 128, 12 (1962).

Trofimenkoff, P.N., Kreuzer, H.J., Wattamaniuk, W.J. and Adler, J.G., Phys. Rev. Lett. 29, 597 (1972).

Wilkins, I.W., Lecture notes on: "Observable Many-body Effects in Metals" (Nordita, 1968).

Solymar, L., "Superconductive Tunneling and Applications", Chapman and Hall Ltd., London (1972).

B30058